# COORDINATE CONTROL OF METABOLIC FLUX WITH LIVER ENERGY STATUS BY AMPK *IN VIVO*

By

Clinton Michael Hasenour

Dissertation

Submitted to the Faculty of the

Graduate School of Vanderbilt University

in partial fulfillment of the requirements

for the degree of

DOCTOR OF PHILOSOPHY

In

Molecular Physiology and Biophysics

August, 2014

Nashville, TN

Approved:

Owen P. McGuinness

Richard M. O'Brien

John M. Stafford

David R. Gius

*To my former students,*

*may you be afforded the same opportunities*

## ACKNOWLEDGMENTS

This work would not have been possible without the enduring support of many people. The Wasserman lab has provided invaluable contributions to my development as a scientist. I am grateful for the support of my mentor, Dr. Wasserman, whose intellectual, financial, and comedic contributions over the last 5yrs are likely to be found on every page of this dissertation. By providing the opportunity to investigate basic control of *in vivo* metabolism, Dr. Wasserman essentially gave me the opportunity to pursue a dream. For this, a single acknowledgments section hardly seems fitting.

Several current and former members of the lab made contributions to this dissertation. Emerson Ridley was crucial for the success of the stable isotope project; his versatility, work ethic, and friendship made his time in the lab far too short. Jeffrey Bonner was always willing to lend a hand, ear, and provide critical advice. Furthermore, Deanna Bracy, Freyja James, Mickael Goelzer, Curtis Hughey, Eric Berglund, Li Kang, Robert Lee-Young provided invaluable surgical and experimental support. The former three members ensure the functions of the lab and, thus, its continued success. I would also like to acknowledge the members of the Mouse Metabolic Phenotyping Center and Vanderbilt Hormone Assay and Analytical Services Core (particularly Pat Donahue and Larry Swift).

My thesis committee members (Owen McGuinness, John Stafford, Richard O'Brien, and David Gius) have provided a strong base of support and constructive criticism. Their expertise and encouragement were paramount for the development of the hypotheses examined in this dissertation. The dedication of our collaborators Jamey Young and Martha Wall made central studies of this dissertation—and many more to come—possible. I would also like to thank my early instructors who were instrumental in preparing me for each phase of education—

particularly Mrs. Steedman, Mrs. Smith, Mr. Martin, Mr. Gardner, and Mrs. Funkhouser. A special thanks to Dr. Wade Hazel for providing >2yrs of science research mentorship at DePauw.

Lastly, I would like to acknowledge my family and friends. My brother and sister have provided constant support, advice and a healthy level of competition over the years. I owe a debt of gratitude to my parents, who have served as exemplars of hard work, creativity, and unconditional love. I would also like to thank the Lorenz family for their support and, in particular, Maggie Lorenz for her patience, dedication and love.

This work would not have been possible without funding from NIH Grants U24 DK59637, R37 DK50277 (David H. Wasserman) and DK20593 (the Diabetes Research and Training Center). This work was also supported by the Molecular Endocrinology Training Program at Vanderbilt.

## TABLE OF CONTENTS

## LIST OF TABLES

**Table** **Page**

## LIST OF FIGURES

## LIST OF ABBREVIATIONS

| | |
|---|---|
| AcAc | Acetoacetate |
| ACC | AcetylCoA Carboxylase |
| AICAR | 5-Aminoimidazole-4-Carboxamide-1-β-D-Ribofuranoside |
| Akt | Protein Kinase B |
| AMPK | AMP-Activated Protein Kinase |
| BCAA/BCKA | Branched-Chain Amino Acid/Keto Acid |
| BCAT | Branched-Chain Aminotransferase |
| BCKDH | BCKA Dehydrogenase |
| CaMKKβ | Calcium/Calmodulin Kinase Kinase β |
| CBP | CREB Binding Protein |
| CBS | Cystathione β-Synthase |
| CE | Cholesterol Ester |
| CPT1 and 2 | Carnitine Palmitoyltransferase 1and 2 |
| CREB | Cyclic AMP Response Element Binding protein |
| CRTC2 | CREB-Regulated Transcription Coactivator 2 |
| DG | Diglyceride |
| DHAP | Dihydroxyacetone Phosphate |
| EC | Energy Charge |
| EndoRa | Endogenous Glucose Production |
| ER | Endoplasmic Reticulum |
| ERK1/2 | Extracellular Signal-Regulated Kinase 1/2 |
| FA and LCFA | Fatty Acid and Long Chain Fatty Acid |
| FAD ($FADH_2$) | Flavin Adenine Dinucleotide |
| FFA (NEFA) | Free Fatty Acids |
| FGF21 | Fibroblast Growth Factor 21 |
| FOXO1 | Forkhead Box Protein O1 |
| F6P | Fructose-6-Phosphate |
| GAP/GA3P | Glyceraldehyde-3-Phosphate |
| GC/MS | Gas Chromatography/Mass Spectrometry |
| GIR | Glucose Infusion Rate |
| G6P | Glucose-6-Phosphate |
| G6Pase | Glucose-6-Phosphatase |
| HDAC | Histone Deacetylase |
| HETE | Hydroxyeicosatetraenoic Acid |
| HMGCoAR | Hydroxy-3-Methylglutaryl-CoA Reductase |
| HMW | High Molecular Weight |
| HNF4α | Hepatocyte Nuclear Factor 4α |
| HODE | Hydroxyoctadecadienoic Acid |
| INCA | Isotopomer Network Compartmental Analysis |

| | |
|---|---|
| LKB1 | Liver Kinase B1 |
| ME | Malic Enzyme |
| MFA | Metabolic Flux Analysis |
| mTORC1 | Mammalian Target of Rapamycin Complex1 |
| NAD+ (NADH) | Nicotinamide Adenine Dinucleotide |
| NAFLD | Non-Alcoholic Fatty Liver Disease |
| NAMPT | Nicotinamide Phosphoribosyltransferase |
| NASH | Non-Alcoholic Steatohepatitis |
| NMP | Nucleotide Monophosphate |
| NMR | Nuclear Magnetic Resonance Spectroscopy |
| OAA | Oxaloacetate |
| OXPHOS | Oxidative Phosphorylation |
| PC | Phosphatidylcholine |
| PE | Phosphatidylethanolamine |
| PEP | Phosphoenolpyruvate |
| PEPCK | Phosphoenolpyruvate Carboxykinase |
| PGC1α | Peroxisome Proliferator-Activated Receptor γ Coactivator 1α |
| PK | Pyruvate Kinase |
| PKA | Protein Kinase A |
| PL | Phospholipid |
| PPARα | Peroxisome Proliferator-Activated Receptor α |
| Ra | Rate of Glucose Appearance |
| RCR | Respiratory Control Ratio |
| Rd | Rate of Glucose Disappearance |
| ROS | Reactive Oxygen Species |
| SAM | S-Adenosylmethionine |
| SCS | SuccinylCoA Synthetase |
| SHP | Small Heterodimer Partner |
| SIK1 and 2 | Salt-Inducible Kinase 1 and 2 |
| Sirts 1 and 3 | Sirtuins 1 and 3 |
| SREBP1c and 2 | Sterol Regulatory Element-Binding Protein 1c and 2 |
| S6K1 | Ribosomal Protein S6 Kinase 1 |
| TAN | Total Adenine Nucleotide pool |
| TCA | Tricarboxylic Acid |
| TG | Triglyceride |
| TSC1 and 2 | Tuberous Sclerosis Complex 1 and 2 |
| T2DM | Type 2 Diabetes Mellitus |
| Ulk1 | Unc-51-Like Kinase 1 |
| VDAC1 | Voltage-Dependent Anion-Selective Channel Protein 1 |

| | |
|---|---|
| VHL | Von Hippel Lindau protein |
| ZMP | 5-Aminoimidazole-4-Carboxamide-β-D-Ribosyl-5-Monophosphate |
| 2PG | 2-Phosphoglycerate |
| 3-OH | 3-Hydroxybutyrate |
| 4E-BP1 | Eukaryotic Initiation Factor 4E-binding Protein |
| 5-methylthioadenosine | MTA |

# Chapter I

## INTRODUCTION

### Cultural-Physiological Context

The alarming incidence of diabetes and obesity has emerged as a byproduct of globalization. Global shifts in economic growth, trade, and urbanization have led to behavioral changes which promote positive energy balance (1). Billions of dollars are spent annually on treating pathologies associated with metabolic dysregulation (1). The US Surgeon General reports that obesity increases risk of premature death from all causes by 50-100%. Moreover, US obesity has doubled in children and quadrupled in adolescents over the last 30yrs (CDC). These statistics convey the serious impact of sedentary lifestyle and overnutrition on physical and financial welfare in the United States.

Glucoregulation is a vital, integrative metabolic process which is often perturbed in overnutritive states. In normal physiology, blood glucose concentrations are maintained within a relatively narrow range despite dramatic changes in fuel flux following a meal, during exercise and fasting (2). The consequences of acute and chronic glycemic dysregulation are, indeed, life threatening—ranging from hypoglycemic seizure and death to metabolic derangements that result from hyperglycemia and insulin resistance (2). Diabetes is generally characterized by a deficit in insulin action and, consequently, an imbalance in the insulin:glucagon ratio. In this context, impairments in insulin-stimulated glucose uptake coincide with increased hepatic glucose, ketone, and triglyceride production.

Modern therapeutics designed to maintain normoglycemia have significant limitations and, in many cases, patients must resort to insulin therapy (3). Furthermore, researchers are still investigating the mechanisms that mediate the effects of the biguanide metformin—a globally prescribed treatment for type II diabetes (3, 4). A clearer understanding of the origins of metabolic dysregulation and drug action will enhance our ability to develop effective treatment strategies. The liver is a major determinant of metabolic state due to its high metabolic activity and diverse functionality. Consequently, overnutrition generates maladaptations in the liver which spur many of the pathogenic symptoms observed in diabetes and obesity. An understanding of the hepatic response to changes in nutritional state is a chief public health concern.

## A Glucagon-Centric View of the Liver in Normal and Pathophysiology

Feeding, fasting, and physical exertion require a complex neuroendocrine response that activates pathways for energy mobilization and utilization (2). The liver is positioned to ensure the body's metabolic requirements during an increase in nutrient demand or scarcity. Nutrients and endocrine signals from the pancreas and gut empty into the portal vein, which drains into the liver. Broadly speaking, this anatomy supports the hormonal control of liver metabolism by the opposing actions of insulin and glucagon (5, 6). Hepatic sinusoids mix the metabolic and endocrine contents delivered by the portal vein with arterial $O_2$. An acute increase in glucose availability elicits an increment in insulin secretion and action at the liver; conversely, glucagon secretion and action increase with a fall in glucose and insulin. In normal physiology, elevated glucagon action occurs in the context of low circulating insulin. Glucagon is a principal regulator

of hepatic metabolic state. Elevated glucagon action transforms the liver into a factory for the production and supply of macronutrients for whole-body metabolism.

A primary function of the liver is to sustain the glucose requirements of the body during fasting and exercise. Glucoregulatory control is so precise that arterial glucose levels are maintained within narrow limits. Two unique properties of the liver support its role in glucose homeostasis: 1) unlike other organs, the liver's glycogen stores are reserved to meet whole-body glucose demands and 2) the liver is uniquely equipped to perform gluconeogenesis, which assembles carbon from amino acids, glycerol, and lactate into new glucose molecules. Most organs catabolize glycogen during fasting and exercise, which generates energy through aerobic and anaerobic glycolysis. The liver retains the highest glycogen concentrations in the body yet degrades its supply to provide glucose for other tissues. This contrasts with the muscle, for example, whose large glycogen reservoirs are retained to meet its own energy needs.

Hepatic gluconeogenesis and associated pathways place an energetic burden on the liver (**Fig. 1.1**). The liver is suited with an enzymatic arsenal uniquely capable of synthesizing glucose and ketones *de novo* from amino acids, glycerol, lactate, and fat (7–11). These processes are necessary to provide a steady source of nutrients to the brain. Glucagon facilitates amino acid extraction and utilization in the liver (8, 11, 12). Muscle proteolysis is a principle supplier of amino acids for gluconeogenesis in starvation (7). However, it has been suggested that glucagon represses hepatic protein synthesis while promoting proteolysis (13, 14), and amino acids liberated via autophagy in the liver may contribute to gluconeogenesis (15). Clearly, multiple mechanisms are in place to supply carbon for glucose synthesis in the liver. Anaplerosis refers to the net entry of carbon into the TCA cycle—which excludes acetylCoA due to the loss of $2CO_2$ in a turn of the TCA cycle. Certain gluconeogenic reactions consume high-energy phosphates

and reducing cofactors; amino acid catabolism necessitates the disposal of $NH_3$ through ureagenesis (**Fig. 1.1**). Accordingly, disrupting gluconeogenic flux through PEPCK prevents the effects of glucagon on liver energy state (16).

Processes that consume large amounts of energy require a commensurate increase in energy production. The liver derives a substantial portion of its energy from fatty acid oxidation. A decline in insulin and increase in adrenergic signaling during fasting and exercise increases lipolysis from adipose tissue (17, 18). Moreover, a reduction in insulin magnifies glucagon action at the liver. *In vivo* studies performed across species demonstrate glucagon's efficacy at promoting substrate (i.e. certain fatty and amino acids) utilization in the liver. Hepatic fat oxidation and ketogenesis are accelerated during exercise due to glucagon action (11). Glucagon controls ketogenesis through intrahepatic mechanisms (18–20) but its effects on fatty acid delivery are controversial (see glucagon.com, Dr. Daniel J Drucker). A detailed analysis of these mechanisms will be provided in subsequent sections. By mass, energy production from fat exceeds that of other endogenous substrates. Though the initial priming of fatty acids requires ATP hydrolysis, subsequent β-oxidation and the complete oxidation of acetylCoA make fatty acids a rich energy source. Indeed, glucagon promotes hepatic mechanisms that support fat oxidation during fasting (21).

The complex function of the liver is integral for whole body energy homeostasis. The liver dictates the flux of multiple fuels in accordance with endocrine state. An imbalance in substrate delivery, uptake, or utilization transforms the liver into a driver of pathophysiology. Metabolic dysregulation may exert pathological changes in insulin (22) and glucagon (5) action at the liver. Defining their contributions to diabetes and obesity poses a significant challenge due to extensive overlap in endocrine, metabolic, and signaling pathways in the liver. Moreover,

insulin regulates glucagon secretion from pancreatic α-cells (23, 24). Pathophysiological glucagon action is most clearly demonstrated in conditions of insulin deficiency (25–27). "Insulin lack" results in severe hyperglycemia and hyperketonemia only if glucagon is present (25). Furthermore, knockout of the glucagon receptor attenuates hyperglycemia and hyperketonemia following β-cell ablation in mice (26, 27).

Deviations in ATP synthesis and/or utilization are observable in ordinary physiology (16, 28–30), pathophysiology (16, 31, 32), and pharmacological intervention (33, 34) in the liver. Hepatic glucagon signaling decreases energy availability (16), despite increasing substrate uptake and utilization (11). This likely stems from the energetic requirement of pathways and processes that support gluconeogenesis in the liver. Pathological glucagon action may contribute to the acceleration in TCA cycle flux, gluconeogenesis, aberrations in oxidation (35), and elevation in the AMP/ATP observed in high-fat feeding (16).

In subsequent sections, substrate flux in and out of the TCA cycle will be evaluated in the context of the current understanding of hepatic signaling mechanisms. The dissertation is structured around physiological and pathophysiological energy stress in the liver. Reductions in ATP and/or increases in AMP are hallmark indices of cellular energy stress. AMP-activated protein kinase (AMPK) serves as the linchpin because glucagon signaling increases the AMP/ATP ratio and drives AMPK activation (16, 36). Glucagon action on macronutrient flux overlaps with AMPK's signaling repertoire (37). Extrapolating from this observation, it is our conjecture that glucagon exerts control over macronutrient flux through AMPK.

## Hepatic Energy State Regulates AMPK Activation

Changes in the AMP/ATP ratio reflect a shift in the balance between ATP production and consumption (38). Adenylate kinase maintains the equilibrium of the adenine nucleotide pool (**Fig. 1.2**). An acute increase in ATP demand results in the generation of ADP. Adenylate kinase senses the imbalance and, to restore equilibrium, drives the reaction toward the production of ATP and AMP. Thus, AMP increases relative to ADP and ATP. A linear increase in the ADP/ATP ratio results in an exponential increase in the AMP/ATP ratio (**Fig. 1.2**).

The importance of ATP requires little explanation, as it is the common currency for the vast majority of energy-consuming reactions in the cell and is a requirement for many kinase reactions. AMP regulation of enzyme activity has been recognized for decades (39, 40). In fact, the cell works to keep ATP high and the AMP/ATP ratio low. Mitochondria are adapted to convert ADP to ATP from the reducing cofactors NADH and $FADH_2$. In some cell types, specialized high-energy phosphate stores rapidly provide energy and protect against changes in ATP. For example, exercise can cause a significant reduction in intramuscular phosphocreatine while ATP levels remain unchanged; in these studies, the AMP/ATP ratio was estimated to be very high despite no observable fall in ATP (41).

Cells may even sacrifice the size of the adenylate pool to maintain energy charge. Evidence for an increase in AMP degradation has been observed in conditions when ATP demand exceeds supply (42–46). Reductions in ATP and $P_i$ can provoke the catabolism of AMP (47, 48) to preserve the relative balance between ATP, ADP, and AMP in the liver (49). Thus, buffering systems have evolved that protect both absolute and relative liver ATP levels.

AMPK extends the capabilities of this sophisticated adenylate buffering network. Rather than directly acting on adenine nucleotides, AMPK's structure is equipped to sense increases in

AMP and direct signaling pathways that control macronutrient flux (50). The heterotrimeric structure of AMPK contains an α (catalytic), β (anchoring), and a γ (nucleotide-sensing) subunit. The nucleotide binding sites in the γ-subunit are constructed from two Bateman units, each with two CBS (helix-β-hairpin-helix) sequence repeats. AMP binding to the γ-subunit makes AMPK a better substrate for its major upstream activators (LKB1 and CaMKKβ) and prevents its dephosphorylation. Once phosphorylated, AMPK activity is enhanced further by AMP activation (51).

## AMPK Signaling in the Control of Energy Producing and Biosynthetic Pathways in the Liver during Fasting and Exercise

### *AMPK Regulation of Hepatic Fat Oxidation and Lipogenesis*

The energetic advantage of fat oxidation stems from the production of NADH and $FADH_2$ through β-oxidation and the TCA cycle. NADH and $FADH_2$ are synthesized during the release of acetylCoA from the hydrocarbon chain of a fatty acid during β-oxidation. Furthermore, acetylCoA catabolism yields 3NADH and $1FADH_2$ in the TCA cycle. The fate of acetylCoA is largely determined by the physiological condition of the liver. During elevated glucagon action, acetylCoA is shunted toward ketogenesis and further oxidation in the TCA cycle and away from lipogenesis (52). AcetylCoA availability does not appear to limit rates of oxidation or ketogenesis during fasting, as it serves as a metabolic node for the entry of carbon from β-oxidation, certain amino acids, and pyruvate. Thus, acetylCoA utilization in fasting and exercise occurs through the synthesis of ketone bodies and oxidation in the TCA cycle.

AMPK may coordinate fatty acid flux into the mitochondria for β-oxidation and ketogenesis during glucagon action (**Fig. 1.3**). MalonylCoA directly inhibits the activity of carnitine palmitoyltransferase I (CPT1) and prevents the initial entry of long-chain fatty acids into the mitochondria for β-oxidation (53, 54). Formation of malonylCoA results from the carboxylation of acetylCoA by acetylCoA carboxylase (ACC) (55). ACC activity is under the biphasic, hormonal control of insulin and glucagon. Insulin potently stimulates while glucagon inhibits ACC activity. AMPK is activated by glucagon in the liver, which inversely corresponds to ACC activity (56). In fact, AMPK's inhibitory effect on ACC was deduced from studies investigating the relationship between glucagon, PKA, and ACC inhibition (57, 58).

The inverse relationship between AMPK and ACC activities may explain aspects of metabolic zonation in the liver. Periportal parenchyma have elevated capacity for gluconeogenesis, ureagenesis, β-oxidation and ketogenesis; these functions correspond to hormonal (e.g. glucagon) and substrate gradients in the liver (59). In the fasted state, AMPK activity is elevated predominantly in the periportal zone and corresponds to reduced ACC activity (60). This is consistent with glucagon concentrations being highest in the periportal region of the liver. As noted above, glucagon promotes fat oxidation in the liver (61). Moreover, high intensity exercise results in reductions in ACC activity, malonylCoA concentrations, increased 3-hydroxybutyrate and AMPK activation (62).

Activation of AMPK may acutely suppress lipid biogenesis and promote fat oxidation in the liver by attenuating the ability of ACC to generate malonylCoA, thus lessening CPT1 suppression. Elevated fatty acid flux at the liver increases the AMP/ATP ratio when coupled with anaplerotic substrate (63), which may contribute to AMPK activation and ACC inhibition. Elevated fatty acids alone—independent of glucagon action—decrease malonylCoA

concentrations (64) and activate AMPK (65). Some evidence suggests that certain fatty acids alter AMPK's conformation and make it a better target for its upstream activator, LKB1 (65). These observations imply multiple mechanisms for the activation AMPK and the inhibition of ACC in the control of fat oxidation and lipogenesis in the liver. Moreover, glucagon represses the expression of SREBP-1c (66), a controller of lipogenesis in the liver. Elegant work with AMPK activators demonstrates that AMPK phosphorylates and reduces SREBP activity (67). It is possible that glucagon, through AMPK activation, might also inhibit SREBP activity (68). Indeed, a block in lipogenesis in fasting is a major determinant of ketogenesis in the liver (69, 70) and, accordingly, the overexpression of hepatic AMPK increases circulating ketones (71).

***AMPK and Amino Acid Utilization in the Liver***

Glucagon is a major hormonal driver of amino acid metabolism in the liver, stimulating the uptake and utilization of specific amino acids and inhibiting signaling pathways that promote protein synthesis (11, 72, 73). Additionally, glucagon potently stimulates autophagy and proteolysis(13, 74, 75). The net effect of these processes would appear to be an increase in amino acid availability for anaplerosis, oxidation, and—potentially—gluconeogenesis.

Mechanistically, glucagon's effects on the aforementioned processes may be mediated by AMPK activation (73). AMPK controls the activity of major hubs of protein synthesis and authophagy—mTORC1 and Ulk1. Glucagon markedly increases AMPK activation while decreasing mTORC1 signaling to 4E-BP1 and S6K1 (73). During periods of elevated glucagon, insulin (an mTORC1 activator) is unable to deactivate AMPK or fully restore mTORC1 signaling (76). Other factors that increase the intrahepatic AMP/ATP ratio or activate AMPK have a similar impact on mTORC1 signaling and protein synthesis (77). Extensive signaling

work has identified at least two sites where AMPK intercedes in the mTORC1 signaling pathway: TSC2 (78) and raptor (79). In both cases, phosphorylation by AMPK leads to a reduction in mTORC1 signaling (**Fig. 1.4**).

Recent research demonstrates that AMPK promotes autophagy during glucose deprivation by activating Ulk1, which is also negatively regulated by mTORC1 (80, 81). The physiological relevance of AMPK, Ulk1, and autophagy in the availability of amino acids for anaplerosis is unresolved. Using an autophagy-deficient mouse model, it was recently demonstrated that amino acids released through autophagy may contribute to gluconeogenesis (15). Glucagon's effects on protein synthesis and degradation align with the effects of AMPK activation. The possibility clearly exists that AMPK facilitates amino acid catabolism during glucagon-mediated uptake and autophagy in the liver.

## A Brief Discussion on the Importance of Carnitine in Mitochondrial Substrate Trafficking and Utilization

The research groups spearheaded by CB Newgard and DM Muoio have utilized the power of metabolomics to investigate the relationship between mitochondrial substrate trafficking in insulin resistant states (82–84). Their research has made substantive contributions to the hypothesis of metabolic overload in overnutrition (84), particularly in skeletal muscle. More importantly, perhaps, this work has emphasized the importance of understanding substrate trafficking in conditions with aberrant signaling, oxidation, and/or nutrient load.

Long-chain fatty acylCoAs are converted to fatty acylcarnitines (CPT1) for transport from the cytosol into the mitochondria. Located on the inner mitochondrial membrane, CPT2 converts acylcarnitines back to their CoA esters for oxidation. This process is particularly

relevant for the acute regulation of fat oxidation by AMPK (**Fig. 1.3**). Furthermore, medium and shorter chain acylcarnitines are generated from their antecedent acylCoA species through carnitine acyltransferases in subcellular organelles (primarily mitochondria) (85, 86). The formation of acylcarnitines from CoA esters can range from long to very short (i.e. acetylCoA→acetylcarnitine, C2). Shorter, odd chain carnitine species (C3 and C5) derive primarily from amino acid catabolism whereas C4 (butyrylcarnitine) may be generated from fatty and amino acid catabolism (85). The metabolic origin of certain stereoisomeric/isobaric carnitine species can be elucidated through LC/tandem-MS. For example, C4-OH carnitine can be generated from L-3-hydroxybutyrate ($_{D\text{-}C4}$-OH-carnitine), $_{L}$-3-hydroxybutyrylCoA ($_{L}$-C4-OH-carnitine) or $_{L}$-3-hydroxyisobutyrylCoA ($_{L}$-isoC4-OH-carnitine) (87).

Certain genetic and nutritional states may also generate an "overloaded"-like condition in the liver. As discussed briefly in the subsequent section, genetic inactivation of VHL impairs respiration, hepatic glucose production, and elevates short-even chain acylcarnitines (88). Chronic overnutrition increases TCA cycle flux, short-even/odd and long chain acylcarnitines, and distorts mitochondrial function in the liver (35). Though these conditions are drastically different, the quantity of available substrate may exceed its rate of removal by the TCA cycle.

## Lessons from Genetic Models Concerning the Coupling of Substrate Utilization with Gluconeogenesis

A relationship between oxidative metabolism and glucose production has been observed for decades (63, 89–93). Glucagon stimulates fat utilization in the liver to support gluconeogenesis and ketogenesis (11, 52). In the absence of changes in insulin and glucagon, an elevation in circulating fatty acids is sufficient to stimulate an increment in gluconeogenesis (94,

95). The delivery of agents that impede CPT1-mediated fatty acid transport and, consequently, β-oxidation abrogate the effects of fatty acids on gluconeogenesis (96, 97). The metabolic products of oxidation are long proposed regulators of gluconeogenic reactions (98). Multiple control mechanisms are in place to accelerate or throttle flux through oxidative, anaplerotic, and cataplerotic pathways during changes in substrate availability and demand (99–102).

The Burgess group at UTSW has implemented state-of-the-art tracer technologies in genetic mouse models to investigate the coupling of metabolic fluxes in the liver. Phosphoenolpyruvate carboxykinase (PEPCK) links TCA cycle flux with gluconeogenesis by converting oxaloacetate to phosphoenolpyruvate (PEP). Unless returned to the TCA cycle through pyruvate (103), PEP undergoes a series of chemical conversions to yield glucose (**Fig.1.1**). Elimination of liver cytosolic PEPCK (PEPCK) and, consequently, a major cataplerotic flux from the TCA cycle results in severe aberrations in oxidative metabolism. Despite a compensatory increase in enzymes that control fat oxidation and the TCA cycle, liver PEPCK deletion causes marked steatosis, a decrease in ketones, and an increase in circulating alanine and fatty acids (104). These changes in metabolites are symptomatic of severe decreases in oxidative metabolism as evidenced by the 10-fold reduction in TCA cycle flux, a more reduced mitochondrial status, and impaired oxygen consumption; as expected, gluconeogenic glucose production from PEP is virtually abolished from the livers of PEPCK knockout mice (105). To a degree, these studies corroborate results obtained through acute, pharmacological PEPCK inhibition *in vivo* (106). Without PEPCK, in fact, glucagon does not exert its depletive effect on liver energy state (16).

The reciprocal question—does impaired oxidative metabolism impinge on cataplerosis-linked gluconeogenesis—was approached with similar methods in mice lacking PGC1α. In this

regard, PGC1α-deficient livers are useful because they exhibit an ordinary fasting-mediated increase in key enzymes for gluconeogenesis but a decrease in those that control the TCA cycle and OXPHOS (107). Whole-body deletion of PGC1α induces liver steatosis, impairs hepatocyte fat oxidation and increases triglyceride synthesis (108). Elegant studies in the perfused liver demonstrate that reduced rates of TCA cycle flux, $O_2$ consumption, β-oxidation, cataplerosis, and pyruvate cycling correspond to a drop in gluconeogenesis from PEP. The deficit in substrate utilization imposed by PGC1α deletion is coupled to trend toward a reduction in ATP and ADP (107). In effect, these studies provide evidence that impairments in gluconeogenic flux to glucose and substrate utilization can result from a primary deficit in oxidative capacity.

Nutrient utilization requires the coordination of neurohormonal inputs with enzymatic and transcriptional activity in the liver. The peroxisome proliferator-activated receptor α (PPARα) regulates the expression of a multitude of enzymes involved in multiple loci of lipid handling in the liver (109). PPARα-/- mice exhibit similar impairments in indices of hepatic metabolism as PGC1α-/- mice. Fasting results in hypoglycemia and hypoketonemia with marked lipid accumulation in the liver (110, 111). Glucagon, which upregulates PPARα expression, fails to acutely stimulate fat oxidation in PPARα-/- hepatocytes (21). Global metabolomics reveals that impairments in oxidation associate with altered substrate selection in PPARα-/- mice (85).

The resemblance between these genetic models and features of the hepatic response to "signaling-hypoxia" are unmistakable. von Hippel-Lindau protein (VHL) directs the hypoxia-inducible factors 1, 2, and 3α for degradation under normoxia (112). VHL deficiency results in hepatic steatosis, impairments in ketogenesis, respiration, and glucose production (112, 113). Accordingly, PPARα target and PGC1α gene expression reduce with VHL deficiency in the liver (112).

These models emphasize the intricate relationship between substrate availability, utilization, and glucose production in the liver. Cataplerosis-linked gluconeogenesis is attenuated by impairments in oxidative metabolism. Reciprocally, anaplerosis and oxidation are limited by defects in cataplerotic flux to PEP. Thus, reactions of the pyruvate and TCA cycles yoke anaplerosis and fat oxidation with gluconeogenic glucose production in the liver (114). The synchronization of these events is visible in physiology during fasting and exercise, when substrate supply and utilization fuel gluconeogenesis.

## An Overlap in Energy Sensor Function and Challenges that Arise from the Use of Pharmacological AMPK Activators

Physiological conditions with sustained or elevated glucagon action result in the uptake and utilization of substrates in the liver. Despite this surplus of oxidizable substrate, a decrease in the AMP/ATP ratio and an increase in AMPK activation are observable (28, 115). Thus, it is unsurprising that absolute and relative NAD+ and NADH levels might also fluctuate during acute, physiological energy stress (116, 117). As discussed, AMPK responds to an increase in the AMP/ATP ratio by controlling signaling pathways that regulate ATP consumption and synthesis. Sirtuins (Sirts), which require NAD+ as a substrate, act on a range of targets that influence hepatic metabolism (117). Sirt1shares a degree of overlap with AMPK signaling and function (117). Increases in the expression and activity of Sirts1 and 3 and AMPK activation may be observable under similar pharmacological, nutritional, and hormonal states (16, 116–119). The outcome of crosstalk between both systems appears to be the protection of energy status by modulating catabolic and anabolic signaling networks (117).

A number of models have been proposed to explain the congruence between AMPK and Sirt1 function. Some propose that AMPK stimulates Sirt1 activity through a NAMPT (120) or β-oxidation dependent (121) mechanism. Many of the metabolic benefits of resveratrol—a compound that targets Sirt1—appear to be dependent on the presence of AMPK *in vivo* (122). The mechanisms that substantiate this relationship require further investigation. For example, AMPK's acute effect on transport-mediated β-oxidation would appear to promote the production of NADH from NAD+ (**Fig. 1.3**). Moreover, AMPK supports glucose uptake in the muscle during contraction, presumably to sustain the ATP pool (123). The relationship between AMPK and Sirt1 is further complicated by studies demonstrating that Sirt1 promotes AMPK activation (124). Much work still remains in elucidating the relationships between the aforementioned enzymes in different physiological states, organs and cellular compartments. Furthermore, a complete description of these complex interactions is well beyond the scope of this dissertation.

***Pharmacological AMPK Activators—the " Known Unknowns"***

There are limitations in the investigation of energy sensors in metabolism using non-specific pharmacological activators (4, 34, 122, 125–128). Biguanides—such as metformin—which inhibit respiratory complex I (128) and glucagon signaling (4), may exert opposing effects on AMPK and Sirt activity. Inhibitors of respiration may decrease NADH and $FADH_2$ oxidation and, consequently, impair ATP synthesis. Indeed, metformin impairs respiration and increases the NADH/NAD+ (Lact/Pyr and 3-OH/AcAc) (125) and AMP/ATP ratio in hepatocytes (34). One might hypothesize an inverse relationship between Sirt and AMPK activity in these conditions—the former low and the latter high. However, dose-dependent and compartmental effects of these pharmacological agents may obscure their mechanisms of action.

Many of the effects of AICAR resemble those of biguanides. For example, AICAR reduces hepatic ATP and alters the adenine nucleotide pool (33, 34) and inhibits respiration (127). Metformin and AICAR exert control over nucleotide sensitive pathways through the aforementioned mechanisms. The conversion of AICAR to ZMP requires ATP (129). ZMP mimics the effects of AMP, which triggers allosteric AMPK activation and phosphorylation (130). Thus, to borrow a phrase from former US Secretary of Defense Donald Rumsfeld, "there are known unknowns—that is to say we know there are some things we do not know" concerning the AMPK-dependent and independent effects of AICAR and metformin on metabolism. Defining these relationships poses a significant challenge (4, 34), when one considers the breadth of enzymes that require ATP for catalysis or are adenine-nucleotide responsive (e.g. Phosphofructokinase (131), Fructose-1,6-bisphosphatase(39), and Glycogen Phosphorylase (132)).

Metformin is used globally to treat type II diabetes. The current diabetes and obesity epidemic make a mechanistic understanding of the effects of antidiabetic compounds imperative. As AMPK activators, AICAR and metformin actions are generally associated with AMPK activation and signaling (133–138).

## AMPK Activation is a Component of Exercise-Mediated Reversal of Fatty Liver

Fatty liver is a condition of excessive lipid infiltration in the liver (>5%) and closely associates with the features of metabolic syndrome (139, 140). Fatty liver is present in 50-60% of T2DM patients, yet fatty liver does not present easily identifiable symptoms (139). Fatty acids in their "free," unesterified or CoA derivatives may exert lipotoxic effects in the liver (141). The mechanisms linking fatty acids with liver injury are extensive (142). Elevated fatty acid β-

oxidation is a proposed component of pathological oxidative stress (142). However, fatty acids may accelerate TCA cycle flux and stimulate ROS formation independent of their entry into the mitochondria (101).Though liver lipid accumulation coincides with metabolic stress, the formation of inert triglycerides may protect the liver from the lipotoxic effects of fatty acids (143, 144).

Obesity drastically alters hepatic metabolic flux in humans and rodents. *de novo lipogenesis* becomes a larger contributor to triglycerides secreted by the liver (145). Recent *in vivo* flux studies performed in humans (146) and rodents (35) have profoundly contributed to a modern understanding of hepatic metabolism in states of overnutrition. An increase in free fatty acid turnover in fatty liver corresponds to conditions with elevated anaplerosis, TCA cycle flux, and gluconeogenesis (146). The metabolic dysregulation caused by high-fat feeding disrupts the coupling of ATP production with $O_2$ consumption (mitochondrial efficiency) in liver mitochondria (35). To compensate, increased rates of TCA cycling may generate enough $NADH/FADH_2$ to increase the NADH/NAD+ ratio (147). The elevation in oxidative metabolism may provide for increased electron deposition in an inefficient electron transport system (35).

High-fat feeding in rodents results in a pathological increase in the hepatic AMP/ATP ratio (16); likewise, aberrations in ATP homeostasis are observable in diabetes (31) and NASH (32) in humans. Exercise intervention improves indices of "hepatic health", alters liver lipid composition and signaling, and/or reduces liver adiposity (36, 148–153). Exercise modalities permit acute and chronic intervention strategies. For example, acute intervention (7days, 85% max HR, 60min in duration) increases liver polyunsaturation and circulating HMW adiponectin (149). Chronic, voluntary exercise reduces hepatic triglycerides and activates AMPK (36). Moreover, early intervention in the development of fatty liver prevents liver triglyceride

accumulation, steatosis, and improves mitochondrial fat processing (151, 154). The physiological effects of exercise training closely associate with an anti-lipogenic, pro-oxidative program in the liver (151, 154).

AMPK's putative role in hepatic fat metabolism (**Fig. 1.3**) may link exercise intervention with the amelioration of fatty liver. Hepatic AMPK is activated in conditions where whole-body nutrient demand and substrate processing in the liver increase. Extra-hepatic nutrient demand provides an outlet for accelerated glucose and associated fluxes in the liver. In this setting, AMPK may route fatty acids and, consequently, acetylCoA toward oxidation and ketogenesis and reduce triglyceride assembly, fatty acid and cholesterol biosynthesis. Thus, AMPK may work to utilize circulating lipids and reduce intrahepatic fat stores to accommodate the energetic demands of exercise, thereby reducing fatty liver.

## AMPK and Hepatic Glucose Production: "A Mystery Inside an Enigma"

The role of AMPK signaling in control of glucose release from the liver can be paraphrased by the words of Sir Winston Churchill. It is a mystery inside an enigma. The results obtained in transgenic and mutant mice are contrary to what one might expect from physiological observations. Hepatic LKB1 deletion causes hyperglycemia and glucose intolerance (137). Likewise, liver-specific AMPKα2 deletion results in glucose intolerance, albeit to a lesser degree than $LKB1^{-/-}$ mice (155). Moreover, overexpression of AMPKα2 in the liver decreases fasting and fed glucose levels and the transcripts encoding the PEPCK and G6Pase enzymes (71). The phenotype of these genetic models would suggest that endocrine mediated activation of AMPK (e.g. glucagon) would result in reduced hepatic glucose production. The enigma is that AMPK is activated in physiology at times when glucose production is high.

Mechanistically, glucagon stimulates the gluconeogenic program in a PKA dependent manner. PKA phosphorylates CREB (156, 157) which upregulates PGC-1α. PGC-1α, in turn, acts to increase the expression of gluconeogenic enzymes (158, 159) and glucose production in hepatocytes (159). PGC-1α's ability to co-activate gluconeogenic gene expression is lost in the absence of hepatocyte nuclear factor 4α (HNF4α) (160). Likewise, PGC-1α co-activates FOXO1 which augments gluconeogenic gene expression in FAO cells (161). AMPK disrupts HNF4α activity through phosphorylation(162) and AICAR-mediated activation of AMPK coincides with reductions in HNF4α protein levels and target gene expression (**Fig. 1.5**) (163). Liver-specific knockout of PGC-1α attenuates fasting-mediated increases in gene expression for the PEPCK and G6Pase enzymes (164). However, livers from PGC-1α-null mice have impaired gluconeogenic glucose production from PEP, despite normal fasting levels of the aforementioned transcripts (107).

CRTC2 (TORC2), a transcriptional co-activator of CREB, could also function as a regulatory point between glucagon, insulin, LKB1, and AMPK signaling in gluconeogenesis (165, 166). While glucagon and forskolin promote CREB-CRTC2 mediated upregulation of gluconeogenic gene transcription, AMPK phosphorylation sequesters CRTC2 in the cytoplasm which reduces its activity (**Fig. 1.5)** (166). Hepatic deletion of LKB1 and AMPK decreases CRTC2 phosphorylation (34, 137). The absence of hepatic CRTC2 results in reductions in gluconeogenic gene expression during fasting. CRTC2-null hepatocytes have impaired glucagon-stimulated glucose production (167).

Recent studies explore a role for Class IIa HDACs and FOXO in glucagon-stimulated gluconeogenesis (168, 169). In response to glucagon, Class IIa HDACs translocate into the nucleus, recruit HDAC3, and promote FOXO-dependent gene transcription of gluconeogenic

targets. LKB1-dependent kinases (e.g. AMPK) phosphorylate and inactivate Class IIa HDACs (HDACs 4/5/7). Interestingly, treatment of hepatocytes with glucagon reduces phosphorylation of HDACs4/5/7 at the sites of LKB1-dependent kinase action. shRNAs targeting these HDACs improve glucose tolerance in *db/db*, *ob/ob*, and high fat fed mice. By increasing the nuclear entry of these HDACS, glucagon could promote, at least in part, FOXO dependent-gluconeogenic gene transcription—another avenue of intervention for glucagon and potentially AMPK in hepatic glucose production (168).

These genetic models and mechanistic data support a regulatory role for AMPK in hepatic glucose production. However, the results obtained with these genetic models do not, in fact, uniformly predict the metabolic response of the liver to the hormones or conditions that regulate the activity of AMPK under physiological conditions. As described earlier, glucagon plays an integral role in maintaining glucose homeostasis by sustaining glucose production during the adaptive response to fasting and exercise. Paradoxically, a genetic increase in AMPK activity in the liver results in an inhibition, and not an increase, in glucose release from the liver (71).

Recent work in liver AMPKα1α2/LKB1 knockout models reveal that the glucose lowering effects of metformin and adiponectin might be AMPK independent (4, 34, 170, 171). Interestingly, mice lacking liver AMPKα1α2 have similar fasting and fed blood glucose levels as WT mice (34). Germline removal of the AMPKβ1 subunit results in significant impairments in hepatic AMPKα1α2 activity (172). Despite elevations in basal gluconeogenic gene transcription, hepatocytes isolated from these mice exhibit normal basal glucose production and similar reductions in glucose output versus control mice when stimulated with the AMPK activators A769662 and AICAR (173). The potential overlap in signaling and function between AMPK and

other LKB1-dependent kinases further complicates data interpretation from *in vivo* and *in vitro* models of AMPK activation or deletion (174). For example, overexpression of salt-inducible kinases (SIK) 1 and 2 reduces fasting glucose levels and gluconeogenic gene expression (166). Moreover, both impair CRTC2 activity by promoting its phosphorylation at S171 and sequestration in the cytoplasm (165, 166, 175).

At present, the results in the literature do not produce sufficient consensus to assign a definitive role for hepatic AMPK in glucose production. Investigators have often made the assumption that changes in gene expression are equivalent to changes in hepatic glucose flux. This is not necessarily true, as mRNA levels of key gluconeogenic enzymes can be poor surrogates for gluconeogenic flux. This is best illustrated by experiments using perfused livers from 24hr fasted mice with graded reductions in PEPCK content (114). Isotopic tracers were used to determine hepatic glucose and TCA cycle fluxes. Metabolic flux analysis of this data indicates that PEPCK has a rather low control coefficient (0.18) for gluconeogenesis from the TCA cycle (114). Although these studies are confined to a very specific set of circumstances (i.e. perfused livers from long-term fasted mice), they do emphasize the need to be cautious when ascribing changes in gene and protein expression to changes in flux.

## Convergence of AMPK and Insulin Signaling Pathways in the Liver

The balance between anabolism and catabolism must be tightly regulated in an organ as dynamic as the liver. Insulin stimulates the synthesis of protein, lipids, and glycogen. By reducing hepatic glucose output, insulin maintains euglycemia during feeding. Insulin and AMPK signaling pathways overlap at key signaling loci to maintain organ homeostasis. An imbalance in insulin and AMPK signaling compromises fuel fluxes and is observable in several

metabolic stresses (diabetes, obesity, under-nutrition). Components of the insulin signaling pathway and AMPK signaling will be briefly juxtaposed to provide a broad perspective of how endocrine inputs may regulate central metabolic processes in the liver.

***Direct Regulation***

Insulin signaling has been shown to reduce AMPK activity in the liver (176). There is evidence that Akt/PKB-mediated phosphorylation of AMPK ($\alpha$1Ser$^{485/}$$\alpha$2Ser$^{491}$) results in a decrease in AMPK-Thr$^{172}$ phosphorylation following insulin pre-treatment (177). Interestingly, AMPK Ser$^{485}$ phosphorylation is elevated while AMPK-Thr$^{172}$ phosphorylation remains unaltered during hyperinsulinemic clamps in the dog—an effect reversed by glucagon, hypoglycemia, or both (178). A direct relationship between Akt phosphorylation and inhibition of AMPK has been further substantiated recently (Hawley et al., 2014 *Biochem J*).

***mTORC1***

mTORC1, a central controller of growth, is activated by insulin, growth factors, and nutrients with the result that translation is increased. Insulin promotes mTORC1 signaling by inhibiting TSC1/TSC2 complex activity, an endogenous mTORC1 repressor (179). During low nutrient availability, however, increases in AMPK activity reduce mTORC1 signaling by promoting TSC1/TSC2 activity and raptor dissociation from mTOR—as previously described. The reciprocity of insulin and AMPK signaling creates sensitive regulation of protein anabolism/catabolism in the liver. As noted, glucagon increases AMPK activation and has been shown to dominantly repress mTORC1 in hepatocytes exposed to both hormones (76).

***Glucose and Lipid Metabolism***

There has been considerable research on the acute and chronic action of insulin and AMPK on hepatic glucose production. Insulin and AMPK share mutual and also use exclusive signaling pathways to reduce the expression of gluconeogenic enzymes. AMPK and related kinases have been suggested to regulate hepatic glucose production through the inhibition of CRTC2 (166), regulation of SHP (180), and, more recently, inhibition of Class IIa HDACs (168). Insulin has been shown to also obstruct a functional CREB-CRTC2-CBP/p300 complex, thus decreasing gluconeogenic gene upregulation (156). Insulin inhibits CRTC2 activity through the activation of SIK2—which, phosphorylates and promotes CRTC2 degradation (165). Insulin also inhibits gluconeogenic gene expression (181) by excluding FOXO1 from the nucleus (182, 183) and by suppressing PGC-1α's impact on gluconeogenic genes (161, 184).

Lipid metabolism and synthesis highlight another juxtaposition of insulin and AMPK action in the liver. As previously discussed, several lines of evidence suggest that AMPK acutely and chronically suppresses lipid biogenesis while promoting fat oxidation. Through increases in cAMP, glucagon and epinephrine activate AMPK, which rapidly inactivates ACC in the liver. On the other hand, insulin decreases AMPK activity (176) while increasing ACC activity (176, 185). The precise mechanism for insulin-mediated activation of ACC remains unresolved (55) but could be due to both covalent and allosteric modifications.

Transcriptional regulation of pro-lipogenic genes by AMPK and insulin converge on SREBP-1c. As mentioned, glucagon (66) and AMPK (67) work to reduce SREBP-1c expression and activity. Thus, intermittent glucagon-stimulated activation of AMPK such as that seen during regular exercise (36) could generate a pro-oxidative, anti-lipogenic tone in the liver through the activation of PPARα and the inhibition of mTORC1 and SREBP-1c. In contrast, insulin plus

glucose increase *Srebf1c* transcription and the expression of target genes (66, 186). Insulin mediated-control of hepatic lipogenesis has focused on SREBP-1c in the normal and insulin-resistant states (22). Recent work demonstrates that insulin works through mTORC1 dependent and independent mechanisms to promote hepatic lipogenesis (186–188).

## AMPK at the Helm in the Coordinate Control of Metabolic Flux and Energy Production in the Liver

Fasting and exercise generate an AMPK activating state in the liver (16, 28–30, 36, 62, 115). In these conditions, hormone-supported nutrient uptake and utilization in the liver sustains hepatic glucose production. A reduction in insulin and increase in adrenergic tone promotes lipolysis in adipose tissue and liberates amino acids from the muscle. Furthermore, lactate and glycerol are utilized for gluconeogenesis. Glucagon plays an indispensable role in substrate uptake and utilization in the liver (5), although it does not substantially contribute to the availability of substrate in the plasma (11). Liver PEPCK deletion impairs glucagon's ability to discharge hepatic energy state and activate AMPK (16). Without PEPCK, in fact, reduction in the liver is high and TCA cycle flux, anaplerosis, ketogenesis (107), and AMPK activation are low (16).

Several molecular signaling mechanisms support a role for AMPK in coordinating the effects of glucagon on metabolic flux in the liver. Glucagon supports fatty acid utilization by promoting flux through CPT1; specifically, glucagon reduces the inhibition of CPT1 by malonylCoA (52). Fatty acid transport into the mitochondria is coupled with an energetic state that inhibits lipogenesis and supports ketogenesis. β-oxidation appears coupled with anaplerosis and, consequently, cataplerosis-linked gluconeogenesis (35, 105, 107). Furthermore, glucagon

regulates SREBP-1c activity (66, 189) and, thus, may reduce the liver's lipogenic capacity. An extensive overlap exists in the regulatory control of hepatic metabolism by glucagon and AMPK (**Table 1.1**).

**Table 1.1**

**The putative effect of AMPK activity on mediators of metabolism in the liver**

1) *AMPK phosphorylates and inhibits ACC activity and decreases malonylCoA concentrations* (190, 191)

2) *AMPK interferes with HMGCoAR* (192–194) *and SREBP2* (67) *activity and, thus, reduces the movement of actetylCoA/HMGCoA through the isoprenoid/cholesterol synthesis pathway*

3) *AMPK phosphorylates and inhibits SREBP activity* (67, 195)*, thereby reducing the liver's lipogenic capacity*

4) *AMPK promotes mitochondrial biogenesis and functions* (126, 127, 196)

5) *AMPK enhances TSC2 activity* (78) *and phosphorylates Raptor* (79) *to deactivate mTORC1 and inhibit protein synthesis* (73)

6) *AMPK promotes autophagy through the inhibition of mTORC1 and the activation of Ulk1* (80, 81)

The metabolic and molecular evidence suggests that AMPK acts as an arbiter of oxidative, anaplerotic and cataplerotic fluxes in the liver. However, 15+yrs of research using pharmacological AMPK activators has placed AMPK at the center of a glucoregulatory paradox (**Fig. 1.5**). The acute effect of glucose lowering agents occurs within minutes of administration (33) which corresponds to AMPK activation. Until recently, mechanisms for AMPK-mediated inhibition of glucose production have primarily been transcriptional (CRTC2, HNF4α, Class II HDACs). However, acute AMPK activation supports a signaling program that fuels, rather than inhibits, hepatic glucose production. *We hypothesize AMPK is essential for the coordinated*

*control of oxidative, anaplerotic/cataplerotic, and glucose flux in the liver but not for the inhibition of glucose production by AICAR.*

The aims of this thesis are designed to

I. *Investigate AMPK's role in the metabolic coupling of oxidation, anaplerosis/cataplerosis, energy status and hepatic glucose production in vivo*

II. *Distinguish between the AMPK-dependent and independent effects of an acute, pharmacological elevation in nucleotide monophosphate (NMP) on hepatic metabolism in vivo*

III. *Establish whether AMPK is essential for the amelioration of fatty liver in the context of exercise training*

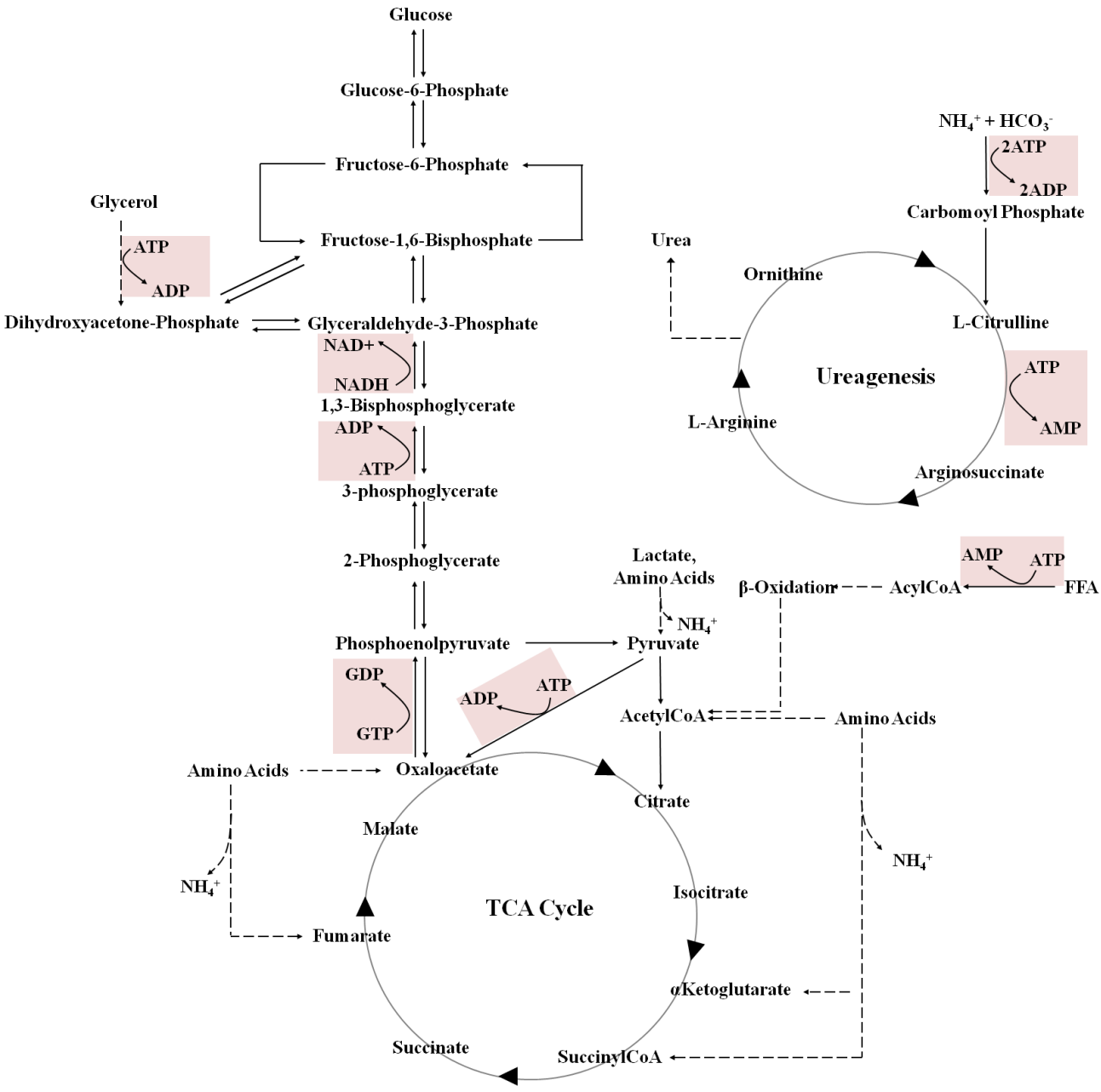


**Figure 1.1 –Energy and cofactor requiring processes associated with gluconeogenesis.** Fluxes associated with gluconeogenesis utilize ATP and reducing equivalents. In the absence of PEPCK, TCA cycle flux, anaplerosis, and ketogenesis are impaired (104, 105) and elevated glucagon action does not deplete ATP (16). *Reactions that compensate for increases in ATP demand were excluded for simplicity.*

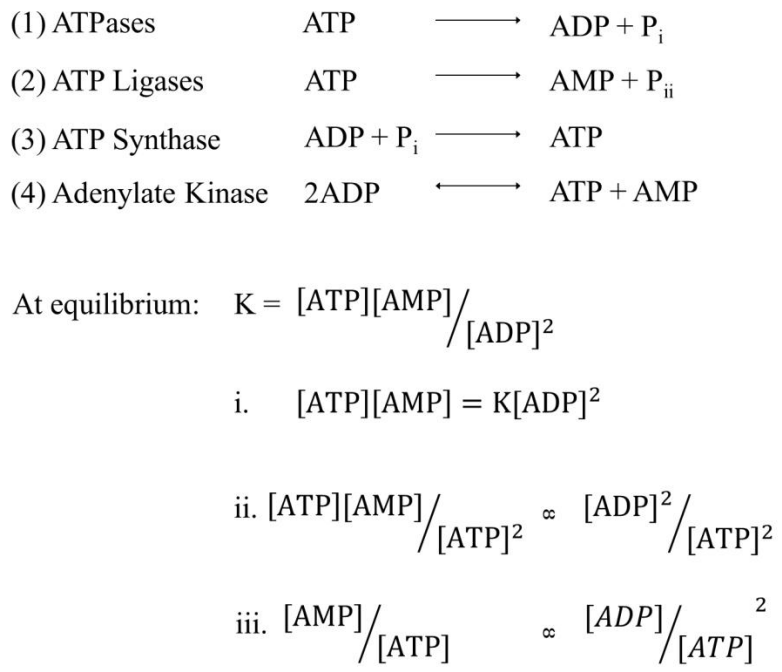


**Figure 1.2** – **Parameters regulating adenylate energy balance.** The ratio of AMP/ATP varies with the square of the ratio of ADP/ATP and, as a result, is subject to large fluctuations. In conditions where ATP demand exceeds synthesis [Rxn (1) > Rxn (3)], the adenylate kinase reaction will proceed from left to right. A subtle rise in ADP (or drop in ATP) magnifies the increase in the AMP/ATP ratio. *Adapted from* (38).

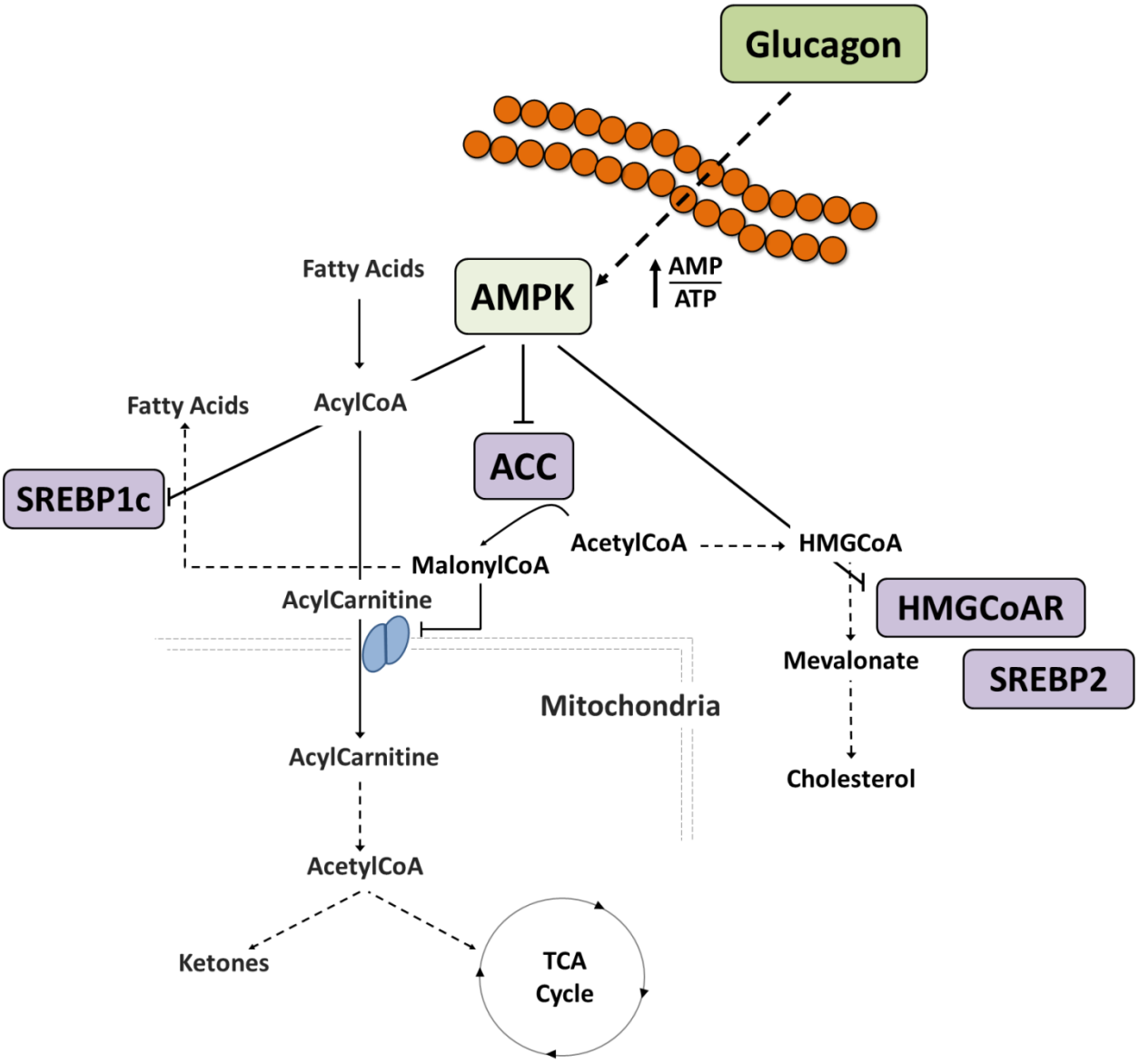


**Figure 1.3** – **Putative regulation of hepatic lipid metabolism through AMPK.** AMPK orchestrates an anti-lipogenic, pro-oxidative signaling program in the liver. Glucagon-mediated AMPK activation appears to navigate fatty acids toward oxidation and ketogenesis while inhibiting *de novo* fatty acid and cholesterol synthesis. It is acknowledged that isoform specific functions of ACC have been proposed (191) which have been consolidated here.

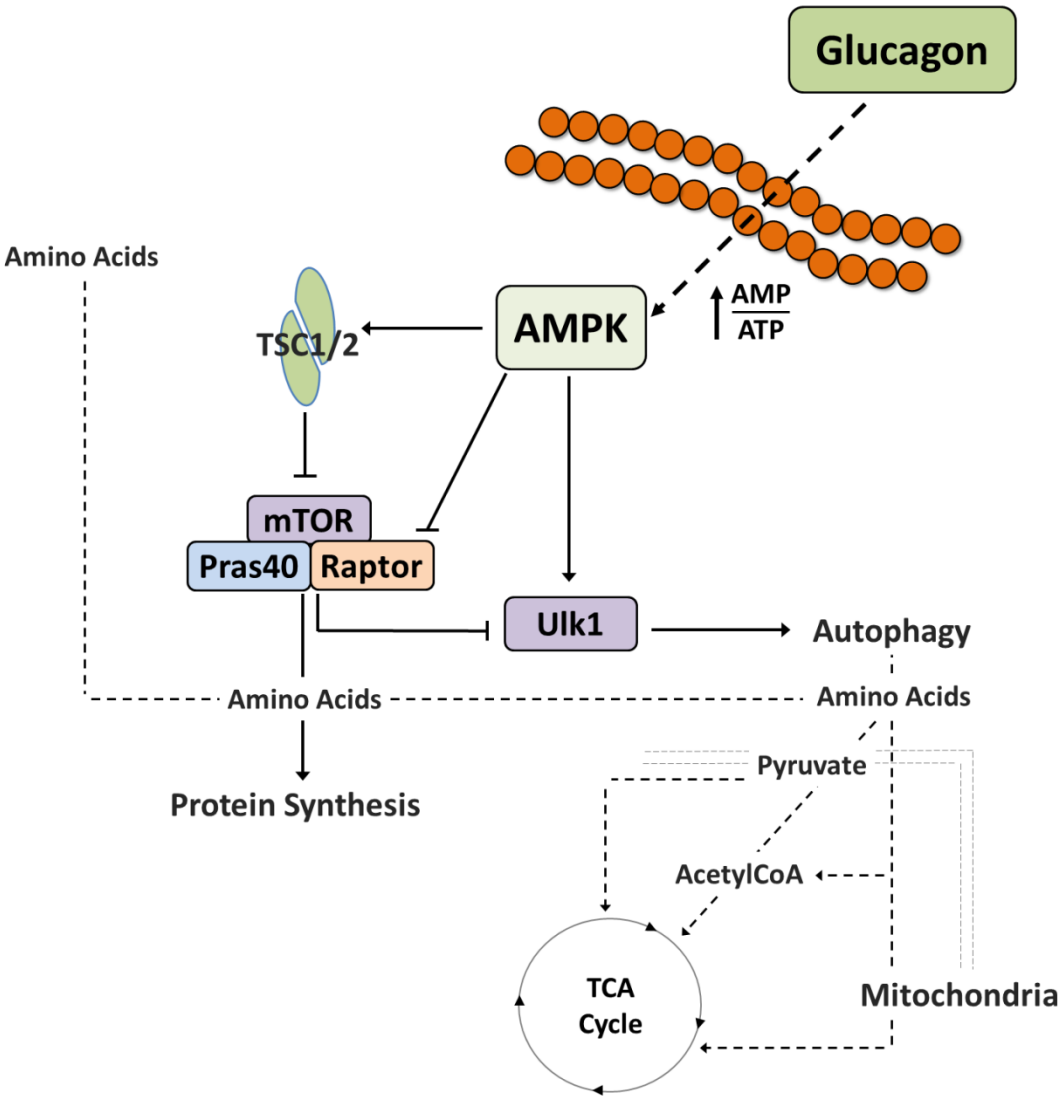


**Figure 1.4 – Putative mechanism for the role of AMPK in amino acid metabolism.** Glucagon regulates the extraction and utilization of certain amino acids. Specific amino acids are considered to be anaplerotic, as their entry into the TCA cycle results in a net provision of carbon. AMPK regulates the activity of mTORC1 and Ulk1, which may route amino acids from protein synthesis and autophagy into anaplerotic pathways.

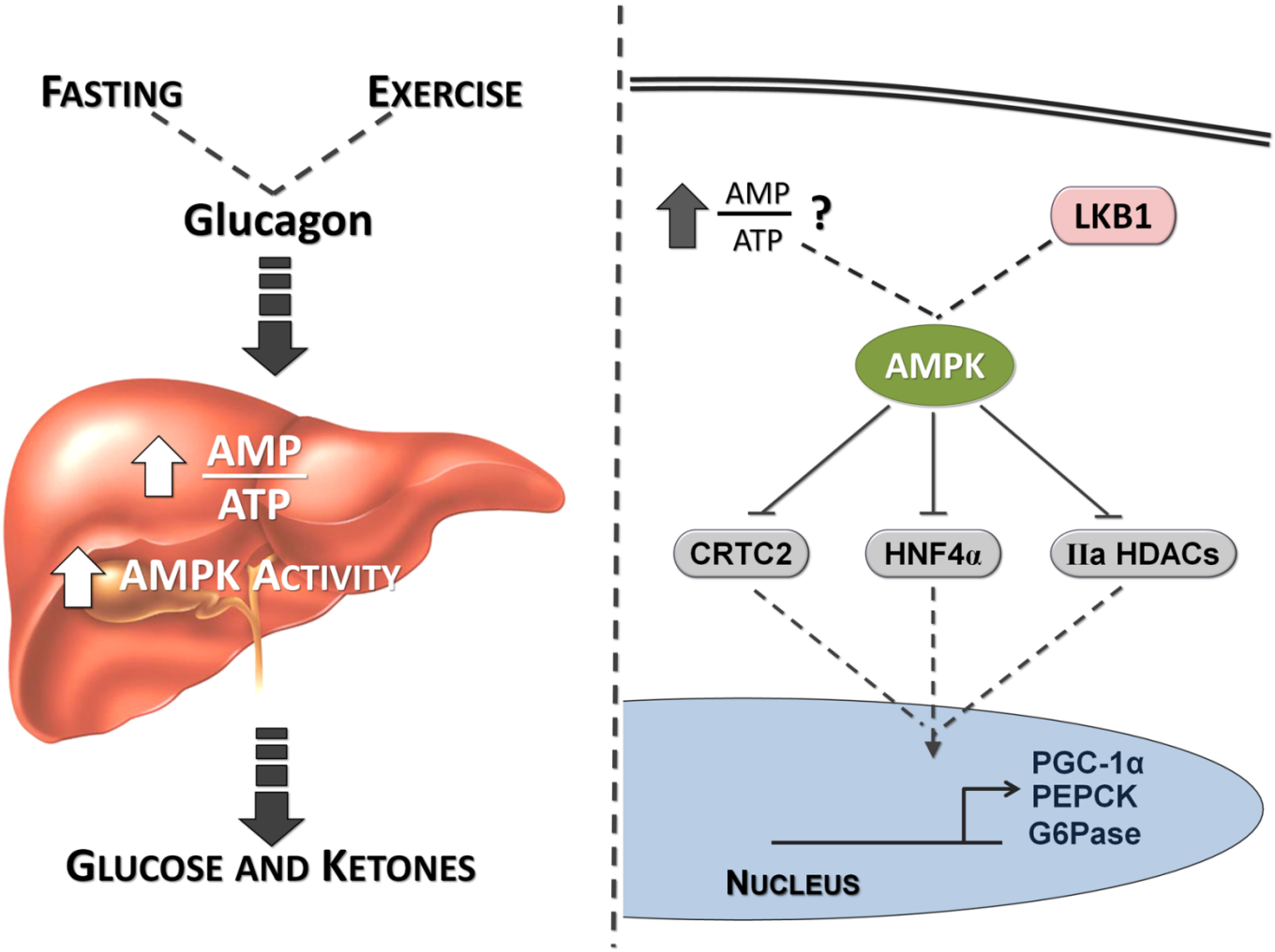


**Figure 1.5 – Paradox of AMPK activation in physiology and signaling.** AMPK activation is highest in physiological conditions characterized by an increased reliance on gluconeogenesis, ketogenesis, and ureagenesis. Acute AMPK activation would appear to route fat and amino acids toward oxidation (**Figs. 1.3, 1.4**), thus providing carbon and ATP for gluconeogenesis. However, *in vitro* studies have demonstrated that AMPK works to downregulate the transcription of gluconeogenic genes.

# Chapter II

## RESEARCH METHODS AND MATERIALS

### Mouse Models

All protocols and procedures were approved by the Vanderbilt University Animal Care and Use Committee. All mice for the studies described herein were generated on a C57Bl/6 background with loxP sites flanking the AMPKα1 and α2 ($\alpha1\alpha2^{lox/lox}$) catalytic subunits (generated by M. Foretz and B. Viollet) ±Albumin Cre Recombinase. Breeder pairs were maintained in Vanderbilt's mouse colony on breeder chow (**Table 2.1**) to generate pups for experimentation. Pups were weaned on a standard chow diet (**Table 2.1**) at 3wks of age and divided by sex. Prior to weaning, mice were individually labeled by ear punching and a small tail clip was removed for genotyping. DNA was isolated using Qiagen's DNEasy Blood and Tissue DNA isolation kit; PCR was performed using the primers listed in **Table 2.2** to verify the floxing of α1 and α2 genes in the presence or absence of Albumin Cre Recombinase. All mice were maintained on a 12:12hr light:dark cycle in a temperature (23°C) and humidity controlled environment. Mice utilized in the investigation of AMPK's role in exercise-mediated reversal of fatty liver were transferred to the Mouse Metabolic Phenotyping Center (MMPC) at Vanderbilt and were fed a high-fat diet (**Table 2.1**) at 6wks of age.

**Table 2.1** – Mouse diet macronutrient composition

| Diet | Fat (%Calories) | Carbohydrate (%Calories) | Protein (%Calories) |
|---|---|---|---|
| Chow | 13.5 | 58.0 | 28.5 |
| Breeder Chow | 25.3 | 54.9 | 19.8 |
| High Fat | 59.0 | 26.0 | 15.0 |

**Table 2.2** - PCR primer sequences for floxed AMPKα1α2 catalytic subunits and Albumin Cre

| Gene Primer | Sequence (5'- 3') | Amplicon Length |
|---|---|---|
| AMPKα1 (+) | TATTGCTGCCATTAGGCTAC | 586(WT); 682(Floxed)bp |
| AMPKα1 (-) | GACCTGACAGAATAGGATATGCCCAACCTC | |
| AMPKα2 (+) | GCTTAGCACGTTACCCTGGATGG | 200(WT); 250(Floxed)bp |
| AMPKα2 (-) | GTCTTCACTGAAATACATAGCA | |
| Cre Recombinase (+) | CCTGGAAAATGCTTCTGTCCG | 400bp |
| Cre Recombinase (-) | CAGGGTGTTATAAGCAATCCC | |

## Surgical Procedures

All equipment and surgical spaces were sterilized to generate an aseptic environment. Mice were maintained under continuous anesthesia (2% isofluorane) through a nose-cone. Hair was removed from the base of the chin to the upper abdomen for catheter insertion; the area extending from the base of the skull to the interscapular region of the back was also shaven for catheter externalization.

Sites for incisions were sterilized with alcohol and betadine. Mice were positioned on their backs and 5mm vertical, midline incisions were made cephalic to the sternum. Forceps were used to reflect the sternomastoid muscle and expose the left carotid artery. Arteries were isolated away from the vagus nerve and ligated at the cephalic end with a silk suture. An additional suture was loosely knotted at the caudal end of the artery. The caudal end was clamped and the artery was cut just below the ligated end. The catheter tip was inserted and extended to the clamp. The clamp was slowly released and the catheter was extended to the silastic-PE junction. Both ligatures were tied securely around the catheter and line patency was checked with a sampling syringe.

To insert the right jugular vein catheter, another insertion was made 5mm from the midline and 2mm caudal to the first insertion. Tissues were moved with forceps to expose the jugular vein, which was ligated at the cephalic end and loosely knotted at the caudal end with

silk suture. A cut was made below the cephalic ligature and catheters were inserted up to the restraining bead, which was secured by tightening a suture behind the bead.

Catheters were tunneled out the back of the mouse and externalized through a third incision made between the shoulder blades. Catheters were secured to stainless steel connectors on the $MASA_{tm}$. The $MASA_{tm}$ was then inserted into the incision between the shoulder blades. Nylon suture was used to close incisions. Catheters were checked using heparinized saline and mice were placed in bedded cages warmed with a heating pad. Mice were observed daily for symptoms of distress (body weight loss, abnormal grooming, etc.) and mice were studied between 5-9days post-surgery. A surgery procedural guide has been detailed thoroughly elsewhere (197).

## *In Vivo* Experiments

### *5-Aminoimidazole-4-carboxamide-1-beta-D-ribofuranoside (AICAR) Euglycemic Clamp*

AICAR is an adenosine analogue that, upon entry of the cell, is phosphorylated by adenosine kinase to yield ZMP (129). ZMP is characterized as an AMP analog due its structural and functional similarities, specifically its ability to allosterically activate AMPK, promote its phosphorylation and activation (129). AICAR has been demonstrated to inhibit endogenous glucose production *in vivo* (133) and glucose production from hepatocytes. The AICAR-euglycemic clamp was designed to elevate circulating AICAR levels (**Fig. 2.6**) and, consequently, intraorgan ZMP concentrations in a setting of well-controlled glycemia.

On the day of study mice were placed in bedded containers without food and water between 07:00 and 08:00 for a 5hr fast (t=-300 to 0min). Infusion lines were connected to the

indwelling catheters 90min prior to infusions to minimize stress. AICAR (Toronto Research Chemicals) or Saline (Sal)-clamps were performed similar to previously described insulin-clamps (198) with minor modifications. At t=-90min, a primed-continuous infusion of [3-$^{3}$H]glucose (2μCi•min$^{-1}$ for 1.2min then 0.04μCi•min$^{-1}$ until t=0min) was administered to determine 5hr fasting and clamp glucose kinetics. Samples were taken at t= -15 and -5min to determine basal blood and plasma parameters followed by the start of a continuous infusion of donor erythrocytes to prevent a fall in hematocrit during the clamp. At t=0min, AICAR or Saline was delivered as a primed (40mg•kg$^{-1}$), continuous infusion (8mg•kg$^{-1}$•min$^{-1}$) followed by a variable infusion of 50% dextrose to clamp blood glucose levels at 110mg•dL$^{-1}$. The AICAR infusion rate was selected to parallel the conditions of earlier clamps in rodents (133, 199), which afforded a more robust basis for comparing AMPK-dependent and independent changes in metabolism. The 0.04μCi•min$^{-1}$ [3-$^{3}$H]glucose infusion was reduced to 0.02μCi•min$^{-1}$ and [3-$^{3}$H]glucose was diluted in the glucose infusate (0.06μCi•μl$^{-1}$) to minimize fluctuations in specific activity during the clamp steady state. Arterial glucose was monitored from a 5μL blood sample (AccuCheck Advantage, Roche Diagnostics) every 10min and the glucose infusion rate (GIR) was adjusted to account for deviations from 110mg•dL$^{-1}$. Glucose kinetics and plasma metabolites were determined from arterial samples taken during the clamp steady state (t=80-120min). Blood samples were collected in EDTA coated tubes, centrifuged, and the plasma layer was stored at -20°C for analysis.

### *Stable-Isotopic Infusions*

*Molecular Modeling*

To date, the most comprehensive method to asses hepatic glucose and oxidative fluxes *in vivo* and *ex vivo* employs $^{2}H_2O$, [$^{13}C_3$]propionate, [3,4-$^{13}C_2$]glucose, and NMR (35). This technique maps rates of glucose production from glycerol, PEP, glycogen, and TCA cycle-related fluxes *in vivo*. Despite the wealth of information provided in the analysis, the time and financial constraints of NMR have limited the broad application of this method. Moreover, the plasma required for NMR analysis exsanguinates the entire blood volume of the mouse. Other methods that measure these fluxes in humans are, to date, impossible in conscious, unrestrained-unstressed mice (200).

Thus, we sought to (1) transform the existent NMR technique to a method more appropriate for genetic mouse models and (2) develop a flux model of hepatic oxidative and glucose metabolism *in vivo* amenable to changes in tracers and flux pathways. Surgical methods (see surgical procedures) developed at Vanderbilt limit the obfuscating variable of stress often present in *in vivo* mouse research. We hypothesized that carbon flux through oxidative and glucose-synthetic biochemical pathways (**Fig. 2.1**) could be determined by measuring isotopic enrichment of glucose through GC/MS and performing mass isotopomer and metabolic flux analysis (MFA).

A method developed by Antoniewicz et al. (201) yields 3 glucose derivatives that allow for independent detection of 6 analytically useful fragments (**Fig. 2.2**) for isotopomer analysis. A model composed of mass balance equations was constructed to (1) determine positional enrichment of glucose and (2) analyze the flow of carbon and hydrogen atoms into plasma glucose from oxidative, anaplerotic and cataplerotic pathways. Dr. Jamey Young guided the

construction of the flux model (Vanderbilt University) in the Isotopomer Network Compartmental Analysis (INCA, devised by Dr. Jamey Young) program. Atomic exchanges and tracer incorporation in a biochemical reaction network are specified by INCA users. INCA analyzes glucose fragment enrichment using a least squares regression in the context of the reaction network. MFA was performed by minimizing the sum-of-squared residuals between simulated and experimentally determined measurements (202).

Isotopic tracers with labeled carbon and hydrogen atoms ($^2H_2O$, [6,6$^2H_2$]glucose, and [$^{13}C_3$]propionate) were used in the studies herein. Thus, the model accounts for carbon and hydrogen atom transitions in the TCA cycle, anaplerotic/cataplerotic reactions, gluconeogenesis from the PEP, gluconeogenesis from glycerol, and glucose derived from glycogen (**Fig. 2.1**). Metabolite chemical formulas in the reaction network were restricted to traceable atoms—carbons, specified by uppercase letters, and hydrogens, specified by lower case letters. Atomic positions and metabolite properties were delineated in an additional interface in INCA (**Fig. 2.3**). Moreover, an additional interface detailed tracer atomic structures, enrichments, and nodes (**Fig. 2.4**). Fragment mass values determined through GC/MS were input for each mouse at each time point of sampling (**Fig. 2.5A,B**). The model assumes the full equilibration of 4C intermediates in the TCA cycle, G6P↔F6P and GAP↔DHAP, no entry of labeled carbon from acetylCoA and no re-entry of $CO_2$ formed in the reaction network. Pyruvate generated from pyruvate kinase and malic enzyme is indistinguishable, as described elsewhere (103).

The reaction network consisted of 19 reactions, 22 metabolite nodes, and 316 mass isotopomer balance equations. Adjustable flux parameters were estimated from 29 independent mass isotopomer measurements for each of three time points taken during the isotopic steady state. Rates were relativized to citrate synthase flux. The sum of squared residuals ranged from

2.30 to 35.20 in $\alpha1\alpha2^{lox/lox}$±Alb*cre* studies. All fits were accepted using a $\chi^2$ test with 24 degrees of freedom ($p<0.05$).

Key: Endogenous glucose production (EndoRa, $\boldsymbol{V_1}$), flux from glycogen to glucose-6-phosphate (G6P) ($\boldsymbol{V_2}$), glycerol to glyceraldehyde 3-phosphate (GA3P) ($\boldsymbol{V_3}$), phosphoenolpyruvate (PEP) to 2-phosphoglycerate (2PG) ($\boldsymbol{V_4}$), oxaloacetate (OAA) to PEP ($\boldsymbol{V_5}$), pyruvate to OAA ($\boldsymbol{V_6}$), OAA to citrate ($\boldsymbol{V_7}$), propionylCoA to succinylCoA ($\boldsymbol{V_8}$), succinylCoA to succinate ($\boldsymbol{V_9}$), the joint contribution of pyruvate kinase and malic enzyme to pyruvate ($\boldsymbol{V_{10}}$), and substrate flux to pyruvate ($\boldsymbol{V_{11}}$). Multiple substrates shuttle through pyruvate to the TCA cycle; thus, $\boldsymbol{V_{11}}$ encompasses all non-PEP, unlabeled sources of substrate flux to pyruvate.

*Stable- Isotopic Infusion Protocols for Conscious Unstressed Mice*

Two protocols were developed for the infusion of stable isotopes in conscious unstressed mice. All continuous infusates were dissolved in 0.9%NaCl-4.5% $^2H_2O$ for both protocols.

(1) A sampling protocol for two isotopic steady states was developed to study the effects of liver AMPK deletion on short and long term fasting glucose and oxidative fluxes *in vivo*. A $^2H_2O$ bolus was infused into venous circulation within 25min to enrich 4.5% total body water ($27\mu L \cdot g^{-1}_{Mouse}$). A [6,6$^2H_2$]glucose prime was dissolved in the bolus ($2.96mg \cdot mL^{-1}$) and a separate continuous infusion line ($0.8mg \cdot kg^{-1} \cdot min^{-1}$) was initiated at the end of the bolus. Three plasma samples were drawn during the first stable-isotopic steady state in 10min intervals, 180min after initiating the $^2H_2O$ bolus and [6,6$^2H_2$]glucose prime. The second stable-isotopic steady state was achieved between 90-110minutes following a primed, continuous infusion of the TCA cycle

tracer [$^{13}C_3$]propionate (sodium salt). The [$^{13}C_3$]propionate prime (108.9mg•kg$^{-1}$, delivered within 10min) and continuous infusion (5.5mg•kg$^{-1}$•min$^{-1}$) was administered 20min after the last sample of the first stable-isotopic steady state. Three plasma samples were collected at 10min intervals 90min following the initiation of the [$^{13}C_3$]propionate prime. Mice were fasted either 3.5 or 14.5hrs prior to the $^2H_2O$ bolus and [6,6$^2H_2$]glucose prime.

(2) The two isotopic steady state protocol was reduced to a single phase. The length of time separating the initiation of the $^2H_2O$ bolus/[6,6$^2H_2$]glucose prime and the [$^{13}C_3$]propionate prime was reduced to 120min. 3 plasma samples were collected in a single, 30min phase 90min after initiating the [$^{13}C_3$]propionate prime. In an effort to optimize the protocol used for studies in this thesis, *in vivo* glucose metabolism in conscious unstressed mice was evaluated in the context of a graded reduction in [$^{13}C_3$]propionate (108.9mg•kg$^{-1}$ prime, 5.5mg•kg$^{-1}$•min$^{-1}$ infusion; 54.5mg•kg$^{-1}$ prime, 2.7mg•kg$^{-1}$•min$^{-1}$; 27.2mg•kg$^{-1}$ prime, 1.4 mg•kg$^{-1}$•min$^{-1}$ infusion).

### *Body Composition*

Body composition was determined using a Bruker Optics mq10 nuclear magnetic resonance analyzer.

## ***In Vitro*** **Experiments**

### *Mitochondrial Isolation and Oxygen Consumption*

Mitochondrial isolation was performed using standard homogenization and differential centrifugation methods as previously described (203). Briefly, liver tissue was weighed and

subsequently minced in 5mL of ice-cold mitochondrial extraction buffer containing 250mM sucrose, 2mM $KH_2PO_4$, 1mM EGTA, and 20mM Tris·HCl (pH 7.2). The minced tissue was washed twice and homogenized at 600rpm with a Teflon Potter Elvehjem pestle (6 up-and-down pulses). The homogenate was centrifuged for 10min at 800g at 4°C. The mitochondria-rich supernatant was then pelleted by centrifugation at 8000g at 4 C for 10min and gently re-suspended in 0.5mL of ice-cold extraction buffer. The mitochondrial sample received a second centrifugation at 8000g at 4°C for 10min and the final pellet was re- suspended in 200µL of extraction buffer. Mitochondrial protein concentration was measured using the Bradford method. The freshly isolated liver mitochondria were used for oxygen consumption measurements. High-resolution respirometry (Oroboros Instruments) was performed in duplicate at 37°C in MiR05 (0.5mM EGTA, 3mM $MgCl_2$ 6H2O, 20mM taurine, 10mM $KH_2PO_4$, 20mM HEPES, 1g/L BSA, 60mM potassium-lactobionate, 110mM sucrose, pH 7.1, adjusted at 30°C) as previously described (204). State 2 oxygen flux was assessed following titration of complex I substrates glutamate (10mM) + malate (2mM) + pyruvate (5mM). State 3 oxygen consumption supported by complex I substrates was evaluated by a 5mM ADP addition. State 4o was determined by titrating oligomycin (2 g/mL). Carbonylcyanide- p-trifluoromethoxyphenyl- hydrazone (FCCP) was added in 0.05 m steps to determine maximal electron transport system (ETS)-mediated oxygen flux. An aliquot of fresh isolated mitochondria was frozen at -80°C for immunoblot analysis.

## Processing Tissue Samples

### *Immunoblotting*

Liver tissue was homogenized in an extraction buffer (1:10 w/v) containing 50mM Tris, 1mM EDTA, 1mM EGTA, 10% glycerol, 1% Triton X-100 (pH 7.5) containing protease (Pierce) and phosphatase inhibitors. Homogenates were centrifuged for 20min at 4500g at 4°C and the supernatants were assayed for protein concentration using the Bradford method. Briefly, samples and standards were loaded into a 96well plate and Bradford Reagent (1:4 MilliQ$H_2O$) was added in equal volume to each well. Plates were read at 595nm in SpectraMax Plus spectrophotometer (Molecular Devices, CA) and a line was constructed from the known standards to determine unknown protein concentrations. The relative sensitivity of enhanced chemiluminescence (ECL) and the anti-AMPKα/pAMPKα$^{T172}$ related antibodies required minimal protein loading for immunoblots. 5-25μg protein were separated in NuPAGE 4-12% (v/v) Bis-Tris gels (Invitrogen) and transferred to a PVDF membrane. Membranes were blocked (1hr room temperature or overnight at 4°C) in 5% milk (w/v) and probed for tAMPK, pAMPKα$^{T172}$, pACC$^{S79}$, tACC, tErk1/2, pErk1/2, tAkt, pAkt$^{S473}$, βActin (Cell Signaling Technology), Total OXPHOS, VDAC1 and GAPDH (abcam). HRP-linked α-rabbit and α-mouse secondary antibodies were applied for ECL and visualization using GE Healthcare Amersham Hyperfilm ECL. Immunoblots for Total OXPHOS were performed on mitochondrial extracts and normalized to VDAC1. ImageJ software was used for gating and densitometry.

***Hepatic Adenine Nucleotides***

Liver tissue excised <20s of cervical dislocation were used to measure hepatic adenine nucleotides. The hypoxia that ensues directly after execution (205) translates to changes in hepatic adenine nucleotides and AMPK signaling. Thus, temporal and procedural criteria were implemented to limit these effects. Freeze-clamped liver tissue was rapidly homogenized (1:10w/v) using a rotor homogenizer or Bullet Blender (bead-based homogenization at recommended settings for liver tissue) in ice-cold, 0.5M $HClO_4$ and 0.5mM EGTA and directly placed on ice. Samples were centrifuged at 3200g at ≤4°C and the supernatants were isolated and neutralized with 0.5M $K_2CO_3$. Samples sat on ice an additional 3min and were re-centrifuged at 3200g for 5min. Supernatants were saved for HPLC analysis in a Supelco Supelcosil LC18-T column (4.6 by 250mm, 5µm particle size) with a Waters 490 detector (254nm at 1.0 AUFS) and constant flow rate of 0.7mL·min$^{-1}$. Adenine nucleotides (AMP, ADP, ATP, ZMP, and AICAR) from samples and standards were spotted using a 12.5min mobile phase A (100nM $KH_2PO_4$, pH 6) and a 3.5min mobile phase B (90:10 100mM $KH_2PO_4$/MeOH), and 44min mobile phase A.

***Metabolomics Profiling***

Liver metabolites were analyzed by Metabolon (Durham, NC). The following description is a slightly modified protocol of that provided by Metabolon. Sample proteins were precipitated with methanol and vigorously shaken for 2min (Glen Mills GenoGrinder 2000) and centrifuged. The sample supernatant was saved and split into equal volumes for LC+, LC-, and GC/MS analysis. The LC/MS portion of the platform incorporates a Waters Acquity UPLC system and a Thermo-Finnigan LTQ mass spectrometer, including an electrospray ionization (ESI) source and linear ion-trap (LIT) mass analyzer. Vacuum-dried samples are reconstituted, one each in acidic

or basic LC-compatible solvents containing 8 or more injection standards at fixed concentrations. Extracts are loaded onto columns (Waters UPLC BEH C18-2.1 x 100 mm, 1.7 μm) and gradient-eluted with water and 95% methanol containing 0.1% formic acid (acidic extracts) or 6.5 mM ammonium bicarbonate (basic extracts). For GC/MS, samples are dried under vacuum desiccation for ≥18 hours before derivatization under nitrogen using bistrimethyl-silyl-trifluoroacetamide (BSTFA). The GC column is 5% phenyl dimethyl silicone and the temperature ramp is from 60° to 340° C in a 17 minute period. A Thermo-Finnigan Trace DSQ fast-scanning single-quadrupole mass spectrometer analyzes all samples using electron impact ionization. Library entries of purified standards are used to identify biochemicals. Using proprietary visualization and interpretation software, chromatographic properties and mass spectra are used to match specific compounds/isobaric entities. Peaks are quantified using area under the curve. The library match for each compound in a sample is verified. Random forest analyses are used to initially classify compounds.

***Liver Glycogen***

Liver glycogen was determined with a modified protocol from Exton and Chan (206). Liver was homogenized in 0.03N HCl (1:10w/v) and incubated at 80°C for 10min. A volume of the digest was applied to chromatography strips (Whatman International, UK), dried, and washed 3X in 70%EtOH and briefly rinsed with acetone. The chromatography strips were incubated in 5mL of 0.04M NaOAc-amyloglucosidase at 37°C in a shaking water bath for 3hrs. Glycogen concentration was determined from the isolate through an enzyme-linked spectrophotometric assay. Briefly, equal volumes of glycogen isolate and glucose standards were pipetted into 96well plates; equal volumes of a buffer (200mM Tris-HCL (pH 7.4), 500mM $MgCl_2$, 5.7mM

ATP, and 2.8mM NADP) containing hexokinase and glucose-6-dehydrogenase. The generation of G6P from the hexokinase reaction was converted to NADPH and 6-phosho-D-gluconolactone by G6PDH. NADPH was quantified at 340nm (SpectraMax Plus spectraphotometer) as a measure of glucose.

***Liver Triglycerides, Diglycerides, Cholesterol Esters, and Phospholipids***

A modification of the method developed by Folch et al. (207) was used to extract hepatic lipids, which were filtered and recovered in the chloroform phase. Extracts were then separated by thin layer chromatography—Silica Gel 60A plates developed in petroleum ether, ethyl ether, and acetic acid (80:20:1)—and visualized by rhodamine 6G. Boron fluoride-methanol was used to methylate fatty acids scraped from plates (208), which were analyzed using an Agilent 7890 gas chromatograph with Helium as a carrier gas (Supelco, PA). The retention times of known standards were used to characterize FA methyl esters. An additional method was used to determine triglycerides in livers from the AICAR-euglycemic clamps. Tissues were placed in an alkaline digest (1mg/μL, 3M KOH in 65% EtOH) and incubated at 70°C for 1hr with intermittent vortexing. Tissues were brought to a total volume of 500μL 2M Tris-HCl (pH 7.5) then diluted further (1:5) in 2M Tris-HCl (pH 7.5). 10μL of the digest (or standards) were added to 1mL pre-warmed, reconstituted GPO reagent (Pointe Scientific, MI) and incubated at 37°C for 5min. 200μL of the reaction mix was then added to a 96well plate in duplicate. A standard curve was generated to calculate unknown triglyceride concentrations.

### *RT-PCR*

Liver RNA was isolated using a RNeasy Mini Kit (Qiagen, MD) and cDNA was synthesized using IScript cDNA synthesis (Bio-Rad, CA) reagents and protocol to generate 1μg cDNA. Taqman Universal PCR Mastermix and primers (Applied Biosystems, NJ) were used for RT-PCR. GAPDH was used as a loading control and relative expression was calculated using the $2^{-\Delta\Delta Ct}$ method.

## Processing Plasma Samples

### *Plasma Glucose and Radioactivity*

Plasma [3-$^{3}$H]glucose concentrations were measured to calculate rates of endogenous glucose production (EndoRa) and disappearance (Rd) from [3-$^{3}$H]glucose infused in the AICAR-euglycemic clamp using a modified version of Steele's non-steady state equations (209). Infusate tracers (1:200 in saturated $C_7H_6O_2$) and plasma samples were deproteinized with $Ba(OH)_2$ and $ZnSO_4$. A volume of the supernatant was dehydrated and reconstituted in $H_2O$ to determine plasma and infusate [3-$^{3}$H]glucose. A separate aliquot was used to determine total [$^{3}$H] in the plasma through liquid scintillation counting (Packard TRICARB 2900, Packard CT). Ultima Gold scintillation fluid (10mL) was added to vials containing infusates and samples. The remaining volume from the sample isolates were utilized to measure plasma glucose levels using the same spectrophotometric assay described for liver glycogen.

***Plasma Non-Esterified Fatty Acids (NEFA)***

Circulating NEFAs were assay directly from the plasma using an enzymatic colorimetric method (HR Series NEFA-HR (2), Wako Diagnostics USA, VA). The assay is designed to conjugate NEFAs to CoA through the provision of AcylCoA synthetase, ATP, and CoA. AcylCoAs are then oxidized by AcylCoA Oxidase to yield peroxide. The addition of peroxidase in the presence of peroxide condenses MEHA and 4-aminoantipyrine to generate a purple pigment detectable at ~550nm. 5µL of each sample was diluted 1:2 in $H_2O$ and added to a 96well plate. Standards (oleic acid) were also loaded onto the 96well plate to generate a curve. 225µL of Reagent A was added to each well, lightly shaken, and incubated at 37°C for 10min. 75µL Reagent B was added, briefly shaken, and incubated at 37°C for 10min. Air bubbles were removed through light aspiration through a clean pipette tip. Plates were read at 560nm on a SpectraMax Plus spectrophotometer.

***Plasma Triglycerides***

Triglycerides were assayed directly from the plasma using an enzymatic colorimetric assay (Raichem, CA). The reaction cleaves the glycerol moeity from triglycerides, which subsequently reacts with glycerol kinase to generate glycerol-1-phosphate. Glycerol phosphate oxidase generates DAP and peroxide from G1P and $O_2$. Similar to the principle behind the NEFA assay, peroxide reacts with 4-aminoantipyrine and 5-dichloro-2-

$$\text{Triglycerides} \xrightarrow{\text{Lipases}} \text{Glycerol} + \text{FFAs}$$

$$\text{Glycerol} + \text{ATP} \xrightarrow{\text{GK}} \text{G1P} + \text{ADP}$$

$$\text{G1P} + O_2 \xrightarrow{\text{GPO}} \text{DAP} + H_2O_2$$

$$H_2O_2 + 4\text{AAP} + \text{DHBS} \xrightarrow{\text{GPOD}} \text{Quinoneimine dye} + 4H_2O$$

hydroxybenzene sulphonate (DHBS) in the presence of peroxidase to generate a red pigmented dye (Quinoneimine) detectible at 520nm (below). Plasma samples were diluted 1:20 in MilliQ $H_2O$; equal volumes of plasma and standard (glycerol) were added in duplicate to a 96well plate and 75µL reconstituted GPO reagent were added to each well, rotated briefly, and incubated at 37°C for 10min. The plate were read directly at 520nm using a SpectraMax Plus spectrophotometer.

***Plasma Lactate***

Plasma isolated directly after blood sample acquisition was added to 4% $HClO_4$ (1:4 dilution), flicked to mix, and spun down. The supernatant was saved to assay plasma lactate. 200µL lactate buffer (glycine, magnesium hexahydrate, hydrazine hydrate, 0.73mM NAD, pH 9.5) was added to 10µL of sample or known standard. The samples were shaken briefly and sat at room temperature for 5min. Baseline fluorescence was measured at an excitation 340nm and emission of 450nm. 10µL lactate dehydrogenase (LDH) buffer (1:15 LDH:Lactate buffer, (v/v)) was added to each well and incubated for 1hr 45min. Excitation and emission of NADH were measured. A standard curve was generated from known standards to calculate unknown sample concentrations.

$$\text{Lactate} + \text{NAD}^+ \xrightarrow{\text{LDH}} \text{Pyruvate} + \text{NADH} + \text{H}^+$$

***Plasma Insulin***

Plasma insulin was measured either by (1) Millipore Rat/Mouse ELISA or (2) 5-day double antibody radioimmunoassay (AICAR-euglycemic clamp). (1) The first method is a basic

sandwich ELISA. 10μL sample plasma and standards were loaded into a microtiter plate pre-coated with anti-rat insulin antibodies; a polyclonal antibody targeting the captured insulin was next applied. Unbound sample/reagents were washed away and HRP was applied to bind the biotinylated antibodies. Next, HRP substrate 3,3'5,5'-tetramethylbenzidine was applied and, after 5-20min incubation, 0.3M HCl was added to quench the aforementioned reaction. The addition of HCl yielded a yellow color that was read on a SpectraMax Plus spectrophotometer at 450 and 590nm. The standards were proportional to increasing concentrations of insulin. Unknown sample concentrations were determined per manufacturer's instructions. (2) Samples and standards were incubated with an anti-rat/mouse insulin detection antibody. 3days later, $^{125}$I-insulin was added to the sample/antibody mix. Secondary antibodies were applied to precipitate antibody-bound insulin. Next, samples were centrifuged and the supernatants decanted; pellet counts were determined using a Cobra II AutoGamma counter (Packard, IL). Counts in the pellet were inversely proportional to insulin concentrations. A standard curve was constructed to calculate unknown insulin concentrations.

## Calculations

The relative contribution of [6,6$^2H_2$]glucose to the otherwise labeled and unlabeled glucose pool was determined through MFA. This relative flux was normalized to the known [6,6$^2H_2$]glucose infusion rate and extrapolated to all reactions in the flux network. The rates measured in these studies are within reasonable agreement with those observed elsewhere (35, 210). Steady state glucose kinetics (Ra, rate of glucose appearance and Rd, rate of glucose disappearance) for AICAR clamps were calculated using the following equation:

$$Ra = Rd = {}^{I}/_{SA} \qquad SA = {}^{Tracer}/_{Tracee}$$

where (*I*) represents the tracer infusion rate and (*SA*) represents the ratio of tracer to tracee. *I* (dpm/min) and *SA* (dpm/mg) were derived through measurement of counts in the infusate and plasma for AICAR clamps. Endogenous Ra was determined by subtracting the clamp glucose infusion rate from Ra.

Energy charge (EC) was calculated from the following equation:

$$EC = {}^{([ATP] + \frac{1}{2}[ADP])}\Big/_{([ATP] + [ADP] + [AMP])}$$

where the numerator represents the total quantity of high energy adenine triphosphate (ATP) and the denominator represents the total adenine nucleotide pool (TAN). The equation for EC was derived from the equilibrium reaction catalyzed by adenylate kinase:

$$2ADP \leftrightarrow ATP + AMP$$

***Statistics***

Data are presented as means±SEM. Differences between groups were determined through student *t tests,* Two-Way ANOVA with ANOVA contrasts (Metabolon metabolites), and Two-Way ANOVA ± Repeated Measures with Fisher's LSD for post-hoc comparisons to determine significance between groups. Significance was set at $p \leq 0.05$.

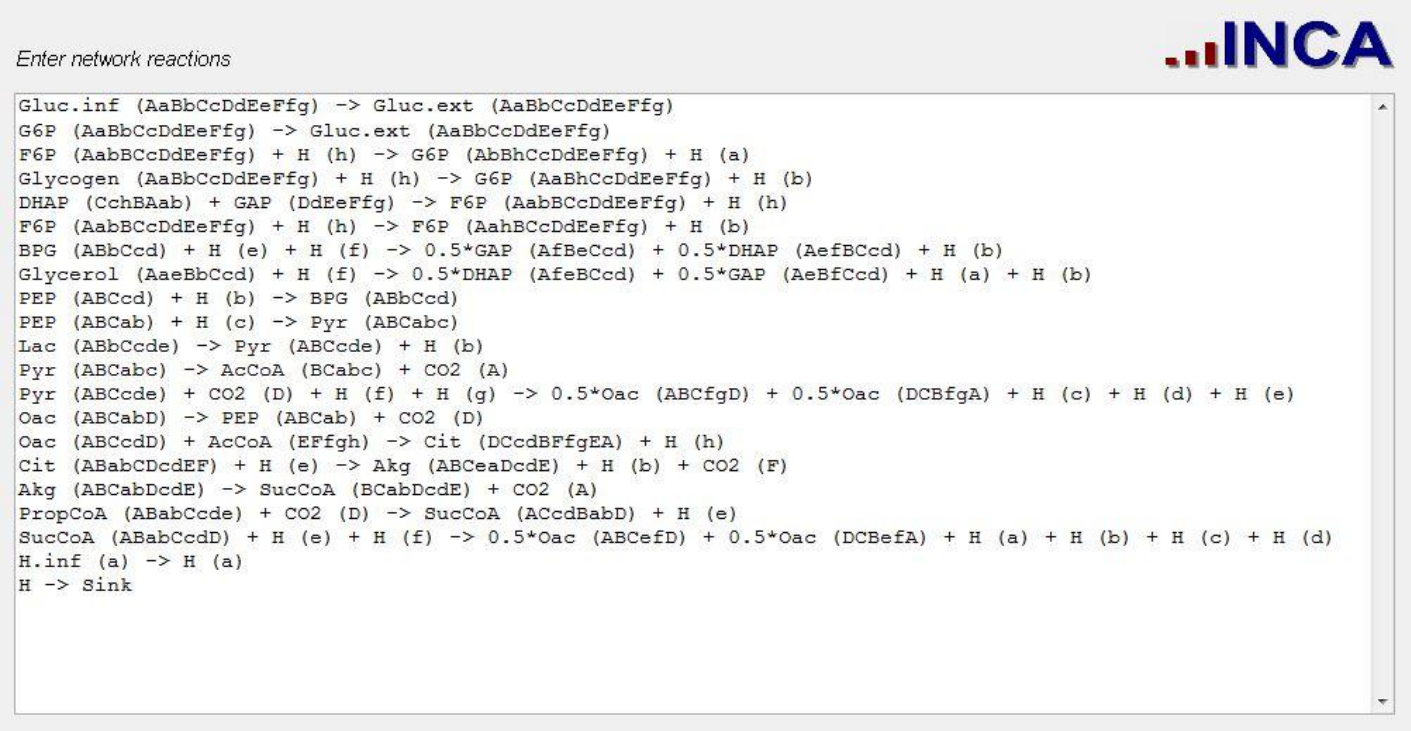


**Figure 2.1 – INCA interface for biochemical reaction network input.** The carbon and hydrogen atom composition of metabolites in the reaction network are designated by uppercase (C) and lower case (H) letters. The network was constructed from known biochemical reactions for gluconeogenesis, glycogenolysis, and the TCA cycle.

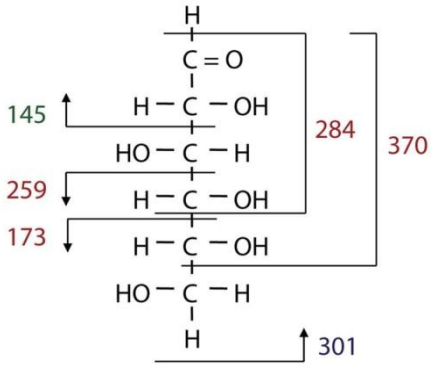


**Figure 2.2 – Atomic positional information is provided by GC/MS analysis of fragments generated from glucose derivatization** (201)

.

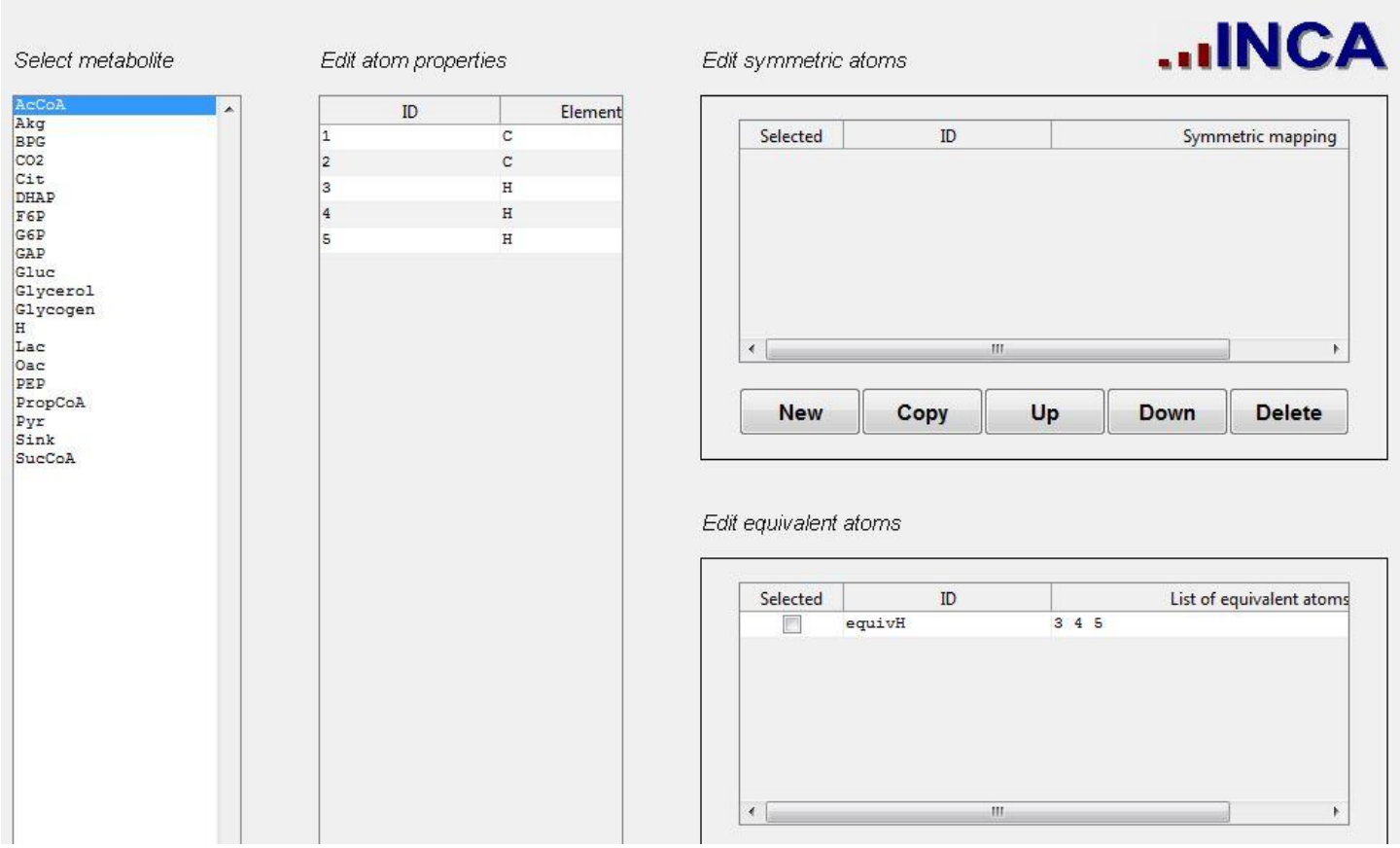


**Figure 2.3 – Atomic properties of each molecule specified in INCA**

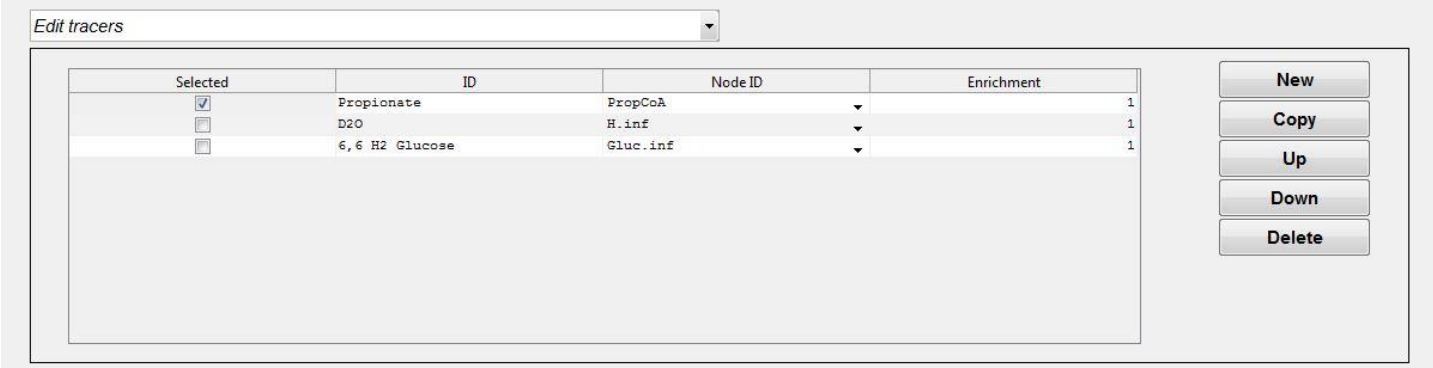


**Figure 2.4- Specification of tracer entry, composition, and enrichment in INCA**


**Figure 2.5A- Specification of labeled and unlabeled atoms in each fragment**

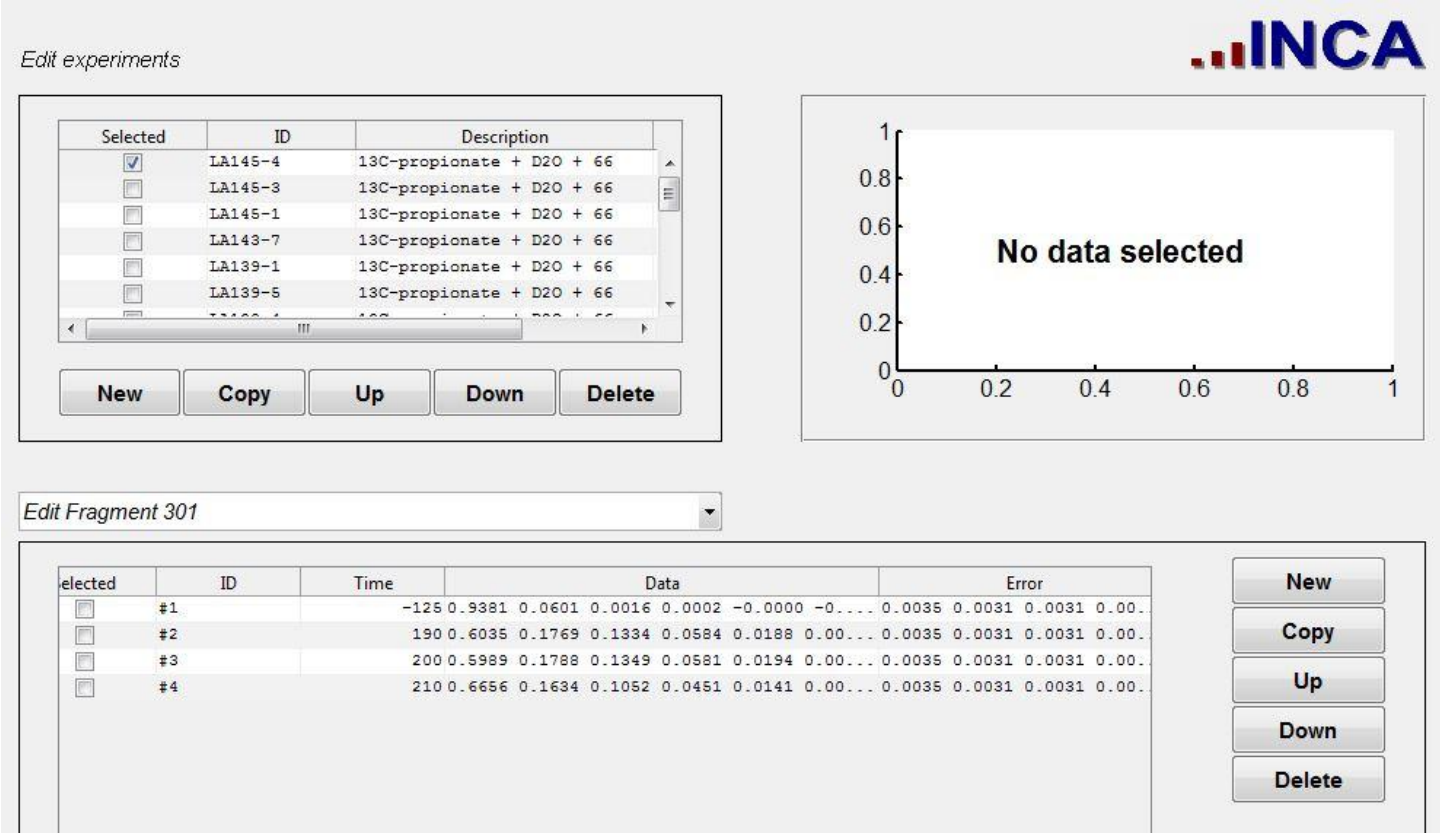


**Figure 2.5B- GC/MS fragment mass input for each sample time point**

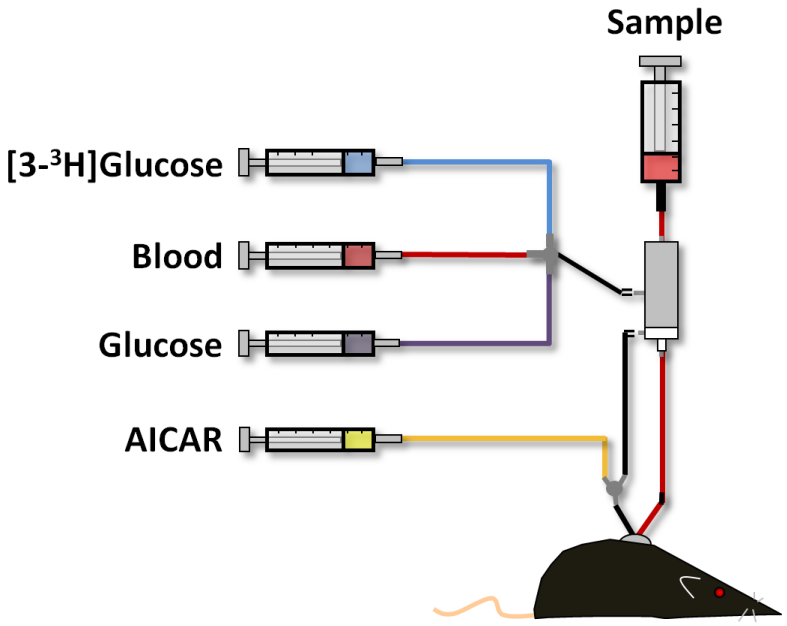


**Figure 2.6- Experimental setup for the AICAR-euglycemic clamp**

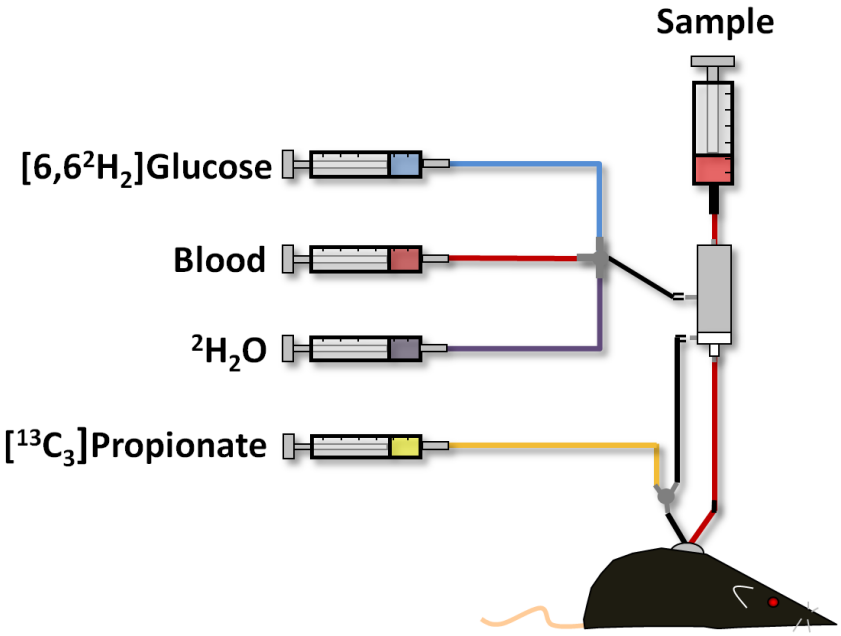


**Figure 2.7 – Experimental setup for stable-isotopic infusions**

# Chapter III

# HEPATIC AMPK SYNCHRONIZES METABOLIC FLUX WITH ENERGY STATUS IN THE LIVER

## Aims

The aims of this chapter were to determine the 1) role of AMPK in liver energy homeostasis in the postabsorptive mouse and 2) extent to which hepatic AMPK coordinates metabolic flux during a physiological decrease in energy state. The hypothesis that AMPK preserves energy homeostasis by supporting oxidative metabolism and, thereby, sustains hepatic glucose production during fasting was tested. Multiple lines of molecular and physiological evidence substantiate the interconnection between fat oxidation, anaplerosis/cataplerosis, and gluconeogenesis in the liver. Moreover, AMPK has been characterized as a control element in buffering against reductions in energy state by either activating or inhibiting mediators of macronutrient flux in the liver (**Table 1.1**). The hypothesis was approached using state-of-the art *in vitro* respirometry and metabolomics methods and *in vivo* metabolic flux analysis in mice with a liver specific deletion of AMPK α1 and α2 catalytic subunits (14-15wk old $\alpha1\alpha2^{lox/lox}$ +Alb*cre* vs. C57Bl/6 floxed controls, $\alpha1\alpha2^{lox/lox}$).

## Experimental Approach

Chapter II provides a detailed account of the methods and models used for studies in Chapter III. Briefly, AMPK effects on a) mitochondrial function were assayed through high resolution respirometry on isolated liver mitochondria, b) liver metabolites were measured using

a multi-mass spectrometry platform and c) rates of oxidative and glucose fluxes were determined through the metabolic flux analysis (MFA) of tracer-enriched plasma glucose in short (7-9hrs) and long term (18-20hrs) fasted mice. The high metabolic rate of the mouse induces a vastly different energy state in the liver within hours of fasting. The decision to vary fast duration provided 1) information concerning the role of hepatic AMPK under different physiological nutritional states and 2) an examination of the metabolic milieu provoked by long term fasting in floxed control mice. The third aim c) was accomplished through the development of a stable-isotopic, *in vivo* tracer technique (**Fig. 2.7**and **3.1**) that extracts biochemical reaction rates from positional glucose enrichment. A model composed of mass balance equations for a network of classical biochemical reactions was constructed using MFA software (INCA) (202) devised by Jamey Young, PhD (see description in **Figs. 2.1-5**). A recent technique developed for plasma glucose derivitization and GC/MS (201) yielded 6 fragments (**Fig. 2.2**) which provided sufficient enrichment information for isotopomer and metabolic flux analysis.

## Results

### *AMPK Restrains Fasting Mediated Changes in Hepatic Glucose and Metabolic Flux*

Post-absorptive conditions in the mouse are reached within a few hours of fasting. Long term fasted $\alpha1\alpha2^{lox/lox}$ and $\alpha1\alpha2^{lox/lox}$+Alb*cre* mice lost ~10% body weight. The transition from a short to long term fast resulted in changes in glucose metabolism consistent with normal physiology in $\alpha1\alpha2^{lox/lox}$ mice (**Fig. 3.2A-C, $V_{1-4}$**). Hepatic glucose production (EndoRa, $V_1$) reduced slightly with long term fasting (**Fig.3.2A-C**). The fasting-mediated decrement in $V_1$ resulted from a complete reduction in glucose flux from glycogen ($V_2$). Accordingly, the fall in

glycogenolytic glucose production (***V₂/V₁***) corresponded to an increased reliance on glucose flux from glycerol (***V₃/V₁***) and PEP (***V₄/V₁***) (**Fig. 3.2D**). Absolute glucose flux from PEP (***V₄***) was unaffected by increasing fast duration (**Fig. 3.2A-C**). Interestingly, flux rates through citrate synthase (***V₇***) decreased with extended fasting but fluxes associated with the entry and removal of pyruvate (***V₅, V₆, V₁₀***) trended toward an increase (**Fig. 3.2A-D**). The flux rates reported here are in reasonable agreement with those estimated using NMR methods in overnight fasted mice (***V₁-₅,₇***) (35, 210).

Hepatic AMPK deletion reduced EndoRa (***V₁***) in the short term fast, stemming primarily from a ~50% reduction in glucose flux from glycogen (***V₂***) (**Fig. 3.2A-D**). The early reduction in glycogenolytic glucose production corresponded to a trend toward increased reliance on gluconeogenesis from glycerol (***V₃/V₁***) and PEP (***V₄/V₁***) in short fasted $\alpha1\alpha2^{lox/lox}$ +Alb*cre* mice (**Fig. 3.2A-D**).Though absolute glucose flux from glycerol (***V₃***) was not significantly different than controls (**Fig. 3.2B,C**), intrahepatic glycerol levels were elevated in $\alpha1\alpha2^{lox/lox}$+Alb*cre* mice (**Fig. 3.9A**). Long term fasting fully diminished glucose flux from glycogen and the liver became more dependent on gluconeogenic fluxes (**Fig. 3.2A-D,** ***V₂-₄***). The rate of glucose production (***V₁***) was low enough in the short fasted $\alpha1\alpha2^{lox/lox}$+Alb*cre* mouse that increasing the fast duration had no statistical effect (**Fig. 3.2A-C**). Intriguingly, citrate synthase flux (***V₇***) was actually elevated in knockout mice compared with controls with increasing fast duration (**Fig. 3.2A-D**). Qualitatively, glucose fluxes in short term fasted $\alpha1\alpha2^{lox/lox}$+Alb*cre* mice more closely resemble those of a long term fasted mouse. Thus, AMPK restrains fasting mediated changes in glucose flux with increasing fast duration.

Despite differences in hepatic glucose and oxidative fluxes, TCA cycle intermediates displayed a relatively uniform response to fasting in $\alpha1\alpha2^{lox/lox}$ and $\alpha1\alpha2^{lox/lox}$+Alb*cre* mice (**Fig.**

**3.9B-D**). The TCA cycle is critical for the provision of reducing equivalents for oxidative phosphorylation in the liver; drastic reductions in oxidative capacity severely impairs hepatic glucose production (107). The modest differences in glucose and oxidative fluxes observed here may be an attempt to compensate for abnormal adenylate energy homeostasis in short and long term fasted AMPK-deficient livers.

***AMPK is Critical for Maintaining Hepatic Energy Homeostasis in Long Term Fasting***

AMPK is generally described as a control element in cellular energy homeostasis. The cell works to keep ATP levels high and the AMP/ATP ratio low. Physiological and pharmacological depletion of ATP increases AMP, which exerts direct control over a number of enzymes, including AMPK. Long term fasting in $\alpha1\alpha2^{lox/lox}$ mice reduced ATP and energy charge while increasing AMP and the AMP/ATP ratio in the liver (**Fig. 3.3A,C,D**). AMP-deaminase works to clear elevations in AMP which, in effect, may reduce the adenine nucleotide pool (46). Indeed, long term fasting reduced TAN (**Fig. 3.3B**). Thus, fast duration reduced hepatic energy state which corresponded to a modest decrease in the rate of flux through citrate synthase ($V_7$, **Fig. 3.2A-C**) in $\alpha1\alpha2^{lox/lox}$ mice. The increase in the AMP/ATP ratio also corresponded to a slight increase in AMPK activation ($pAMPK^{T172}$/AMPK) and the phosphorylation of its downstream target, AcetylCoA Carboxylase ($pACC^{S79}$/ACC) (**Fig. 3.4A,B**). Phosphorylation of the aforementioned target is undetectable in the absence of hepatic AMPK (See **Chapter IV**, **Fig 4.3A,B**). Decreases in Akt and ERK1/2 phosphorylation were also observed in the long term fast (**Fig. 3.4C,D**).

The absence of hepatic AMPK provoked a larger decrement in hepatic energy state in long term fasting. Indeed, ATP and ADP levels were significantly lower in long term fasted

α1α2$^{lox/lox}$+Alb*cre* mice compared to controls (**Fig. 3.3A**). TAN levels were reduced in short term fasted α1α2$^{lox/lox}$+Alb*cre* mice which was exacerbated by extending fast duration (**Fig. 3.3B**). These data imply that AMPK-deficient livers resort to greater AMP degradation to limit the rise in AMP/ATP and preserve energy charge (**Fig. 3.3C,D**). Paradoxically, the decrease in ATP availability spurred by fasting did not correspond to a decrease $V_7$ in α1α2$^{lox/lox}$+Alb*cre* mice; rather, the drop in energy availability corresponded to a relative increase in flux through citrate synthase in the absence of liver AMPK (**Fig. 3.2A-D**). These results demonstrate a defect in the coupling of oxidative metabolism with energy status in the absence of hepatic AMPK.

### *Mitochondria from α1α2$^{lox/lox}$+Albcre Mice Display Impairments in Function*

Livers from α1α2$^{lox/lox}$+Alb*cre* mice demonstrate an impaired capacity to maintain normal energy state in a short and long term fast. Moreover, differences in *in vivo* oxidative and glucose fluxes are observable in the absence of hepatic AMPK. Given the importance of oxidative phosphorylation in these interrelated processes, we hypothesized that hepatic mitochondria from α1α2$^{lox/lox}$+Alb*cre* mice would demonstrate impairments in integrative oxidative phosphorylation function compared with floxed littermates. Polarographic oxygen consumption measurements were performed on mitochondria isolated from the livers of α1α2$^{lox/lox}$ and α1α2$^{lox/lox}$+Alb*cre* mice. The absence of hepatic AMPK had no effect on glutamate, malate, and pyruvate supported basal oxygen consumption (State 2) (**Fig. 3.5A**). ADP-stimulated oxygen consumption (State 3), however, was attenuated in α1α2$^{lox/lox}$+Alb*cre* mice (**Fig. 3.5A**). The addition of the ATP-synthase inhibitor oligomycin demonstrated that non-phosphorylating oxygen consumption was no different between α1α2$^{lox/lox}$ and α1α2$^{lox/lox}$+Alb*cre* mice (**Fig. 3.5A**). Absolute FCCP-stimulated, uncoupled respiration was significantly higher in

$\alpha1\alpha2^{lox/lox}$ mice (**Fig. 3.5A**) but equaled $\alpha1\alpha2^{lox/lox}$+Alb*cre* when normalized to State 3 and Leak respiration (**Fig. 3.5D**). Impaired State 3 respiration in $\alpha1\alpha2^{lox/lox}$+Alb*cre* mice led to a reduction in the respiratory control ratio (RCR) — an index of mitochondrial efficiency—compared with $\alpha1\alpha2^{lox/lox}$ controls (**Fig. 3.5B**). These data indicate that hepatic AMPK supports efficient coupling of ADP phosphorylation and oxygen consumption. In addition, the removal of hepatic AMPK was sufficient to reduce the expression of mitochondrial complexes II and III (**Fig. 3.5C**). These results are consistent with the demonstration that hepatic AMPK activity is protective against a greater reduction in energy state during extended nutrient deprivation.

### *An Early Elevation in Fatty Acids Precedes Normal Triglyceride Accumulation in Liver AMPK Knockout Mice*

Prolonged fasting promotes adipose tissue lipolysis through a decrease in circulating insulin and increases in glucocorticords and (nor) epinephrine (211). Fatty acids (FAs) sequestered by the liver are oxidized or re-esterified, leading to profound increases in liver TGs in the mouse. Indeed, increasing fast duration elevated hepatic triglycerides (TGs), diglycerides (DGs), and cholesterol esters (CEs) in $\alpha1\alpha2^{lox/lox}$ and $\alpha1\alpha2^{lox/lox}$+Alb*cre* mice, respectively (**Fig. 3.6A-C**). CE formation may protect against the lipotoxic effects of unesterified cholesterol and fatty acids. CEs were elevated in long term fasted $\alpha1\alpha2^{lox/lox}$+Alb*cre* mice compared to controls (**Fig. 3.6C**). AMPK deletion had no impact on fasting mediated increases in absolute TGs and DGs (**Fig. 3.6A,B**). Hepatic long chain FAs (LCFAs) exhibited a similar trend. Livers of control and liver-AMPK knockout mice experienced equal fasting mediated increases and decreases in LCFAs (**Fig. 3.7**).

Despite no differences in TGs and DGs in short term fasting, several long chain (**Fig. 3.7**), but not short chain (**Fig. 3.11A-E**) FA species were elevated in the absence of hepatic AMPK. The early rise in liver LCFAs resulted from increases in saturated (14:0, 15:0, 16:0, 20:0), monounsaturated (17:1, 18:1, 22:1), and polyunsaturated (18:2, 18:3, 22:2) species in $\alpha1\alpha2^{lox/lox}$+Alb*cre* mice (**Fig. 3.7**). The rise in LCFAs corresponded to an increase in endogenous PPAR agonists that stem from linoleic and arachidonic acid (**Fig. 3.10A-C**, 9,13HODE and 12,15HETEs) (212). Additionally, liver phospholipids were significantly reduced (35±2.9%) in short term fasted $\alpha1\alpha2^{lox/lox}$+Alb*cre* mice (**Fig. 3.6D**). The aforementioned changes in FAs, metabolite signals, and phospholipids were equalized by long term fasting.

***Liver AMPK Deletion Elevates BCAA/BCKA-Related Metabolites***

Acylcarnitine species of varying lengths are formed from their antecedent acylCoA species (83). Catabolism of branched chain amino and keto acids (BCAA and BCKAs), yields reduced cofactors, acetylCoA and succinylCoA for further oxidation in the TCA cycle and electron transport chain (82). Though leucine, isoleucine, and valine levels were no different in $\alpha1\alpha2^{lox/lox}$ and $\alpha1\alpha2^{lox/lox}$+Alb*cre* mice (data not shown), several BCAA/BCKA-related metabolites were elevated in the livers of short term fasted $\alpha1\alpha2^{lox/lox}$+Alb*cre* mice (**Fig. 3.8**).

4-methyl-2-oxopentanoate, which results from leucine deamination, was increased compared with controls (**Fig. 3.8A**). Further leucine degradation yields the intermediates isovalerylCoA and 3-methylglutarylCoA. Metabolites formed from intermediates in leucine metabolism (β-hydroxyisovalerate and 3-methylglutarylcarnitine) were elevated in the livers of $\alpha1\alpha2^{lox/lox}$+Alb*cre* mice in short fasting (**Fig. 3.8B-D**). Isobutyrylcarnitine, a metabolite generated from isobutyrylCoA in valine catabolism, was also elevated in the absence of AMPK

(**Fig. 3.8E**). Moreover, a metabolite associated with lysine catabolism—glutarylcarnitine (non-BCAA/BKAA, but also an amino acid whose metabolism yields acetylCoA and/or acetoacetate)—was also increased in short-fasted liver AMPK knockout mice (**Fig. 3.8G**). The elevation in the majority of these hepatic metabolites in $\alpha1\alpha2^{lox/lox}$+Alb*cre* mice corresponded to increased pyruvate (**Fig. 3.9E**) and a trend toward elevated acetylcarnitine (**Fig. 3.8H**). Hydroxybutyrylcarnitine was the only small chain acylcarnitine to reduce with liver AMPK deletion (**Fig. 3.8F**). Intriguingly, this 4-carbon metabolite may emanate from processes related to fatty acid metabolism, in addition to BCAA/BCKA metabolism (87).

Fasting resulted in an increase in the majority of the aforementioned hepatic metabolites in control mice (**Fig. 3.8B-H**). In several cases, AMPK deletion led to further elevations in short chain acylcarnitine species in long term fasting: 2-methylbutyrylcarnitine (isoleucine catabolism), 3-methylglutarylcarnitine (leucine catabolism), and, interestingly, propionylcarnitine (**Fig. 3.8D,I,J**). PropionylCoA enters the TCA cycle as succinylCoA, the catabolic product of valine, isoleucine, and certain FAs. Thus, the aberrant oxidative flux ($\boldsymbol{V_7}$) and deficit in energy state spurred by AMPK deletion coincides with an atypical elevation in BCAA/BCKA-related metabolites in long term fasting.

## Discussion

Characterizing the fundamental role of AMPK in different physiological states has proven to be a difficult task due to the enzyme's diverse functionality. Nevertheless, genetic models with inhibitory or activating effects on hepatic AMPK have provided valuable insight into AMPK function. The use of *in vivo* and *ex vivo* technologies to map the catabolism and interconversion of metabolites in the mouse liver have been paramount to understanding

molecular control of liver metabolism (35, 105, 107, 114). Similar technologies were used here to investigate hepatic AMPK action in two linked—yet distinct—physiological energy states. These studies revealed that hepatic AMPK works to resist the fasting-mediated decline in energy state and associated changes in glucose flux. In the absence of both AMPKα1 and α2 catalytic subunits, citrate synthase flux is increased and aberrant BCAA/BCKA-related metabolism correspond to deficits in energy state and mitochondrial function.

These studies add another layer of complexity to AMPK's role in glucoregulatory control. An increase in AMPK activation by the administration of metformin and AICAR implicates AMPK in the inhibition of glucose production (34, 133, 136, 213). Removal of hepatic LKB1—AMPK's major upstream activator—results in marked hyperglycemia (137). Moreover, AMPK negatively regulates mediators of gluconeogenic gene expression (162, 163, 166, 168). However, acute control of glucose production and gluconeogenic gene expression by multiple pharmacological agents *in vitro* and *in vivo* may occur through an AMPK-independent reduction in energy state (4, 34).

Physiologically, a decrease in hepatic energy state and AMPK activation correspond to endocrine states characterized by increased glucagon action, substrate oxidation, and sustained gluconeogenesis (11, 16, 28). These observations are consistent with AMPK's putative role in oxidative metabolism (71, 155), as data here and elsewhere demonstrate that AMPK deletion impairs respiration (127). These studies identify a novel, physiological role for AMPK in maintaining a metabolic state in the liver that sustains glucose production. Indeed, hepatic glucose fluxes in short term fasted, liver AMPK knockout mice more closely resemble those of a prolonged fast.

The reduction in EndoRa in short term fasted α1α2$^{lox/lox}$+Alb*cre* mice primarily results from a reduction in glycogenolytic glucose production. Though liver glycogen only trended lower for these studies (**Fig. 3.11H**), reductions are observable in the knockout model used here (See **Chapter IV**, **Table 4.2** and **Chapter V, Fig. 5.8A**) and mice with a whole-body deletion of the AMPKβ2 subunit (214). A mechanism responsible for this phenotype is presently unclear. Impairments in the generation and/or oxidation of reduced cofactors from fat in α1α2$^{lox/lox}$+Alb*cre* mice may make the liver more reliant on glycolytic ATP production. As a result, less glucose may be available for glycogenolytic glucose production. These studies demonstrate that flux from PEP does not compensate for reductions in glucose production from glycogen.

The relationship between oxidative capacity and gluconeogenic glucose production has been demonstrated in liver's lacking PGC1α (107) and hypoxia-inducible factor activation driven by VHL inactivation (113). Whole-body deletion of PGC1α and disruption of hepatic VHL both result in marked liver steatosis and impairments in fat oxidation (107, 108, 112, 113). The reduction in oxidative capacity in PGC1α-null livers corresponds to drastic defects in $\boldsymbol{V_4}$, $\boldsymbol{V_5}$, pyruvate cycling, and $\boldsymbol{V_7}$ despite a normal induction of gluconeogenic enzyme expression with fasting (107). This model is consistent with impairments in mitochondrial respiration provoked by VHL inactivation. In addition to impairments in gluconeogenic glucose production, both models demonstrate abnormal glycogen metabolism and impaired ketogenesis (107, 113, 215).

Liver AMPK knockout impairs mitochondrial efficiency. This defect, perhaps, triggers the larger deficit in energy state observed in long term fasted AMPK-deficient livers. α1α2$^{lox/lox}$+Alb*cre* mice exhibit a much milder glucose and oxidative phenotype *in vivo* than the aforementioned models. Short term fasting results in a reduction in glycogenolytic glucose

production, yet gluconeogenic flux from PEP remains intact in the absence of hepatic AMPK. Several LCFAs increase with short term fasting, yet liver AMPK deletion does not cause abnormal triglyceridemia in response to a short or long term fast. Long term fasting normalizes the impairments in hepatic glucose fluxes exhibited in short term fasted liver AMPK knockout mice. Evidence presented here supports a fundamental role for AMPK in suspending the transition from a short to long term fasted condition in the liver. As noted, short term fasted $\alpha1\alpha2^{lox/lox}$+Alb*cre* mice exhibit several metabolic characteristics of the livers of long term fasted mice. Liver AMPK knockout promotes an early change in ERK1/2 phosphorylation, phospholipids, the total adenine nucleotide pool, BCAA/BCKA related metabolites, and the aforementioned changes in glucose fluxes and fatty acids. Extending the fast duration normalizes the majority of these effects.

Fasting mediated reductions in energy state correspond to a modest decrease in citrate synthase flux in control mice. Paradoxically, citrate synthase flux is actually elevated despite larger reductions in hepatic ATP levels in $\alpha1\alpha2^{lox/lox}$+Alb*cre* mice, demonstrating inefficient hepatic substrate oxidation and energy production in the absence of AMPK *in vivo*. As previously noted, liver mitochondria from $\alpha1\alpha2^{lox/lox}$+Alb*cre* mice display defects in function (lower State 3 respiration and State 3/State 2). Others have measured metabolic flux in conditions with an imbalance between substrate availability, energy state and TCA cycle flux in the liver. Satapati et al. (35) have recently shown that 32wks of HF-feeding may impair the coupling of oxidative metabolism with ATP synthesis (lower State 3/State 4)—despite an elevation in the rate of TCA cycle flux *in vivo*. Aberrant hepatic ATP homeostasis is also characteristic of chronic high fat feeding (16), diabetes (31), and NASH (32).

Elevations in short-chain acylcarnitine species in the liver have been observed in conditions of aberrant oxidative metabolism (35, 113). The accumulation of short and medium chain acylcarnitine species in the liver may provide evidence of incomplete fatty acid oxidation (113). The relationship between these metabolites and acetylCoA oxidation in the TCA cycle may be dependent on metabolic state. For example, an elevation in acylcarnitines corresponds to accelerated TCA cycling, $\boldsymbol{V_4}$, and an increase in EndoRa during fatty liver (35). Short, even-chain acylcarnitines are also elevated with liver VHL inactivation, however, glucose production, ketogenesis, and respiration are blunted (113). If liver acylcarnitines are assumed to equilibrate with their antecedent acylCoA species, substrate load may exceed its rate of disposal in the TCA cycle and ketogenesis in both conditions.

AMPK deletion shares a degree of similarity with the aforementioned liver phenotypes—albeit more modest. The elevation in LCFAs in the short term fast corresponds to a reduction in deoxycarnitine and CoA (the immediate precursor for carnitine synthesis, **Fig. 3.9G,H**). Pyruvate and lactate are elevated in the short and long term fast, respectively (**Fig. 3.9E,F**). Furthermore, BCAA/BCKA-related metabolites (short and medium chain acylcarnitines and 4-methyl-2-oxopentanoate) increased in livers lacking hepatic AMPK. The abundance of these metabolites coincides with abnormally high citrate synthase flux, normal rates of glucose flux from PEP, and exacerbated fasting-mediated deficits in hepatic ATP. It is plausible that impairments in fatty acid transport and mitochondrial function shift liver metabolism toward alternative substrates that yield reduced cofactors, acetylCoA and anaplerotic carbon, thus fueling the TCA cycle in long term fasting. Clearly, AMPK deletion impairs the appropriate coupling of energy state with substrate load and utilization in the liver.

Energy status has been a long proposed regulator of metabolism (38, 46, 216). In conditions with available gluconeogenic substrate, an increase in fatty acid delivery decreases liver energy state and supports hepatic glucose output (63). The physiological decline in hepatic energy state with long term fasting corresponds to a modest decrease in citrate synthase flux, which does alter gluconeogenic glucose production from PEP in floxed control mice. These studies demonstrate that hepatic AMPK is a vital component of a molecular signaling network that restrains metabolic adaptations to increasing fast duration. AMPK promotes mitochondrial function, protects against a decline in energy state and the accumulation of oxidizable substrate. In its absence, a disconnect between substrate abundance, oxidation, and ATP production leads to greater energy deficits in long term fasting *in vivo*.

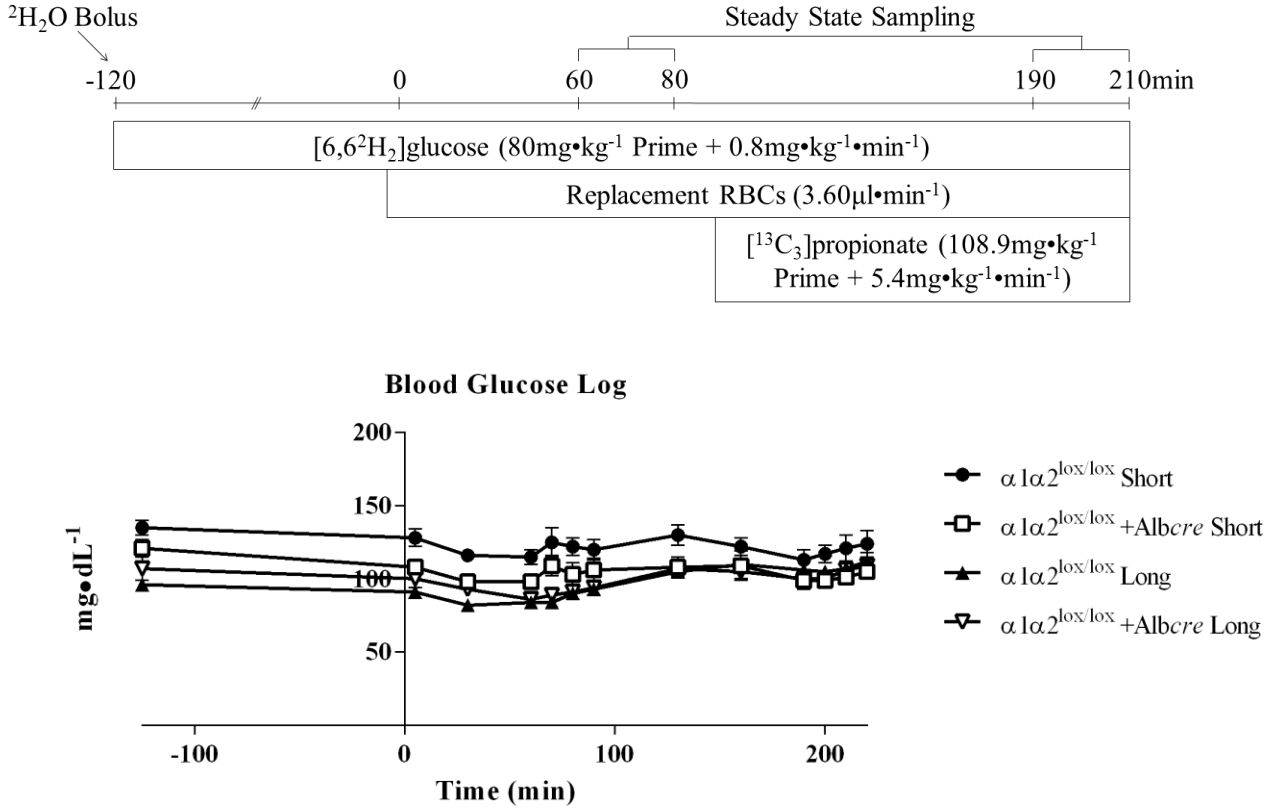


**Figure 3.1—Schematic for stable-isotopic infusions and Blood Glucose Log.** α1α2$^{lox/lox}$ and α1α2$^{lox/lox}$+Alb*cre* mice were either fasted for 3.5 or 14.5hrs prior to the $^2H_2O$ bolus (delivered as a continuous infusion for 25min, beginning at t= -120min). The [6,6$^2H_2$]glucose prime was dissolved in the $^2H_2O$ bolus. A continuous infusion of [6,6$^2H_2$]glucose started directly following the bolus. 3 steady-state plasma glucose samples were taken 180min after the initiation of the $^2H_2O$ bolus, 10min prior to the primed, continuous infusion of [$^{13}C_3$]propionate. 3 steady-state plasma glucose samples were drawn between 90-110min following the initiation of the propionate prime.

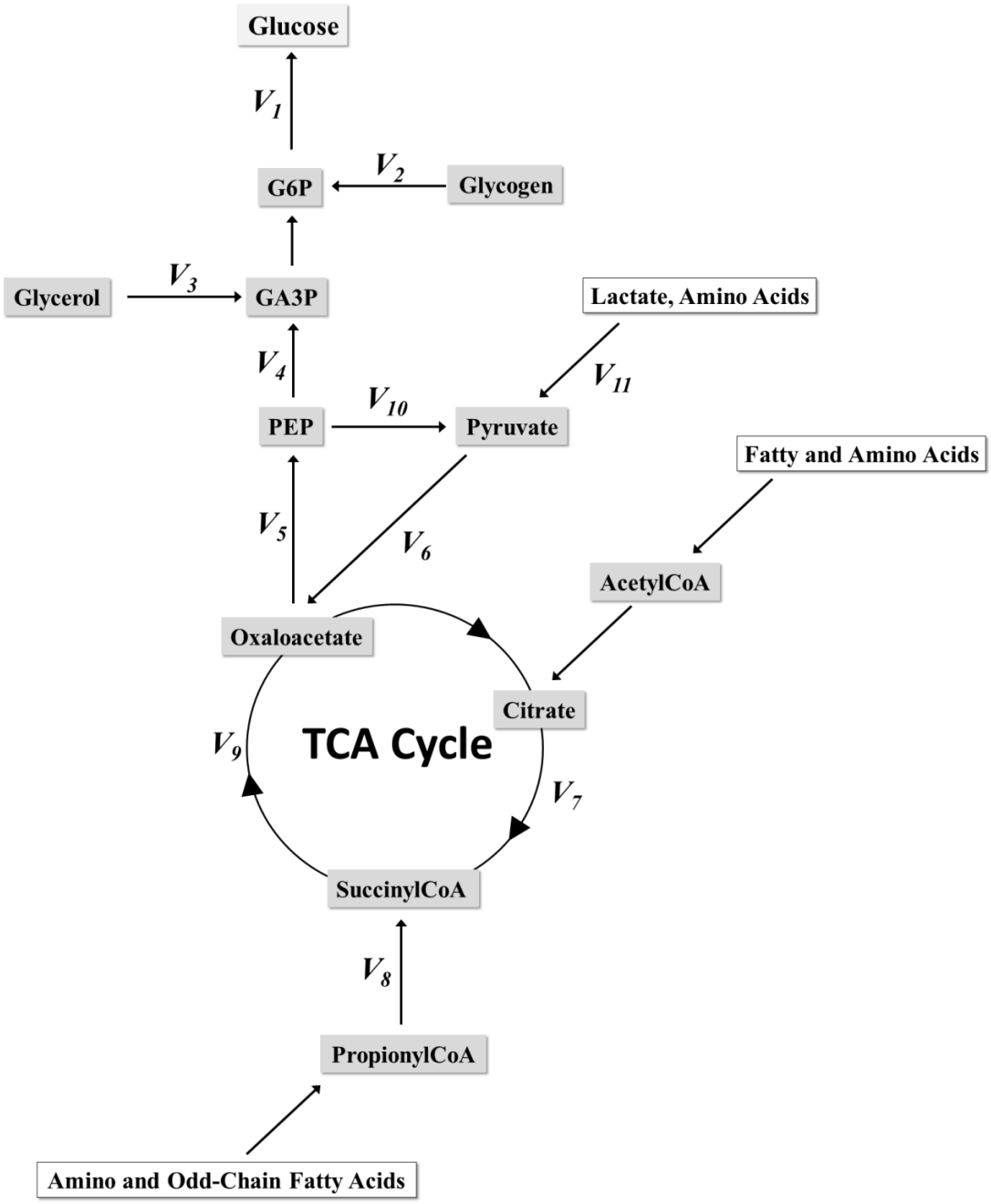


**Figure 3.2A-D—Abnormal glucose and oxidative fluxes in mice lacking hepatic AMPK.** A scheme (**A**) describing the fluxes measured in these studies is provided for clarity. Absolute (μmol·min$^{-1}$ (**B),** μmol·kg$^{-1}$·min$^{-1}$ (**C**)) and relative (**D**) fluxes were determined for α1α2$^{lox/lox}$ and α1α2$^{lox/lox}$+Alb*cre* mice in short and long term fasting. Stable-isotopic enrichment of plasma glucose was used to determine flux rates using GC/MS and metabolic flux analysis (MFA). Fluxes were converted to hexose units where necessary and expressed in three different formats for a comparison to the validation work performed elsewhere using NMR (210). Data are expressed as means ±SE, *n=5-8* in each group. **p≤0.05* vs. short term fasting; †*p≤0.05* vs. α1α2$^{lox/lox}$ mice.

Key: $V_1$= EndoRa, $V_2$= Glycogen→G6P, $V_3$=Glycerol→GA3P, $V_4$= PEP→2PG, $V_5$= Oxaloacetate→PEP, $V_6$= Pyruvate→Oxaloacetate, $V_7$= Oxaloacetate→Citrate, $V_8$= PropionylCoA→SuccinylCoA, $V_9$= SuccinylCoA→Succinate, $V_{10}$= PK and ME, $V_{11}$= Anaplerotic Substrate→Pyruvate

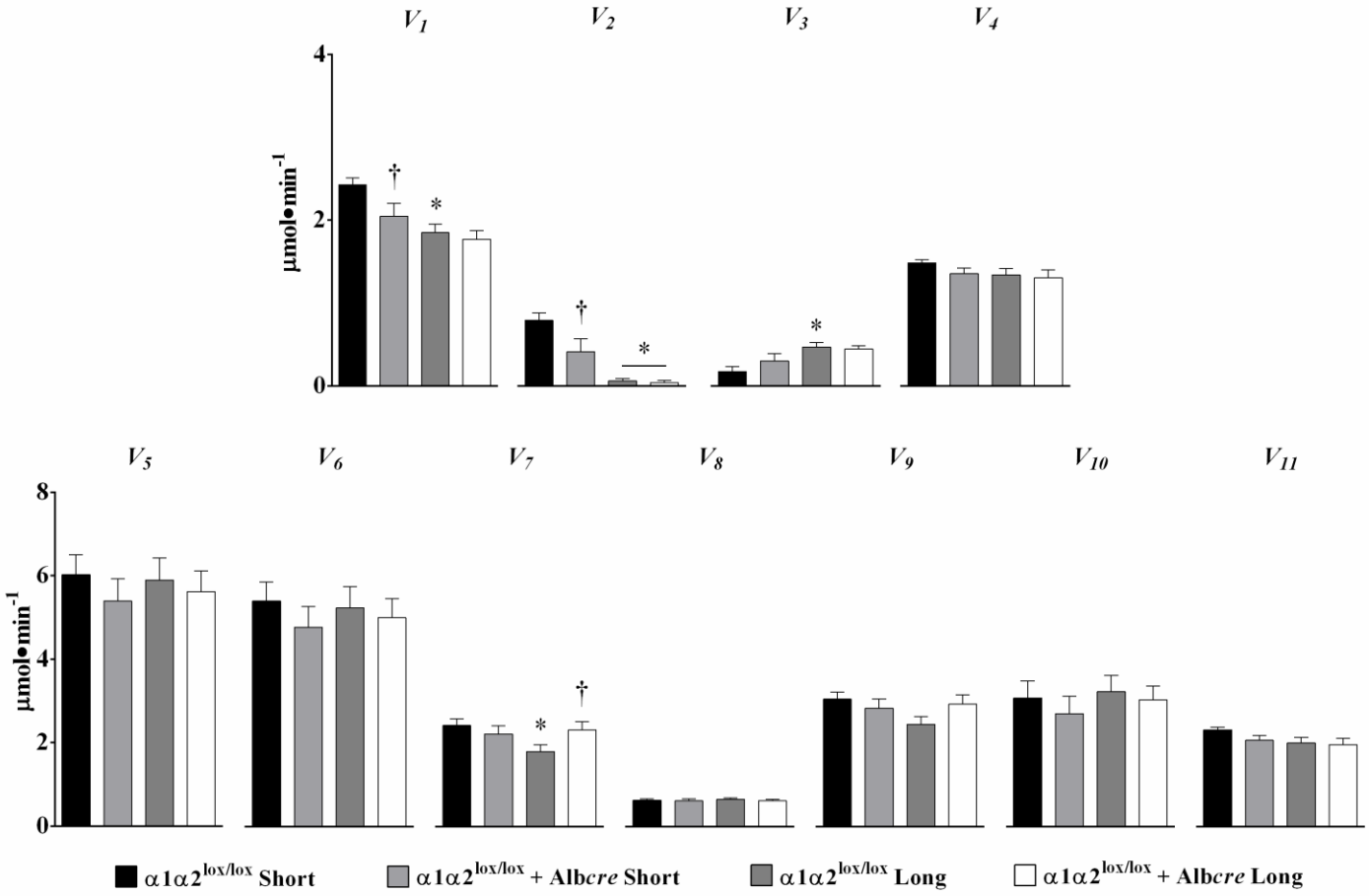


**Figure 3.2B –Abnormal glucose and oxidative fluxes in mice lacking hepatic AMPK—µmol·min$^{-1}$.** Data are expressed as means ±SE, *n=5-8* in each group. *$p \leq 0.05$ vs. short term fasting; †$p \leq 0.05$ vs. α1α2$^{lox/lox}$ mice.

Key: $V_1$= EndoRa, $V_2$= Glycogen→G6P, $V_3$=Glycerol→GA3P, $V_4$= PEP→2PG, $V_5$= Oxaloacetate→PEP, $V_6$= Pyruvate→Oxaloacetate, $V_7$= Oxaloacetate→Citrate, $V_8$= PropionylCoA→SuccinylCoA, $V_9$= SuccinylCoA→Succinate, $V_{10}$= PK and ME, $V_{11}$= Anaplerotic Substrate→Pyruvate

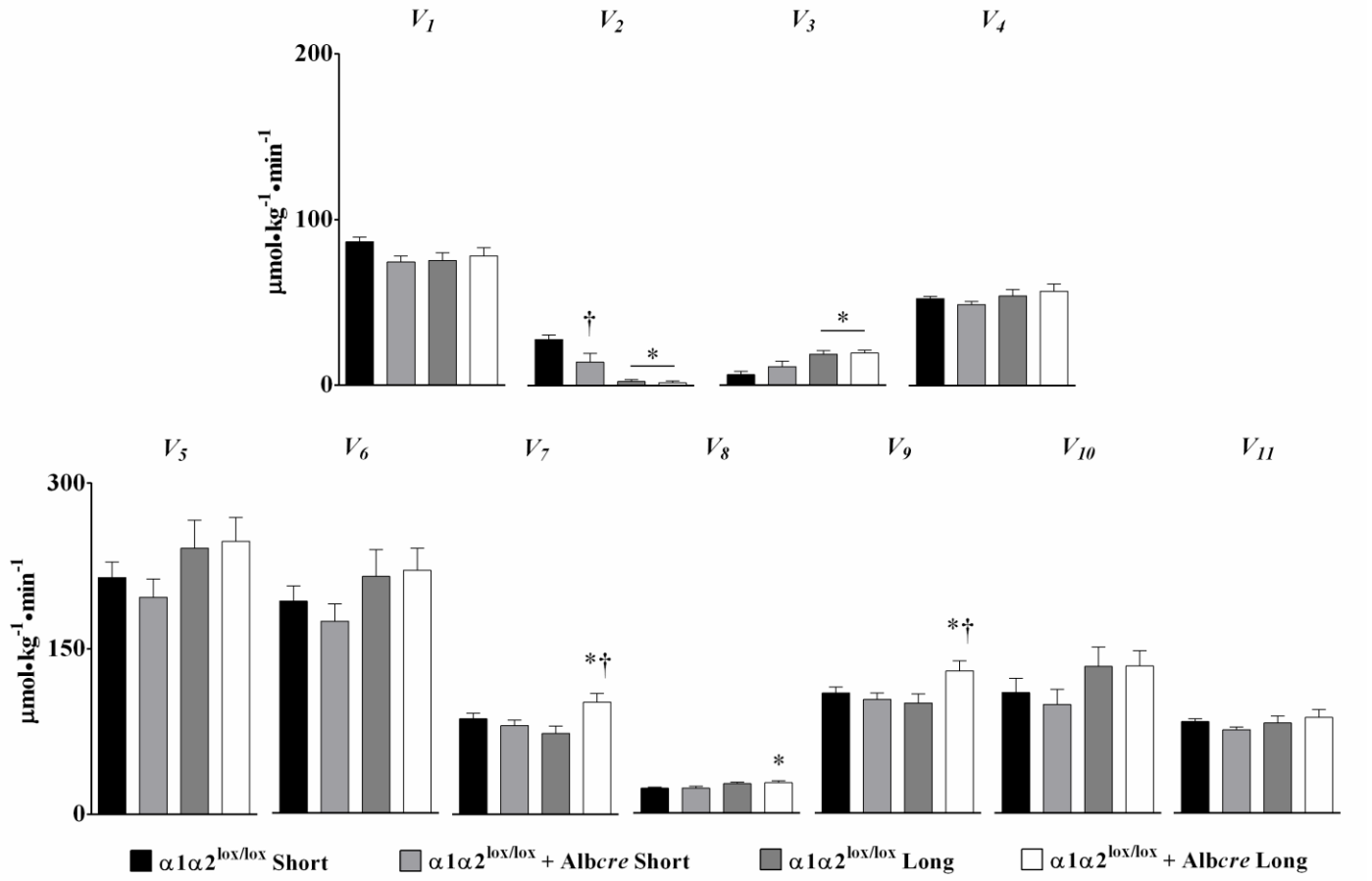


**Figure 3.2C –Abnormal glucose and oxidative fluxes in mice lacking hepatic AMPK—µmol·kg$^{-1}$·min$^{-1}$.** Data are expressed as means ±SE, *n=5-8* in each group. *$p \leq 0.05$ vs. short term fasting; †$p \leq 0.05$ vs. $\alpha 1\alpha 2^{lox/lox}$ mice.

Key: $V_1$= EndoRa, $V_2$= Glycogen→G6P, $V_3$=Glycerol→GA3P, $V_4$= PEP→2PG, $V_5$= Oxaloacetate→PEP, $V_6$= Pyruvate→Oxaloacetate, $V_7$= Oxaloacetate→Citrate, $V_8$= PropionylCoA→SuccinylCoA, $V_9$= SuccinylCoA→Succinate, $V_{10}$= PK and ME Flux, $V_{11}$= Anaplerotic Substrate→Pyruvate

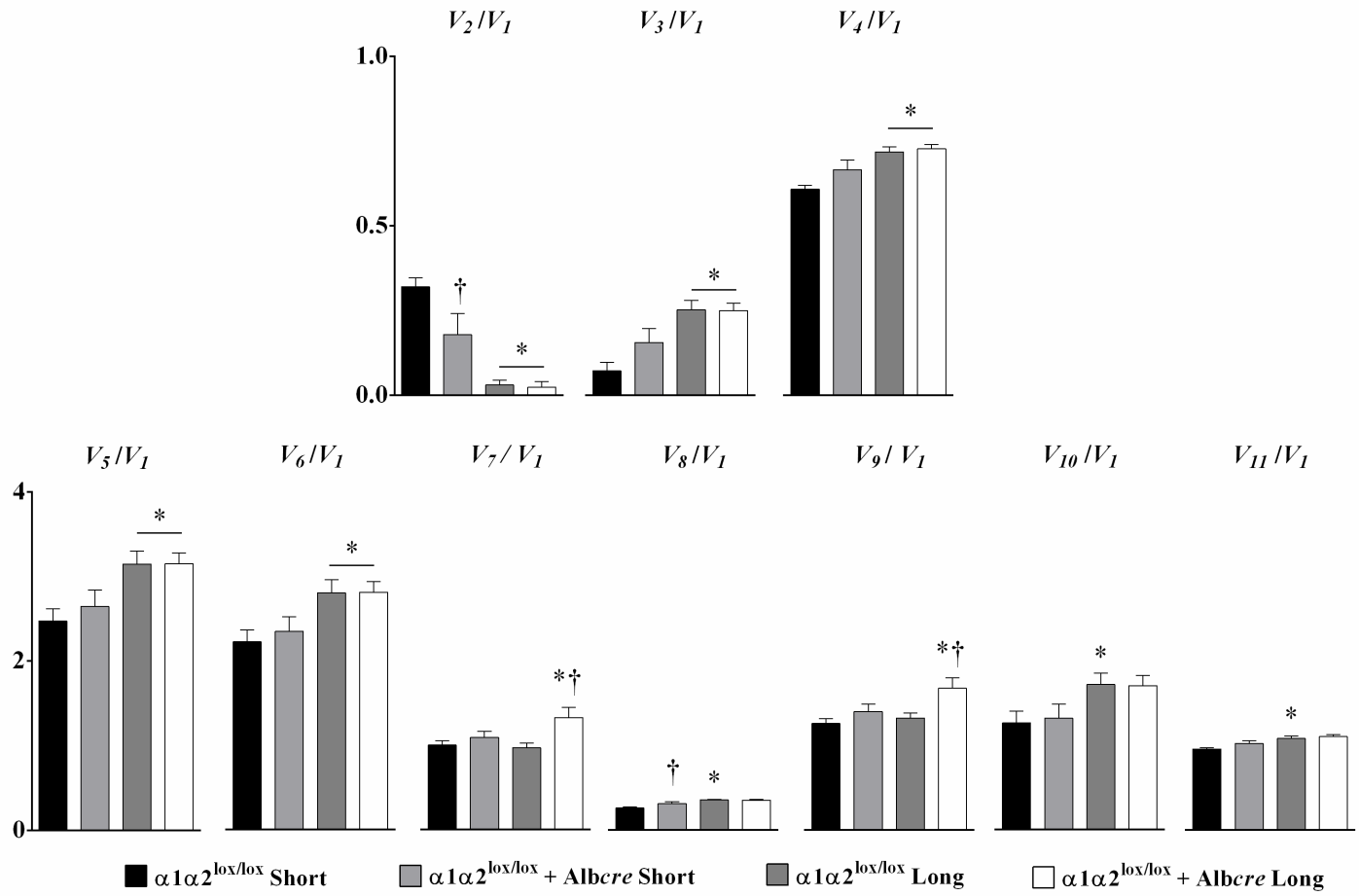


**Figure 3.2D –Abnormal glucose and oxidative fluxes in mice lacking hepatic AMPK—Relative to EndoRa.** Data are expressed as means ±SE, *n=5-8* in each group. *$p \leq 0.05$ vs. short term fasting; †$p \leq 0.05$ vs. $\alpha 1\alpha 2^{lox/lox}$ mice.

Key: $V_1$= EndoRa, $V_2$= Glycogen→G6P, $V_3$=Glycerol→GA3P, $V_4$= PEP→2PG, $V_5$= Oxaloacetate→PEP, $V_6$= Pyruvate→Oxaloacetate, $V_7$= Oxaloactate→Citrate, $V_8$= PropionylCoA→SuccinylCoA, $V_9$= SuccinylCoA→Succinate, $V_{10}$= PK and ME Flux, $V_{11}$= Anaplerotic Substrate→Pyruvate

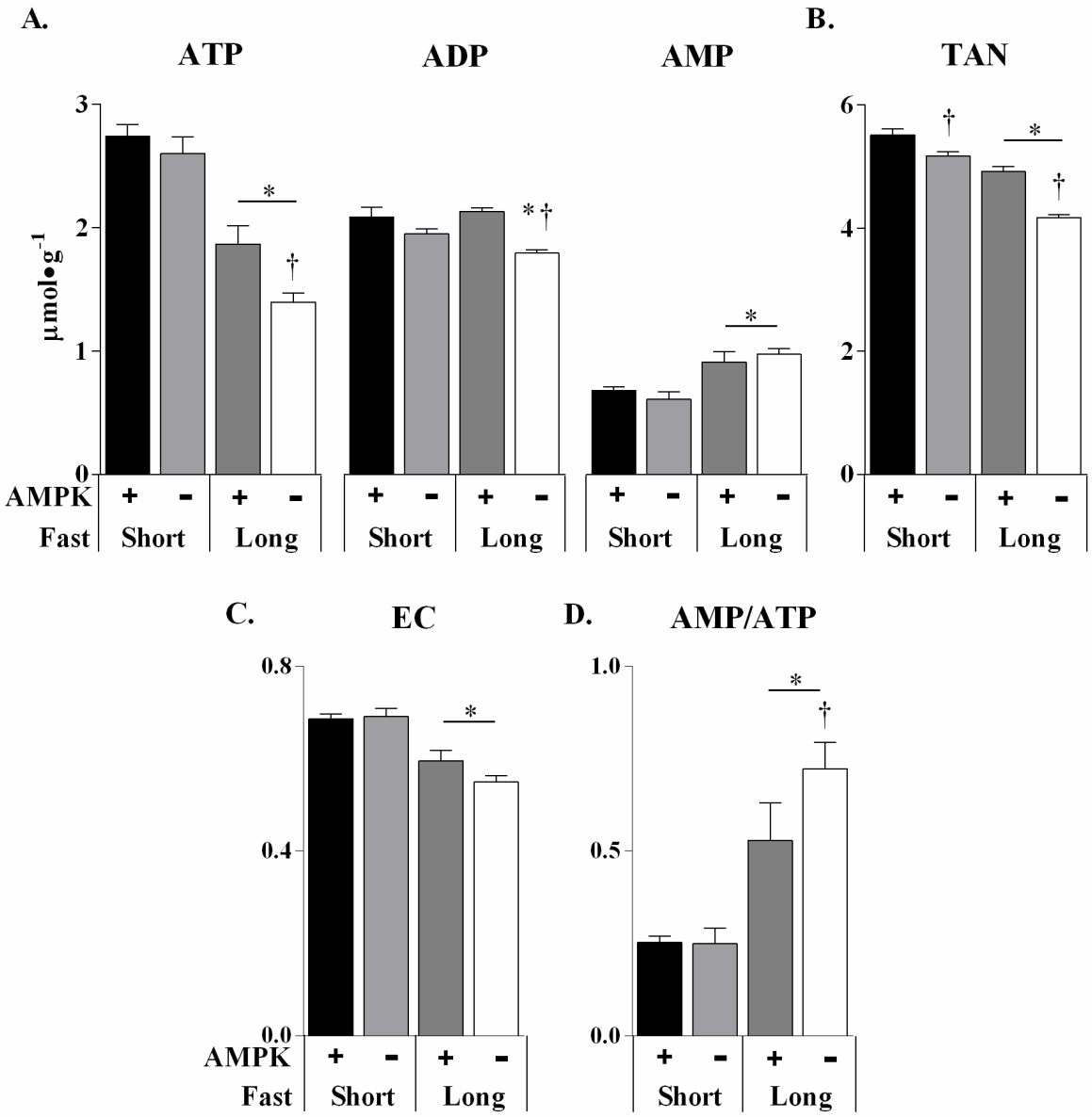


**Figure 3.3—AMPK protects against fasting-mediated reductions in energy state.** Hepatic adenine nucleotides (**A.**), the total adenine nucleotide pool (TAN= ATP+ADP+AMP, **B.**), energy charge (EC= [ATP+0.5ADP]/[TAN], **C.**), and the AMP/ATP ratio (**D.**) were determined for $\alpha1\alpha2^{lox/lox}$ and $\alpha1\alpha2^{lox/lox}$+Alb*cre* mice in short and long term fasting. Liver tissue was rapidly excised and freeze-clamped following cervical dislocation to preserve hepatic energy state. HPLC analysis was performed on neutralized, perchloric acid extracts of liver tissue as described elsewhere (16). Data are expressed as means ±SE, *n=6-7* in each group. *$p \leq 0.05$ vs. short term fasting; †$p \leq 0.05$ vs. $\alpha1\alpha2^{lox/lox}$ mice.

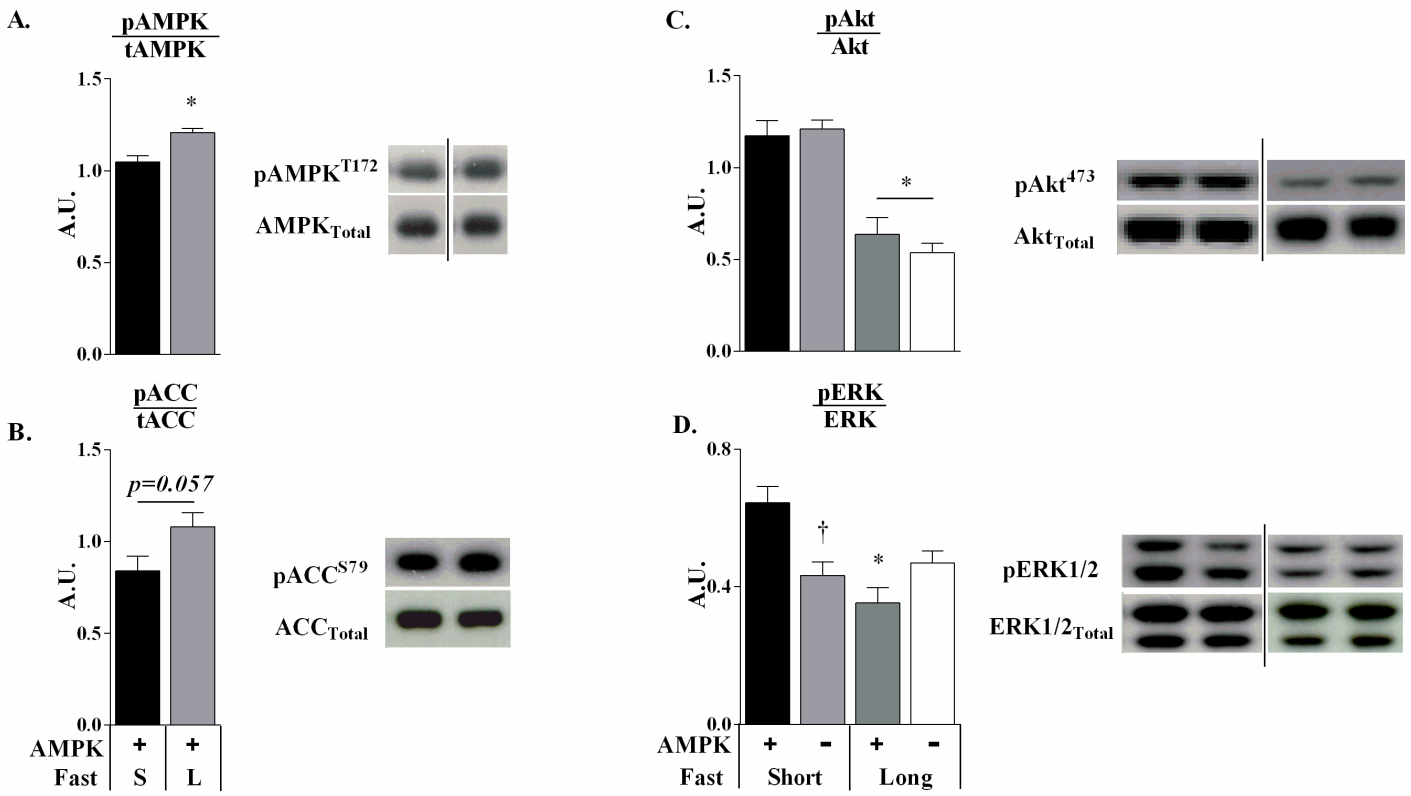


**Figure 3.4—Fasting-mediated changes in liver AMPK, ACC, Akt, and ERK1/2 phosphorylation state.** Liver AMPK (**A,B.**), Akt (**C.**), and ERK1/2 (**D.**) signaling in short and long term fasted $\alpha1\alpha2^{lox/lox}$ and $\alpha1\alpha2^{lox/lox}$+Alb*cre* mice. Activating (**A,C,D.**) and inhibitory (**B.**) phosphorylation to total AMPK, ACC, AKT, and ERK1/2 are provided as ratios (A.U.). Data are expressed as means ±SE, *n=6-7* in each group. *$p \leq 0.05$ vs. short term fasting; †$p \leq 0.05$ vs. $\alpha1\alpha2^{lox/lox}$ mice.

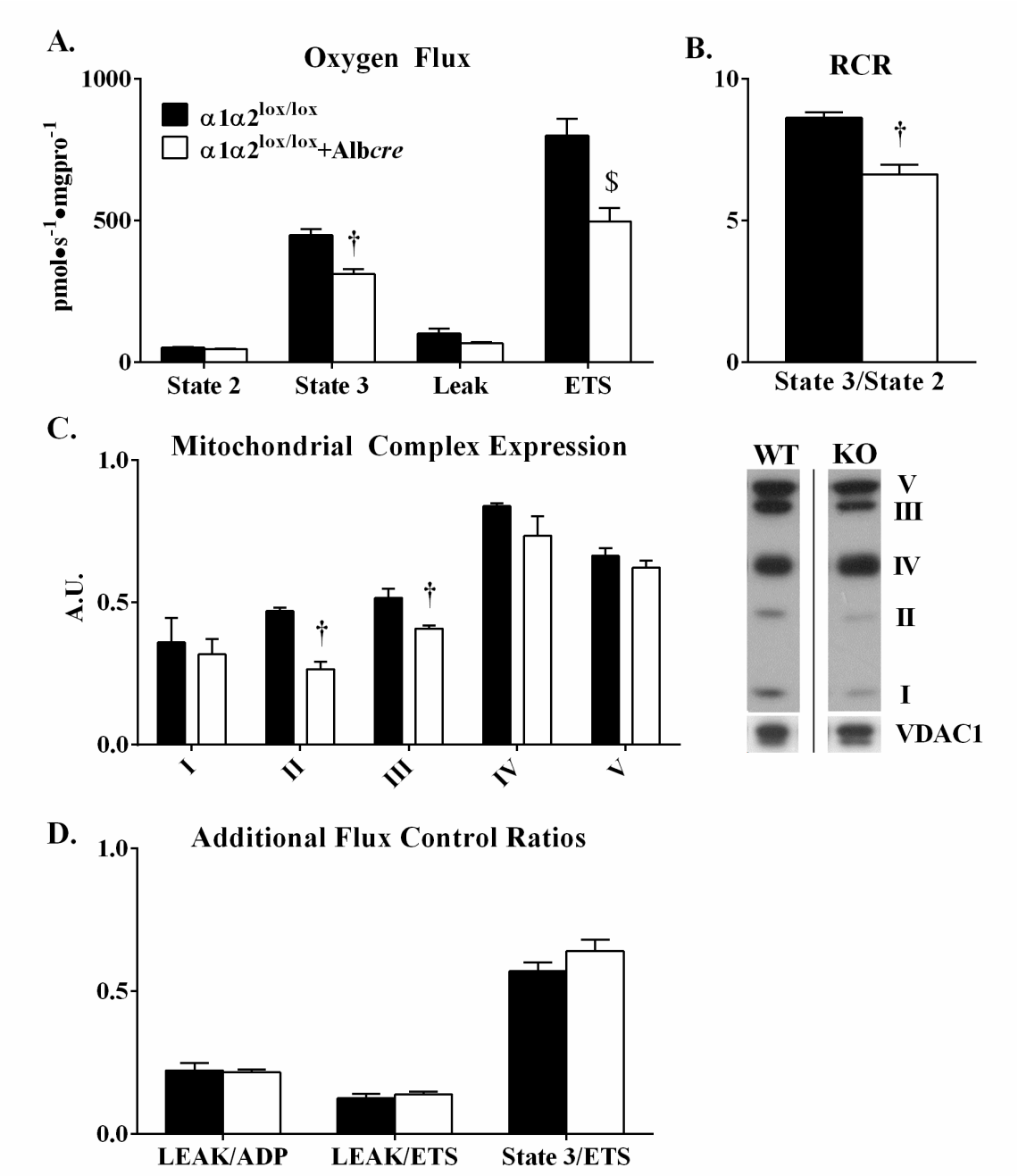


**Figure 3.5 –Oxygen flux data from mitochondria isolated from the livers of α1α2$^{lox/lox}$ and α1α2$^{lox/lox}$+Alb*cre* mice.** Mitochondrial respiration (A.) was measured in the presence of the OXPHOS substrates glutamate, malate, and pyruvate (State 2) in the presence of saturating ADP (State 3), oligomycin (LEAK), and FCCP (ETS). The respiratory control ratio (RCR) (B.) is defined as the ratio of State 3 to State 2 oxygen consumption. Mitochondrial complex expression (C.) in isolated mitochondria from the livers of α1α2$^{lox/lox}$ and α1α2$^{lox/lox}$+Alb*cre* mice was measured through western blotting (normalized to VDAC1). The representative images are lanes obtained from different parts of the same immunoblot. Control ratios for ETS, normalized to State 3 and LEAK respiration (D.). Data are expressed as means ±SE, n=5-6 in each group. †$p \leq 0.05$ vs. α1α2$^{lox/lox}$ mice; $ absolute rate of ETS is significant but not when normalized to Leak or State 3 (D.).

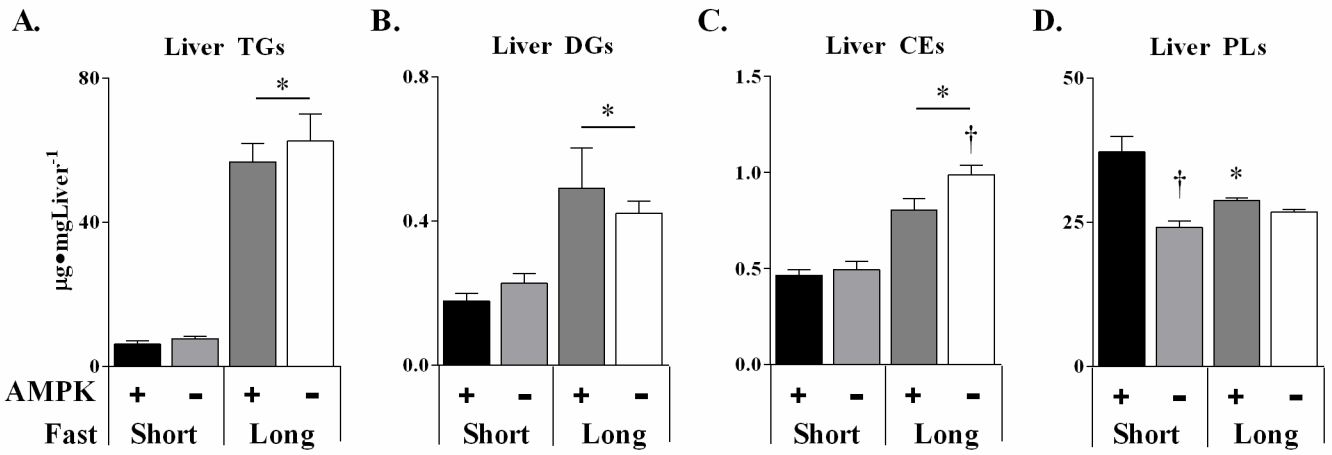


**Figure 3.6 –Liver AMPK-dependent and independent effects of fast duration on liver lipids.** Hepatic lipids in $\alpha1\alpha2^{lox/lox}$ and $\alpha1\alpha2^{lox/lox}$+Alb*cre* mice following a short and long term fast. Liver triglycerides (TGs, **A.**), diglycerides (DGs, **B.**), cholesterol esters (CEs, **C.**), and phospholipids (PLs, **D.**) were isolated through Folch extraction (207) and measured as described (36). Data are expressed as means ±SE, *n=6-7* in each group. **p≤0.05* vs. short term fasting; †*p≤0.05* vs. $\alpha1\alpha2^{lox/lox}$ mice.

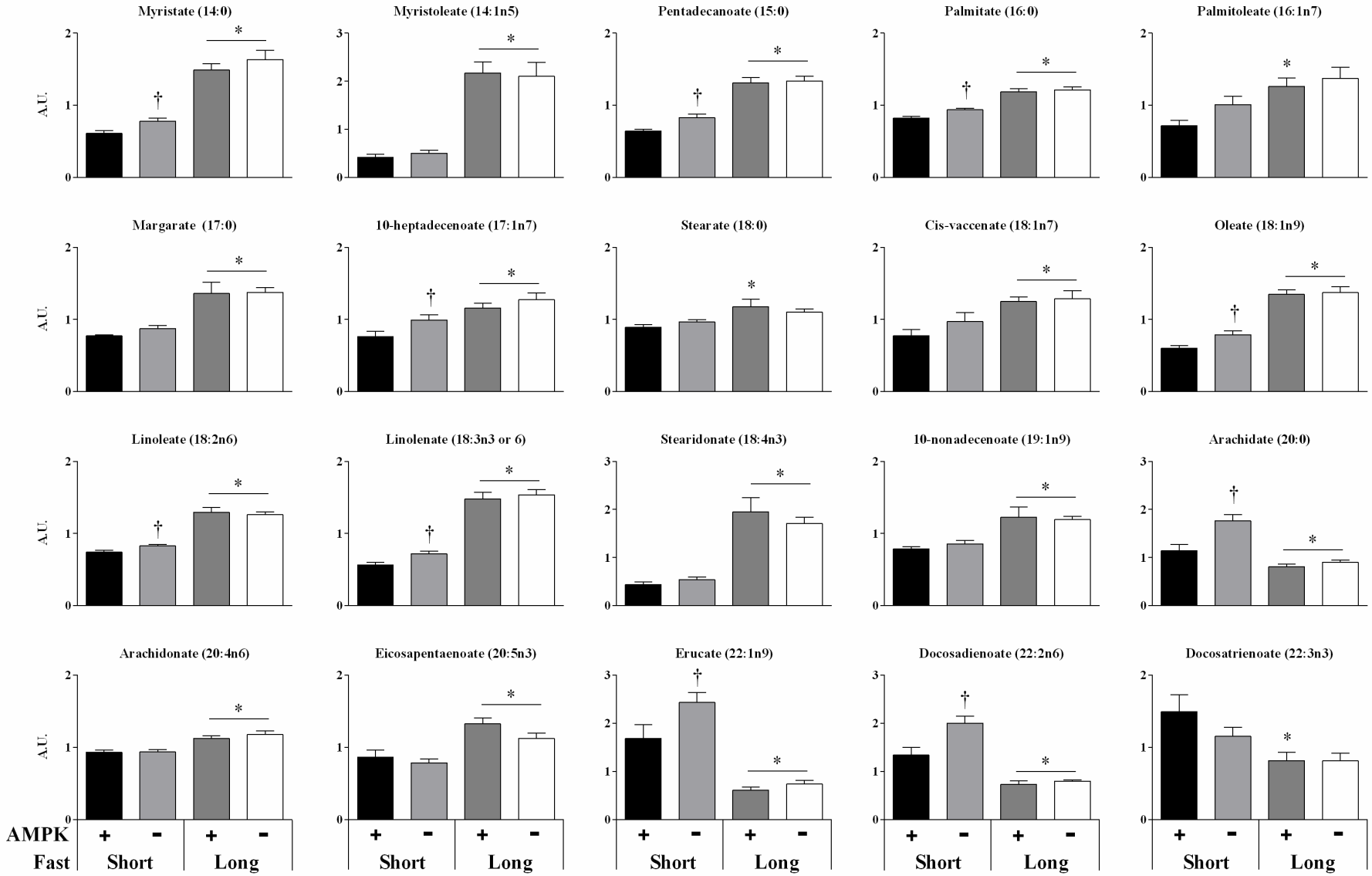


**Figure 3.7 –AMPK attenuates elevations in hepatic long chain fatty acids in short term fasting.** Liver fatty acid species determined for short and long term fasted $\alpha1\alpha2^{lox/lox}$ and $\alpha1\alpha2^{lox/lox}$+Alb*cre* mice. Data are expressed as means ±SE, *n=7-8* in each group. **p≤0.05* vs. short term fasting; *†p≤0.05* vs. $\alpha1\alpha2^{lox/lox}$ mice.

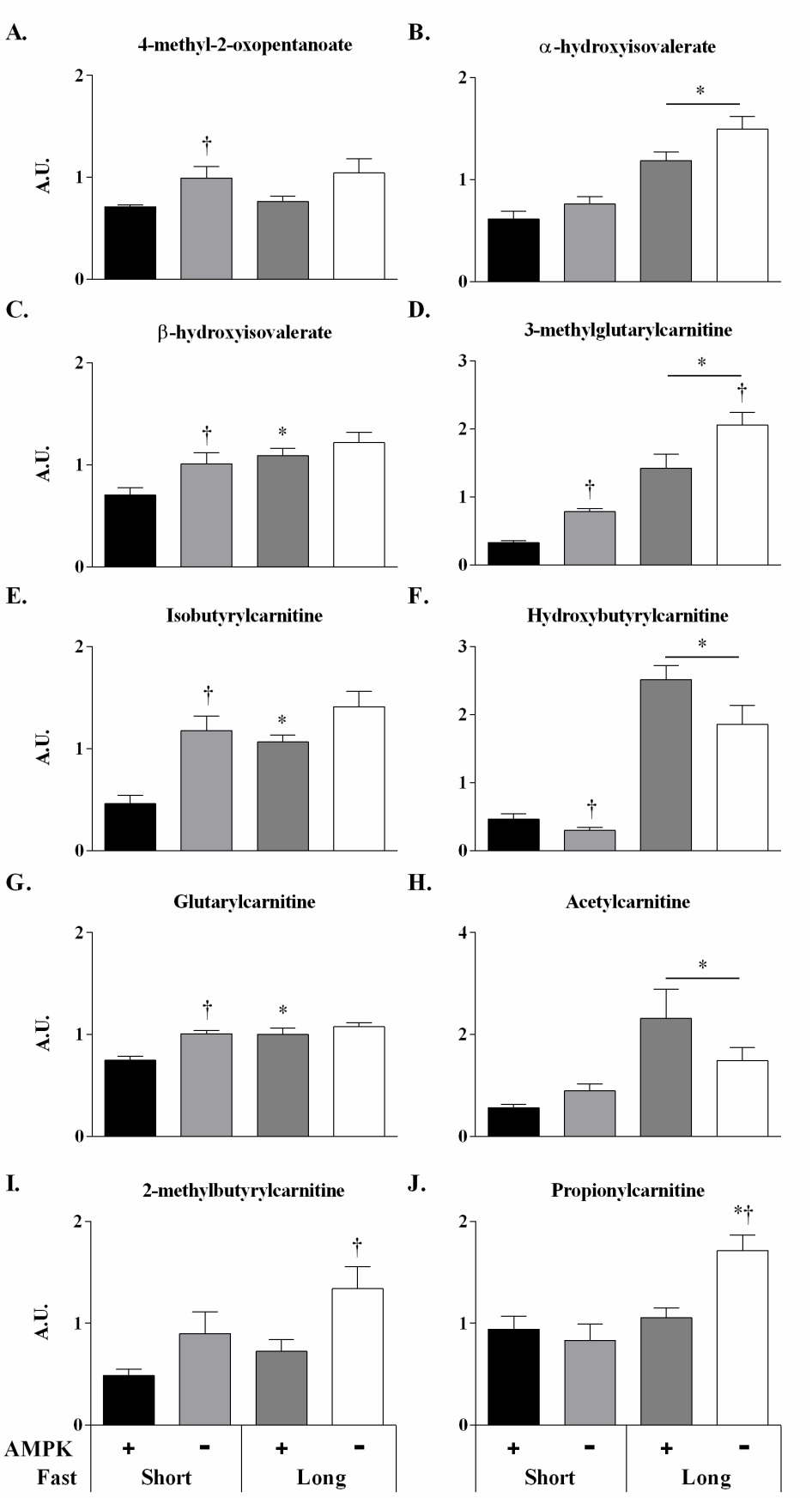


**Figure 3.8 –AMPK deletion results in aberrant BCAA/BCKA-related metabolism.** Liver BCAA/BCKA-related metabolites in short and long term fasted $\alpha 1\alpha 2^{lox/lox}$ and $\alpha 1\alpha 2^{lox/lox}$+Alb*cre* mice (**A-J.**). Medium and short chain acylcarnitine species derive from the metabolism of BCAA/BCKAs, amino acids, and certain fatty acids. Elevations in medium and short acylcarnitines (**D-J.**) have been linked with aberrant oxidative metabolism in liver. Data are expressed means±SE, *n=7-8* in each group. **p≤0.05* vs. short term fasting; †*p≤0.05* vs. $\alpha 1\alpha 2^{lox/lox}$ mice.

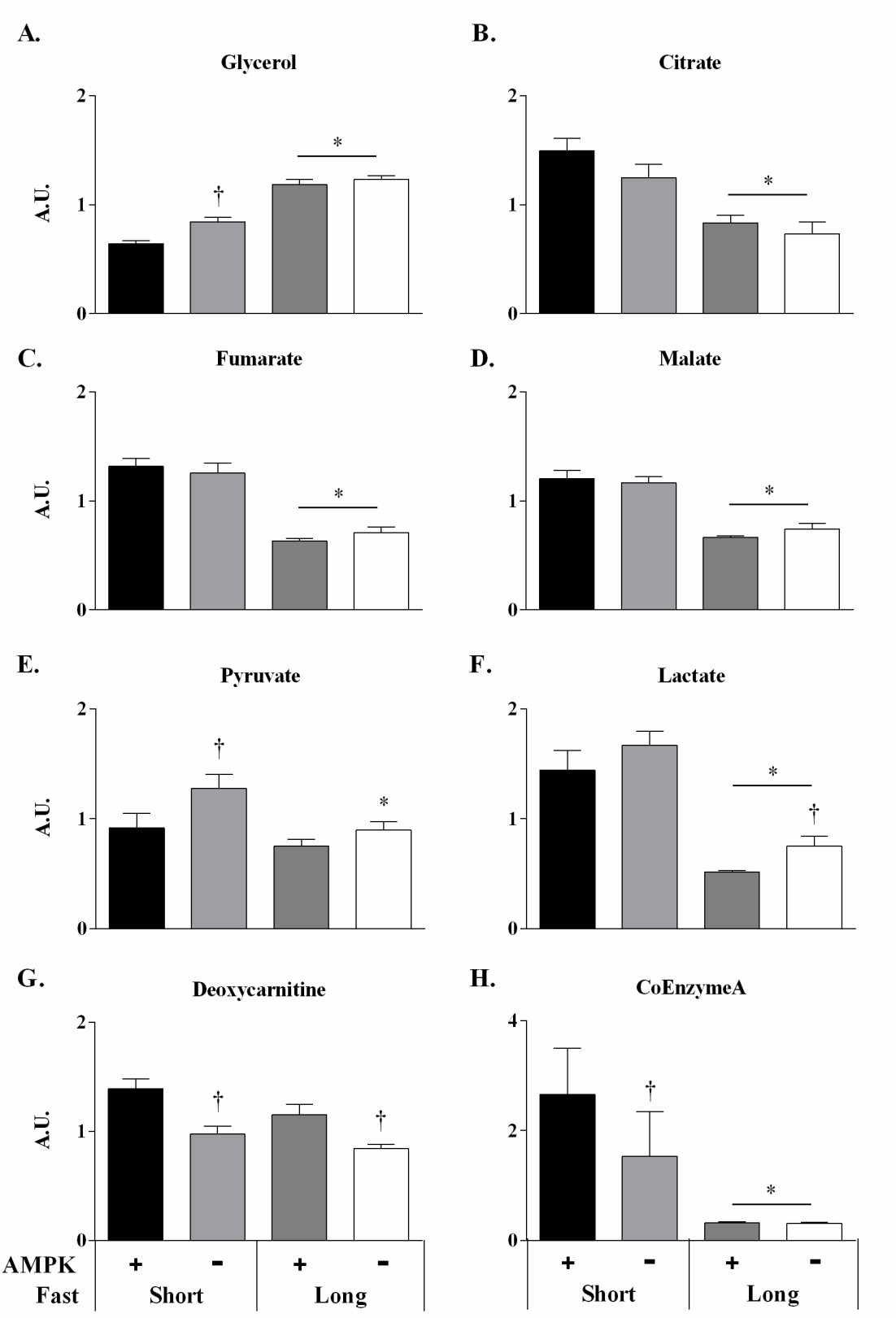


**Figure 3.9 –AMPK deletion alters oxidative metabolites but not TCA cycle intermediates.** Central metabolites for liver glucose production and oxidative metabolism in the liver in short and long term fasted $\alpha1\alpha2^{lox/lox}$ and $\alpha1\alpha2^{lox/lox}$+Alb*cre* mice (**A-H.**). Data are expressed as means±SE; *n=7-8* in each group. *p≤0.05* vs. short term fasting; †*p≤0.05* vs. $\alpha1\alpha2^{lox/lox}$ mice.

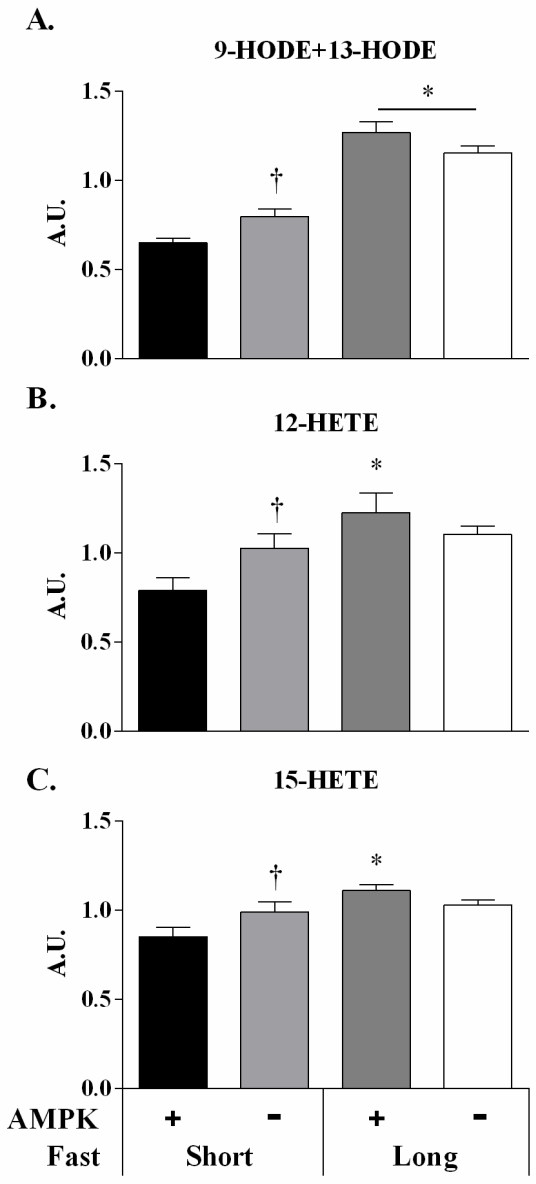


**Figure 3.10 –Lipid signaling molecules in the livers of α1α2$^{lox/lox}$ and α1α2$^{lox/lox}$±Alb*cre* mice.** Fatty acid species derived from the lipoxygenation of linoleic (**A.**) or arachidonic (**B,C.**) acids. Data are expressed as means±SE; *n=7-8* in each group. **$p \leq 0.05$* vs. short term fasting; *†$p \leq 0.05$* vs. α1α2$^{lox/lox}$ mice.

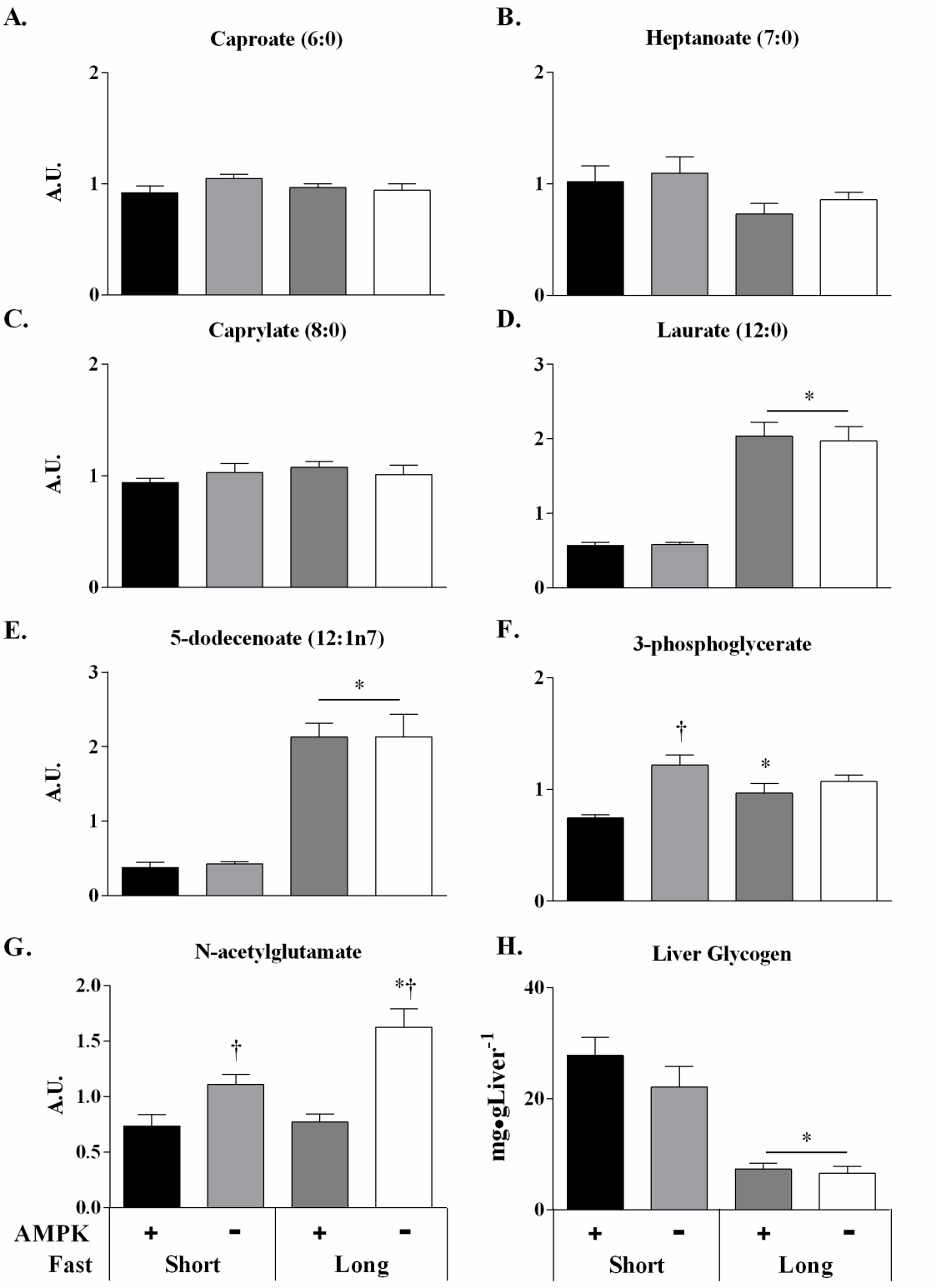


**Figure 3.11 –Liver medium chain fatty acids are unaffected by hepatic AMPK deletion.** Medium chain fatty acid species (**A-E.**), 3-phosphoglycerate (**F.**), N-acetylglutamate (**G.**), and glycogen (**H.**) in the liver of short or long term fasted $\alpha1\alpha2^{lox/lox}$ and $\alpha1\alpha2^{lox/lox}$+Alb*cre* mice. All data are expressed as means±SE; *n=7-8* in each group. **p≤0.05* vs. short term fasting; †*p≤0.05* vs. $\alpha1\alpha2^{lox/lox}$ mice.

# Chapter IV

## 5-AMINOIMIDAZOLE-4-CARBOXAMIDE-1-B-D-RIBOFURANOSIDE (AICAR) EFFECT ON GLUCOSE PRODUCTION, BUT NOT ENERGY METABOLISM, IS INDEPENDENT OF HEPATIC AMPK *IN VIVO*

### Aims

The coincidence of AMPK activation and the inhibition of glucose production by biguanides and AICAR suggest an overlap in function. This observation has led to the discovery of targets of AMPK action that exert control over the transcription of gluconeogenic enzymes (see **Chapter I**). Moreover, deletion of LKB1—which phosphorylates and activates AMPK—causes marked hyperglycemia *in vivo*. These compelling data have led investigators to equate AMPK activation with the inhibition of glucose production. However, the increase in nucleotide monophosphate (NMP) induced by AICAR and biguanides may be sufficient to acutely suppress glucose production *in vivo* (4, 34). The capacity of nucleotides to regulate metabolic flux has been recognized for decades (40, 216). The aims of this chapter are to determine if AMPK is necessary for the effects of an increment of NMP on 1) glucoregulation and 2) liver energy homeostasis *in vivo*. AMPK is clearly essential for the ordinary coupling of substrate utilization with energy production in the liver under physiological energy stress (**Chapter III**). Here we tested the hypothesis that hepatic AMPK is necessary for protecting liver energy status, but not the inhibition of glucose production, during an acute elevation in NMP *in vivo*. AICAR-euglycemic clamps were performed in mice with a liver-specific deletion of AMPK ($\alpha1\alpha2^{lox/lox}$ and $\alpha1\alpha2^{lox/lox}$+Alb*cre*) to limit fluctuations in arterial glucose and circulating hormones.

## Experimental Approach

Male $\alpha1\alpha2^{lox/lox}$ and $\alpha1\alpha2^{lox/lox}$+Alb*cre* were catheterized (**Chapter II**, Surgical Procedures) at 14wks of age for a primed continuous infusion of AICAR during euglycemia. A schematic for the experimental design is provided in **Fig. 4.1**. Tissue and plasma parameters were measured as specified in the Chapter II. The AICAR infusion rate ($40mg\cdot kg^{-1}$prime; $8mg\cdot kg^{-1}\cdot min^{-1}$ infusion) was selected based on the following two considerations:

1) AICAR-euglycemic clamps were performed in rats infusing comparable doses ($7.5\text{-}10mg\cdot kg^{-1}\cdot min^{-1}$) (133, 134, 199), which would afford a more robust basis for determining AMPK-dependent AICAR effects.

2) The infusions in rats hedged on the higher end of doses. We rationalized that the relatively high metabolic rate of the mouse would increase AICAR turnover and, thus, temper the perceived dose. In this setting, we would be able to test the AMPK-independent effectiveness of AICAR while limiting its associated complications (i.e. rhabdomyolysis).

## Results

### *Body Composition and 5hr Fasted Metabolites*

A cohort of 14wk-old $\alpha1\alpha2^{lox/lox}$ and $\alpha1\alpha2^{lox/lox}$+Alb*cre* mice were assayed to determine whether the absence of hepatic AMPK impacted whole body weight and composition. There were no apparent differences in body composition (Table 4.1). Arterial glucose, plasma insulin,

free fatty acids (FFAs), lactate, and triglycerides (TGs) were not different between $\alpha1\alpha2^{lox/lox}$ and $\alpha1\alpha2^{lox/lox}$+Alb*cre* after a 5hr fast (**Table 4.1**).

***AICAR-Mediated Inhibition of Glucose Production is Independent of Acute AMPK Activation***

*In vivo* and *in vitro* delivery of AICAR to hepatocytes inhibits glucose production (34, 133). To test whether AICAR requires AMPK for the inhibition of endogenous glucose production (EndoRa), AICAR was continuously infused at 8mg•kg$^{-1}$•min$^{-1}$ and blood glucose was clamped at ~110mg•dL$^{-1}$. During the experimental period, the glucose infusion rate (GIR) required to maintain euglycemia (**Fig. 4.2A**) was similar between genotypes in both Saline and AICAR-clamps (**Fig. 4.2B**); however the sustained elevation in GIR was significantly higher with the infusion of AICAR than Saline controls. EndoRa and glucose disappearance (Rd) were indistinguishable between genotypes prior to and during the AICAR or Saline-clamp (**Fig. 4.2C,D**). AICAR inhibited EndoRa equivalently in $\alpha1\alpha2^{lox/lox}$ and $\alpha1\alpha2^{lox/lox}$+Alb*cre* mice (0.8±1.4 and 1.1±2.4mg•kg$^{-1}$•min$^{-1}$). Likewise, AICAR induced an equal increment in Rd in $\alpha1\alpha2^{lox/lox}$ and $\alpha1\alpha2^{lox/lox}$+Alb*cre* mice (31.0±1.2 and 32.8±1.5mg•kg$^{-1}$•min$^{-1}$). Plasma insulin levels were indistinguishable between the Saline and AICAR-clamp groups (**Table 4.2**). The data show that the inhibition of EndoRa by AICAR (**Fig. 4.2C,D**) is disassociated from its capacity to activate AMPK (**Fig. 4.3A**) *in vivo.* AMPK deletion also provoked a reduction in liver glycogen (**Table 4.2**), which did not impact AICAR-mediated inhibition of EndoRa.

The 2hr AICAR infusion blunted plasma FFA and plasma TG concentrations in $\alpha1\alpha2^{lox/lox}$ and $\alpha1\alpha2^{lox/lox}$+Alb*cre* mice (**Table 4.2**). Indeed, AICAR was so potent at clearing FFAs that circulating levels were undetectable in $\alpha1\alpha2^{lox/lox}$ mice (**Table 4.2**). AICAR elicited a 6.6±0.6 and 5.2±0.5 fold increase in plasma lactate over Saline in $\alpha1\alpha2^{lox/lox}$ and

$\alpha1\alpha2^{lox/lox}$+Alb*cre* mice, respectively. The elevation in plasma lactate, however, was partially attenuated in $\alpha1\alpha2^{lox/lox}$+Alb*cre* mice (**Table 4.2**).

AMPK activation during energy stress is implicated in fat utilization in the liver (68). Liver TG levels in $\alpha1\alpha2^{lox/lox}$ and $\alpha1\alpha2^{lox/lox}$+Alb*cre* mice at the end of the Saline infusion were not statistically different (24.6±0.8 and 29.1±2.0 mg/gLiver) (**Table 4.2**). The AICAR infusion in $\alpha1\alpha2^{lox/lox}$ mice reduced hepatic TG concentrations compared to Saline controls (19.7±1.5 vs. 24.6±0.8mg/gLiver, *p=0.08*). $\alpha1\alpha2^{lox/lox}$+Alb*cre* did not experience the same AICAR-mediated reduction as hepatic TG concentrations were significantly higher than $\alpha1\alpha2^{lox/lox}$ (26.7±2.7 and 19.7±1.5 mg/gLiver) (**Table 4.2**). Inhibitory phosphorylation of acetyl-CoA carboxylase ($pACC^{S79}$) was similar between $\alpha1\alpha2^{lox/lox}$ Saline and AICAR groups at the end of the clamp (**Fig. 4.3B**). Indeed, AICAR can promote carnitine palmitoyl-transferase-1 (CPT-1) activity independent of changes in malonylCoA (217)**.** Thus, AICAR facilitates a decrease in liver TGs via hepatic AMPK.

### *AMPK Counters a Decrease in Hepatic Adenylate Energy Charge During an Acute AICAR Challenge In Vivo*

The primed, AICAR infusion resulted in comparable hepatic ZMP levels in the two genotypes (**Fig. 4.4C**). The conversion of AICAR to ZMP utilizes ATP (129) and ZMP has been demonstrated to inhibit complex I respiration in isolated mitochondria (127). Adenylate kinase maintains the equilibrium between ATP, ADP, and AMP; physiological and pharmacological perturbations in metabolism can alter this balance (4, 16, 28, 34, 36). Thus, hepatic ATP, AMP, and ADP were measured to investigate how an acute AICAR infusion perturbs hepatic adenylate energy balance in a euglycemic, *in vivo* setting. Liver ATP levels were comparable in $\alpha1\alpha2^{lox/lox}$

and $\alpha1\alpha2^{lox/lox}$+Alb*cre* mice (1.7±0.12 vs. 1.5±0.09μmol·$g^{-1}$) that received the Saline infusion (**Fig. 4.4A**). The AMP/ATP ratio and EC were similar to previous measurements taken under post-absorptive conditions (28). The AICAR infusion resulted in a significant reduction in the total adenine nucleotide (TAN) pool (3.3±0.09 to 1.6±0.02μmol·$g^{-1}$) in $\alpha1\alpha2^{lox/lox}$ and mice lacking hepatic AMPK (3.1±0.06 to 1.4±0.08μmol·$g^{-1}$) (**Fig. 4.4B**). Hepatic AMP levels were equivalent (0.43±0.04 vs. 0.47±0.03 μmol·$g^{-1}$) in Saline control groups. However, AICAR elicited a significant increase in AMP in $\alpha1\alpha2^{lox/lox}$+Alb*cre* over $\alpha1\alpha2^{lox/lox}$ mice (0.43±0.02 vs. 0.61±0.09 μmol·$g^{-1}$) (**Fig. 4.4A**). AICAR also elicited a reduction in ATP and ADP levels in both groups (**Fig. 4.4A**). The fall in ATP was exacerbated in the absence of hepatic AMPK. AICAR's deleterious effect on the adenylate pool is exemplified by the magnitude of change in EC and the AMP/ATP ratio. $\alpha1\alpha2^{lox/lox}$ mice sustained a ~20% reduction in EC whereas $\alpha1\alpha2^{lox/lox}$+Alb*cre* incurred a nearly two-fold greater reduction (**Fig. 4.4D**); the relative amount of available high energy, adenylate phosphate was severely reduced as reflected by the ~3 and ~6 fold rise in the AMP/ATP ratio in $\alpha1\alpha2^{lox/lox}$ and $\alpha1\alpha2^{lox/lox}$+Alb*cre* mice, respectively (**Fig. 4.4E**). Thus, AMPK limits the fall in energy charge induced by an acute AICAR infusion *in vivo.* These data are consistent with the effects of metformin and AICAR *in vitro* (34).

## Discussion

Compounds (endogenous and pharmaceutical) and conditions that increase hepatic AMPK activity have been demonstrated to mitigate hepatic processes central to the etiology of diabetes and obesity (4, 33, 34, 135, 170, 171, 180, 213, 218–222). Here we use genetic tools to distinguish between the AMPK-dependent and independent effects of AICAR *in vivo*. Recent evidence challenges the role of AMPK as an indispensable arbiter for the anti-glycemic action of

biguanides and adiponectin in hepatocytes (4, 34, 171). The studies herein define the regulatory role of energy state in terms of those metabolic effects that are mediated by hepatic AMPK and those that are not. This was accomplished by increasing the NMP concentration in the presence of a fixed glucose concentration using an AICAR-euglycemic clamp technique in the presence and absence of hepatic AMPK *in vivo*.

AMPK activation is broadly implicated in the transcriptional control of mediators of gluconeogenesis (71, 166, 168, 223–226). Cre-mediated removal of the AMPKα2 catalytic subunit from the liver results in substantial increases in fasting glucose and insulin (155). It has also been demonstrated that the overexpression of constitutively active AMPKα2 reduces fasting glucose with a concomitant attenuation of PEPCK and G6Pase gene expression (71). Moreover, AICAR attenuates the gene expression of PEPCK and G6Pase; this effect has been attributed to AMPK activation (166, 223, 226), but the requirement for this enzyme in acute control has recently been strongly contested in primary hepatocytes and metabolic tests *in vivo* (34). We demonstrate that the genetic removal of both AMPKα1 and α2 catalytic subunits from the liver has no impact on rates of endogenous glucose production or disappearance in the conscious, 5hr fasted mouse. During euglycemia, liver AMPK is neither required for the AICAR-mediated inhibition of EndoRa nor its stimulation of glucose disappearance. These data impart two important results regarding the role of AMPK in the acute glucoregulation: the genetic deletion of AMPK from the liver (1) does not affect 5hr fasting glucose kinetics and (2) is unnecessary for the AICAR mediated suppression of EndoRa in the short-fasted mouse.

Though these studies highlight the power of AICAR to inhibit glucose production *in vivo*, the results do not discount the possibility that hepatic AMPK participates in the regulation of glucose flux under other conditions. The experiments were designed to study glucose flux in the

short-fasted, post-absorptive mouse to limit the effects of fast duration on hepatic nucleotides and AMPK signaling. These and other recent studies (4, 16, 34) emphasize the need to demarcate the *in vivo* effects of AMPK in physiology from pharmacology.

Recent literature on glycemic regulation by glucagon (16) and biguanides (4, 34) has reinvigorated the conversation surrounding AMP and energy charge as regulatory variables (40, 216). Glucagon-mediated flux through PEPCK appears to generate an autoregulatory feedback loop limiting the fall in ATP due to gluconeogenesis (16). These studies demonstrate that the unique plasticity of liver EC has an important function in response to a normal elevation in endocrine action. Indeed, glucagon provokes distinct changes in liver function which correspond to a relative decrease in available ATP (16), despite the stimulation of fat oxidation and suppression of triglyceride synthesis (21).

A therapeutic advantage of AMPK-activators like AICAR and biguanides is that they are not dependent on cataplerotic flux to glucose for an increase in the AMP/ATP ratio. Rather, metformin has been shown to inhibit mitochondrial complex I activity (125, 128), depress energy charge and activate AMPK (34). AMP has the capacity to inhibit fructose 1,6-bisphosphatase (39) and adenylyl cyclase (4). ZMP, the AMP mimetic generated from AICAR, also inhibits the former (222) and interferes with complex I activity in isolated mitochondria (127). In well-controlled conditions in which glucose is tightly regulated, the AICAR infusion induces a large drop in the total adenine nucleotide pool, EC, and an increase in the AMP/ATP ratio. The AICAR stimulated fall in ATP is even larger in the absence of hepatic AMPK, which manifests into a greater drop in EC and increase in AMP/ATP. *In vivo* (33, 125) and *in vitro*(34, 127) delivery of AICAR can disrupt the hepatic adenylate energy pool and induce a drop in ATP.

AMPK clearly plays a protective role, maintaining energy state in the presence of the metabolic challenge induced by nucleotide phosphate disequilibrium.

Substrate utilization and energy production are functionally linked through oxidative phosphorylation. Physiological conditions characterized by decreases in ATP also correspond to elevations in fat, amino acid, glycerol, and lactate utilization in the liver (11). The AICAR infusion provokes a fall in available energy. Liver AMPK knockout impairs mitochondrial function and increases hepatic fatty acids, which may exacerbate AICAR's effects on hepatic energy state (See Chapter III, **Fig. 3.5A,B**). Energy production from fat primarily results from the generation of reducing cofactors for oxidative phosphorylation. Additionally, AMPK promotes mitochondrial complex II and III expression, which serve as sites for the provision of reducing equivalents (**Fig. 3.5C**). During AICAR delivery, the efficient coupling of reduced cofactors with ATP production may be vital to preserving energy charge. Reductions in complex II and III expression and mitochondrial efficiency may trigger the larger increment in the AMP/ATP ratio observed in AMPK-deficient livers. It should be noted that impairments in hepatic energy homeostasis in $\alpha1\alpha2^{lox/lox}$+Alb*cre* mice only emerged with AICAR administration. No differences in adenine nucleotides, EC, or AMP/ATP were observed in short-fasted, euglycemic $\alpha1\alpha2^{lox/lox}$ and $\alpha1\alpha2^{lox/lox}$+Alb*cre* mice receiving the Saline infusion. Thus, defects in substrate utilization and mitochondrial function in $\alpha1\alpha2^{lox/lox}$+Alb*cre* mice only affect liver energy state when linked with elevated metabolic stress.

Similar to the effects of metformin, ZMP interferes with complex I and impairs state 3 respiration (127). AICAR may promote AMPK-dependent and independent fat transport into the mitochondria yet impede cofactor oxidation. As a result, liver energy charge may decline despite

a relative abundance of substrate, NADH and $FADH_2$. A similar hypothesis has been proposed for the actions of metformin (227).

The deleterious effect of AICAR on EC may be compounded by the inhibition of hepatic glucose uptake. AICAR delivery into the portal vein renders the liver insensitive to net hepatic glucose uptake, even during hyperglycemia and hyperinsulinemia (228). *In vitro* work confirms that AICAR reduces glucokinase translocation and glycolysis in hepatocytes (229), in AMPK-dependent (230) and independent (231) conditions. Our AICAR delivery rate was selected to permit a reasonable physiological comparison between our results and earlier AICAR-euglycemic clamps in rodents (133, 134). The resulting dose was sufficient to perturb hepatic adenylate energy balance and we expect that the depletion of ATP could contribute to an inhibition of liver glycolysis (230, 231). AICAR also elevates plasma lactate *in vivo* (33, 133), which may result from increased production from muscle (232) and impaired uptake in the liver (222). Since AICAR induced an equal increment in glucose disappearance in both genotypes, it is reasonable to assume muscle lactate production is unaffected by liver AMPK knockout. The attenuated elevation in plasma lactate in $\alpha1\alpha2^{lox/lox}$+Alb*cre* mice may instead reflect a switch in substrate uptake and utilization in the liver during AICAR administration.

The metabolic challenge induced by AICAR inhibits both glucose flux in and out of the liver effectively generating a condition in which the liver may become more reliant on fat oxidation. Ample molecular and physiological evidence connects AMPK activation with fat utilization in the liver. AICAR reduces hepatic TGs under various conditions in rodents (135, 213, 218) and increases fatty acid oxidation in hepatocytes (136, 217, 233). Knockout of the AMPKα2 subunit in the liver (155) results in increased circulating fatty acids, TGs, and a decrease in β-hydroxybutyrate. Whereas, the short-term overexpression of a constitutively active

form of AMPKα2 reduces plasma TGs and increases β-hydroxybutyrate (71). Together, this suggests AMPK mediates fatty acid uptake and oxidation. Our data demonstrate that AICAR's acute effect on hepatic TGs requires liver AMPK. $pACC^{S79}$ is undetectable in $\alpha1\alpha2^{lox/lox}$+Alb*cre* mice and, thus, higher in AICAR-treated $\alpha1\alpha2^{lox/lox}$ mice (**Fig. 4.3B**), implicating increased CPT-1 activity as a potential mechanism for elevated fat oxidation in the liver. However, $pACC^{S79}$ was not different between $\alpha1\alpha2^{lox/lox}$ Saline and $\alpha1\alpha2^{lox/lox}$ AICAR. It is plausible that increased NMP drives fatty acid flux away from *de novo lipogenesis* and through CPT-1 (217), in an AMPK-dependent and $pACC^{S79}$-independent manner.

Lastly, AMPK has been shown to regulate mediators of TG and cholesterol synthesis (67, 194, 234, 235). At the end of the AICAR infusion, higher liver TGs in $\alpha1\alpha2^{lox/lox}$+Alb*cre* mice could conceivably result from an impaired inhibition of TG synthesis (*de novo* synthesis or FA re-esterification) or a reduction in TG export. If this were the case, one might expect circulating TGs to follow a similar trend, yet circulating TGs were equivalent in $\alpha1\alpha2^{lox/lox}$ and $\alpha1\alpha2^{lox/lox}$+Alb*cre* mice. Evidence from these studies point to impairments in fat utilization as a source of elevated TGs in the livers of $\alpha1\alpha2^{lox/lox}$+Alb*cre* mice following AICAR administration.

Collectively, the data provide *in vivo* support for the energy sensor paradigm (38)—AMPK acts as a sensor and safeguard of the hepatic adenylate energy pool during an acute challenge to the energy status of the liver. The absolute amounts of ATP, ADP, and AMP in the liver are dictated by changes in synthesis and breakdown, with adenylate kinase coordinating their relative balance. Genetic deletion of AMPK exacerbates the AICAR-mediated disturbance of the adenylate pool and a larger reduction in available ATP. The evidence suggests that AMPK works to promote fat utilization and mitochondrial function during a pharmacological increase in ATP consumption, as liver AMPK knockout leaves liver TGs elevated. These data prove that

AMPK is not required for the acute inhibition of endogenous glucose production during elevations in AMP, the AMP/ATP ratio, or ZMP *in vivo*. This and other recent research (4, 34, 171) has important implications for therapeutics designed to target the pathogenesis of diabetes and metabolic diseases.

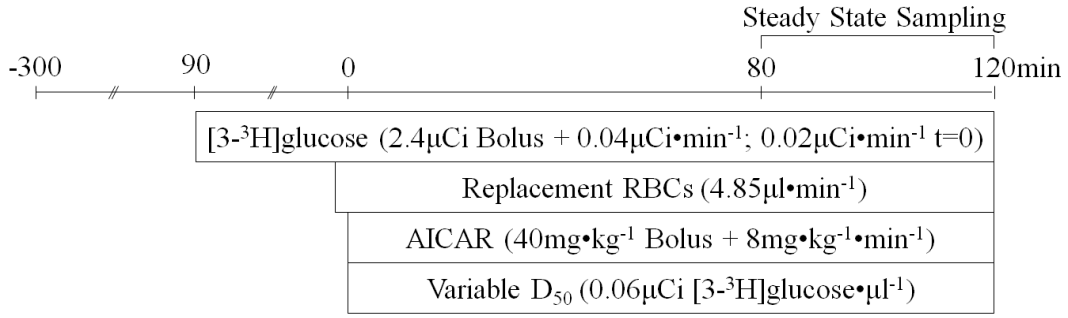


**Figure 4.1 –Schematic for AICAR-euglycemic clamps.** α1α2$^{lox/lox}$ and α1α2$^{lox/lox}$+Alb*cre* mice were fasted for 3.5hrs prior to the primed, continuous delivery of [3-$^{3}$H]glucose. Basal (5hr fasted) glucose kinetics and circulating parameters were determined from arterial plasma samples taken directly prior to the ACIAR infusion. At t=0, AICAR was delivered as a primed continuous infusion (40mg·kg$^{-1}$bolus, 8mg·kg$^{-1}$·min$^{-1}$ infusion). Blood glucose was monitored over the 120min time course and glucose was infused to minimize deviations from ~110mg·dL$^{-1}$. 5 steady state plasma samples were drawn between 80-120min to determine clamp glucose kinetics and circulating parameters.

| | **α1α2$^{lox/lox}$** | **α1α2$^{lox/lox}$ + Alb*cre*** |
|---|---|---|
| Body Composition | | |
| Body Weight (g) | 28.3±1.0 | 28.2±0.8 |
| Fat (%) | 9.3±1.1 | 10.6±0.5 |
| Muscle (%) | 87.6±3.1 | 86.9±0.5 |
| Plasma Metabolites | | |
| Blood Glucose | 118±3 | 117±4 |
| Insulin (ng/mL) | 1.9±0.3 | 2.1±0.4 |
| Triglycerides (mg/dL) | 95±8 | 82±7 |
| Lactate (mmol/L) | 0.7±0.1 | 0.6±0.1 |
| Free Fatty Acids (mEq/L) | 0.30±0.03 | 0.38±0.07 |

**Table 4.1 –Body composition and 5hr fasted metabolites of α1α2$^{lox/lox}$ and α1α2$^{lox/lox}$+Alb*cre* mice.** Plasma metabolites were isolated from arterial blood samples taken from 5hr fasted α1α2$^{lox/lox}$ and α1α2$^{lox/lox}$+Alb*cre* mice. Body composition was performed on a separate cohort of α1α2$^{lox/lox}$ and α1α2$^{lox/lox}$+Alb*cre* mice. Data are expressed as means ±SE, *n=5-13* in each group.

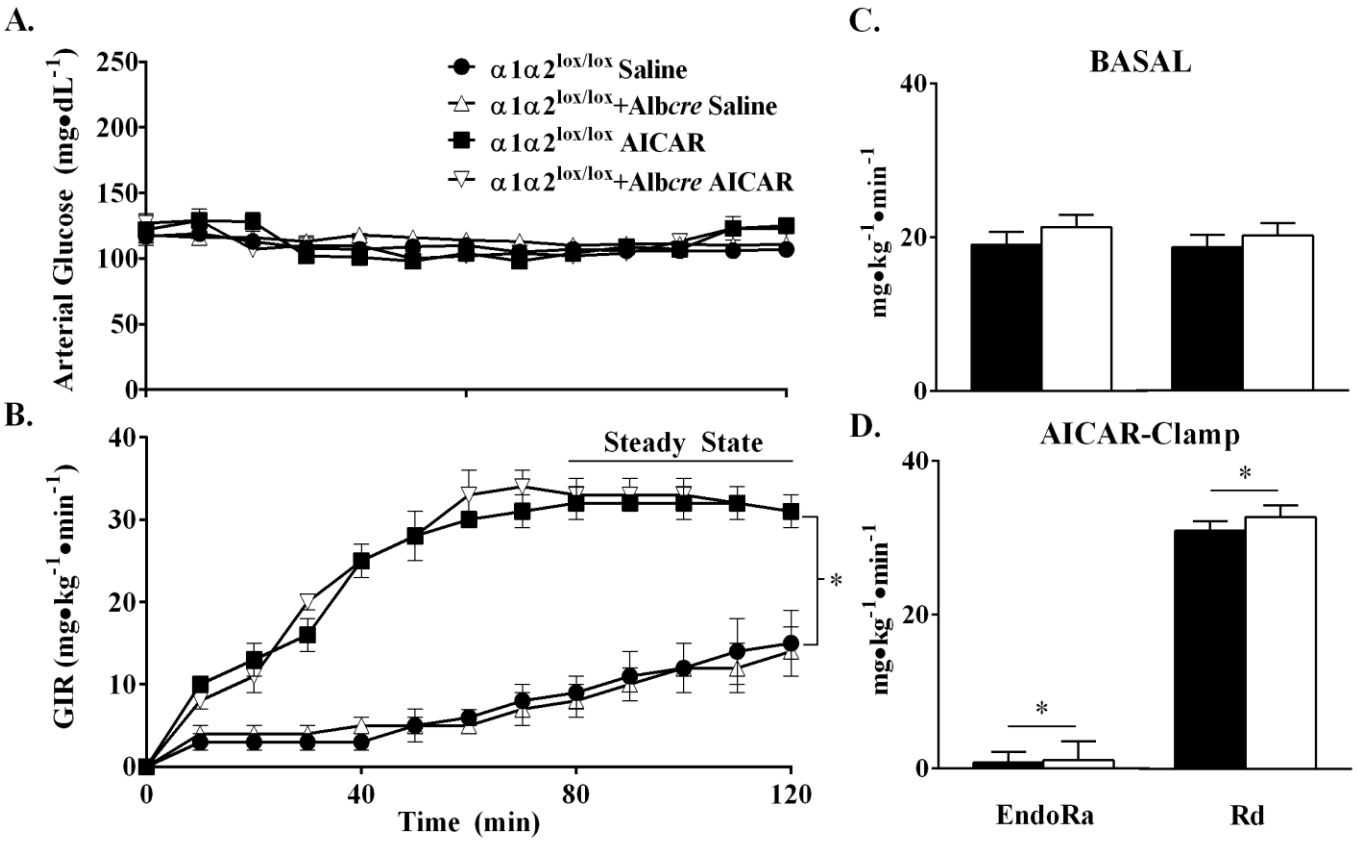


**Figure 4.2 –Acute inhibition of glucose production by AICAR is independent of hepatic AMPK.** Arterial glucose (**A.**) and glucose infusion rate (GIR) (**B.**) during AICAR and Saline clamps in $\alpha1\alpha2^{lox/lox}$ and $\alpha1\alpha2^{lox/lox}$+Alb*cre* mice. Mice were fasted 5hr prior to the primed (40mg•kg$^{-1}$) infusion of AICAR (8mg•kg$^{-1}$•min$^{-1}$) or Saline. Blood glucose was clamped at 110mg•dL$^{-1}$ and the time course is displayed to demonstrate experimental quality. 50% dextrose was infused to maintain euglycemia during the steady state of the clamp (t=80-120min). Endogenous glucose production (EndoRa) and disappearance (Rd) during the Basal period (5hr fasted) (**C.**) and steady state of the AICAR-clamp (**D.**) in $\alpha1\alpha2^{lox/lox}$ (■) and $\alpha1\alpha2^{lox/lox}$ +Alb*cre* (□). GIR means from the experimental period were analyzed for significance. Data are expressed as means ±SE, *n=5-12* in each group. *$p\leq0.05$ vs. Sal.

| | $\alpha1\alpha2^{lox/lox}$ | $\alpha1\alpha2^{lox/lox}$ + Alb*cre* |
|---|---|---|
| Blood Glucose(mg/dL) | | |
| Saline-Clamp | 109±4 | 113±4 |
| AICAR-Clamp | 111±2 | 112±5 |
| Insulin (ng/mL) | | |
| Saline-Clamp | 4.1±0.5 | 3.0±0.7 |
| AICAR-Clamp | 6.9±1.5 | 4.5±1.6 |
| Triglycerides (mg/dL) | | |
| Saline-Clamp | 41±5 | 45±5 |
| AICAR-Clamp | 17±1* | 22±4* |
| Lactate (mmol/L) | | |
| Saline-Clamp | 0.8±0.1 | 0.7±0.1 |
| AICAR-Clamp | 5.0±0.5* | 3.7±0.3*† |
| Free Fatty Acids (mEq/L) | | |
| Saline-Clamp | 0.47±0.06 | 0.48±0.07 |
| AICAR-Clamp | ND* | 0.06±0.02* |
| Liver Triglycerides (mg/gLiver) | | |
| Saline-Clamp | 24.6±0.8 | 29.1±2.0 |
| AICAR-Clamp | 19.7±1.5$ | 26.7±2.7† |
| Liver Glycogen (mg/gLiver) | | |
| Saline-Clamp | 7.2±2.2 | 3.1±0.8 |
| AICAR-Clamp | 14.6±3.4* | 2.1±0.4† |

**Table 4.2 –AICAR-euglycemic clamp metabolites.** Plasma and liver metabolite concentrations during the Saline or AICAR ($8mg \cdot kg^{-1} \cdot min^{-1}$) euglycemic-clamp from $\alpha1\alpha2^{lox/lox}$ and $\alpha1\alpha2^{lox/lox}$ + Alb*cre* mice. Plasma metabolites were isolated from arterial blood samples drawn from externalized catheters in conscious, unstressed mice during the clamp steady state. Liver triglycerides and glycogen were measured from freeze-clamped tissue excised at the end of the clamp. Blood glucose means from the experimental period were analyzed for significance. Data are expressed as means ±SE, *n=4-7* in each group. Values lower than detectable range (ND);*$p \leq 0.05$ vs. Sal; †$p \leq 0.05$ vs. $\alpha1\alpha2^{lox/lox}$; \$$p=0.08$ vs. Sal.

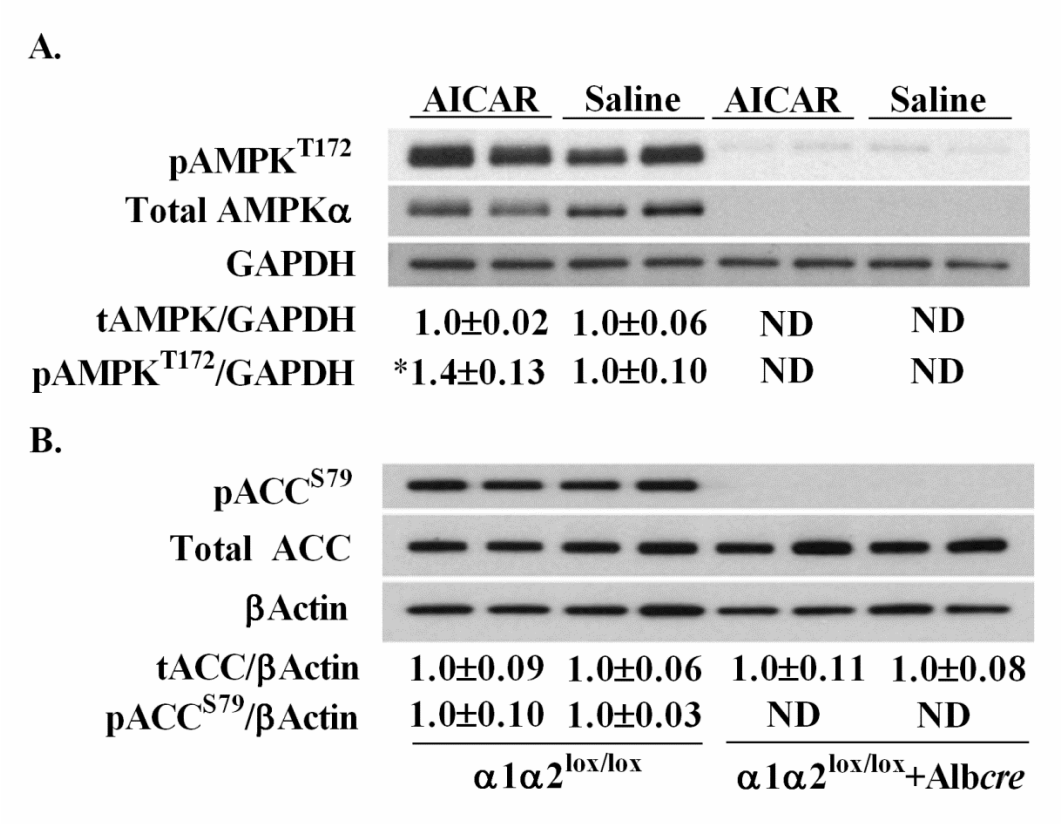


**Figure 4.3 –Effect of AICAR on liver AMPK activation state.** Total, pAMPK$^{T172}$ (**A.**) and total, pACC$^{S79}$ (**B.**) from the livers of α1α2$^{lox/lox}$ and α1α2$^{lox/lox}$+Alb*cre* mice following the AICAR or Saline clamp. Data are normalized to GAPDH or βActin and expressed as means ±SE; values below the blots are arbitrary units normalized to α1α2$^{lox/lox}$ Saline controls, *n=5-6* in each group. *$p \leq 0.05$ vs. Sal. ND, values lower than detectable range.

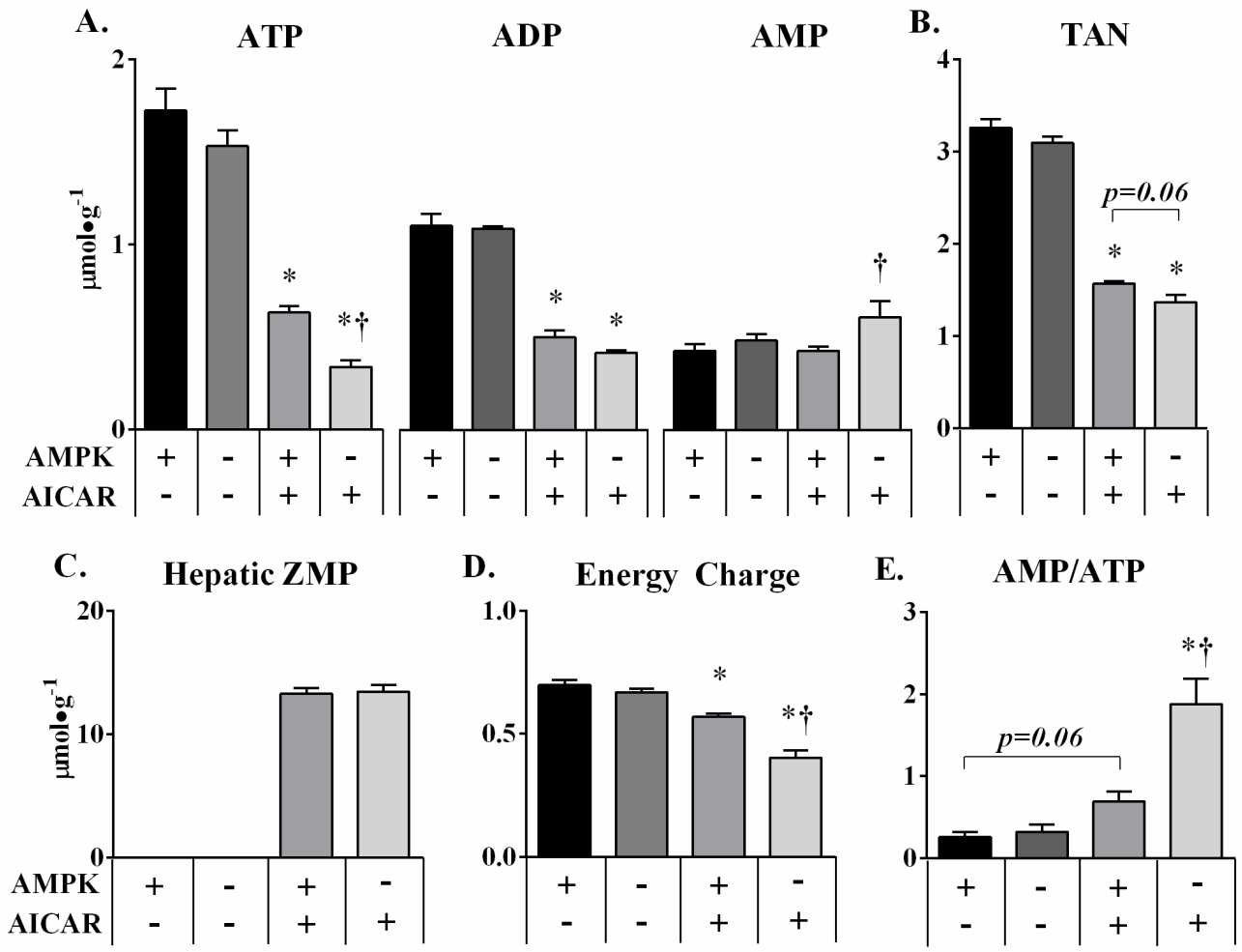


**Figure 4.4 –Liver AMPK deletion exacerbates AICAR effects on hepatic energy state.** Hepatic adenine nucleotides (**A.**) and the total adenine nucleotide pool (TAN) (**B.**) were measured by HPLC from liver extracts taken from $\alpha1\alpha2^{lox/lox}$ and $\alpha1\alpha2^{lox/lox}$+Alb*cre* mice at the end of the AICAR or Saline clamp. Hepatic ZMP levels (**C.**) were also measured to assess the quality of AICAR delivery into the liver. Energy charge (**D.**) was calculated by the following equation, ([ATP]+0.5[ADP])/([ATP]+[ADP]+[AMP]), to assess the energy state of the liver. The AMP/ATP ratio (**E.**) was provided for each clamp group. Data are expressed as means ±SE, *n=5-6* in each group. *$p \leq 0.05$ vs. Sal; †$p \leq 0.05$ vs. $\alpha1\alpha2^{lox/lox}$.

# Chapter V

## EXERCISE TRAINING ATTENUATES METABOLIC ABNORMALITIES IN THE LIVERS OF HIGH-FAT FED MICE LACKING HEPATIC AMPK

### Aims

The aim of this chapter was to determine the AMPK-dependent effectiveness of regular, voluntary exercise on 1) the amelioration of fatty liver and 2) energy state during HF-feeding. An increment in glucagon action couples substrate utilization and hepatic glucose flux to accommodate the body's increased energetic demands during exercise (2, 9, 236, 237). Glucagon action is necessary for the exercise-mediated reversal of fatty liver (36). Moreover, glucagon administration can prevent and attenuate fatty liver (238, 239). These results add to the body of literature substantiating the invaluable role of glucagon in control of hepatic metabolic flux (8, 10, 18, 20, 21, 240). Glucagon regulates molecular mechanisms that support fat oxidation *in vitro* (21) and *in vivo* (36). Regular bouts of exercise may exert tonic effects on fat oxidation through PPARα (21, 36, 109) and FGF21 (36, 241, 242). Glucagon may also regulate lipogenesis by suppressing SREBP-1c expression and activity (66, 189).

Importantly conditions characterized by elevated glucagon action activate hepatic AMPK (16, 21, 28, 36). An extensive overlap exists between the effects of glucagon and AMPK activity on mediators of fat oxidation and synthesis (68). AMPK phosphorylation interferes with the expression and activity of SREBP-1c (67) and ACC (190, 191) which, in turn, inhibits lipogenesis and promotes fat oxidation. Chronic exercise reduces the expression of mediators of lipogenesis and promotes fatty acid transport into the mitochondria (243). Furthermore, AMPK

supports mitochondrial function and the maintenance of hepatic energy charge (**Chapter III**). Despite the overlap between elevated glucagon action and AMPK activation, the requirement of AMPK for exercise-mediated reductions in fatty liver has not been elucidated. These studies tested the necessity of AMPK for the amelioration of fatty liver by exercise.

## Experimental Approach

Fatty liver was induced in floxed control ($\alpha1\alpha2^{lox/lox}$) and liver-specific AMPKα knockout ($\alpha1\alpha2^{lox/lox}$ +Alb*cre*) mice through 6wks of high-fat (HF) feeding. For an additional 10wks, mice were maintained on a HF-diet with access to operable ($RW_{EX}$) or inoperable (Sed) running wheels (**Fig. 5.1A**). Running wheel activity was continuously monitored using a digital revolution counter. Body weight, composition, and plasma parameters were measured throughout the fatty liver induction and intervention phases. 48hrs after the last bout of exercise (~16wks of HF-dieting ± 10wks $RW_{EX}$), mice were sacrificed by cervical dislocation and liver tissues were analyzed through standard biochemical and state-of-the-art metabolomics methods (as detailed in **Chapter II**).

## Results

### *Liver AMPK Deletion does not Affect Changes in Body Weight and Composition during the Induction Phase*

Body weight and composition were no different between $\alpha1\alpha2^{lox/lox}$ and $\alpha1\alpha2^{lox/lox}$+Alb*cre* mice at 6wks (**Fig. 5.1B-D**). 6wk-old male mice were HF-fed for 6wks to induce fatty liver. Both groups experienced a progressive increase in body weight over the 6wk

Induction Phase (**Fig. 5.1B**) and exhibited no genotype specific differences. From 6 to 12wks, absolute lean (14.7±0.56 to 19.8±0.49g and 14.2±0.74 to 20.5±0.52g) and fat mass (1.3±0.05 to 9.6±0.6g and 1.4±0.09 to 10.1±1.0g) significantly increased in $\alpha1\alpha2^{lox/lox}$ and $\alpha1\alpha2^{lox/lox}$+Alb*cre* mice. 6wks of HF-feeding caused an equal increase and decrease in %Fat and Muscle, respectively, in both genotypes (**Fig. 5.1C,D**).

***Exercise Training Mediates Improvements in Whole-Body Health Independent of Hepatic AMPK***

Body weight, composition, blood glucose, insulin, and leptin were no different in untrained $\alpha1\alpha2^{lox/lox}$ and $\alpha1\alpha2^{lox/lox}$+Alb*cre* mice at 12wks (**Fig. 5.2B-G**). HF-feeding increased total body weight over the 10wk Intervention Phase in $\alpha1\alpha2^{lox/lox}$ and $\alpha1\alpha2^{lox/lox}$+Alb*cre* Sed mice (**Fig. 5.2B**). Running wheel activity during the Intervention Phase was not statistically different between $\alpha1\alpha2^{lox/lox}$ and $\alpha1\alpha2^{lox/lox}$+Alb*cre* mice (**Fig. 5.2A**). $RW_{EX}$ resulted in a reduction in body weight and fat mass compared to sedentary controls. Lean mass, however, did not differ (**Fig. 5.2B-D**). The absence of hepatic AMPK had no impact on diet or $RW_{EX}$-mediated alterations in body weight or composition.

Glucose and insulin means were no different between $\alpha1\alpha2^{lox/lox}$ and $\alpha1\alpha2^{lox/lox}$+Alb*cre* Sed mice during the Intervention Phase (**Fig. 5.2E,F**). Insulin increased in sedentary controls over the 10wk Intervention Phase (**Fig. 5.2F**), which corresponded to a reduction in blood glucose by 22wks (**Fig. 5.2E**). $RW_{EX}$ reduced blood glucose within 5wks of training, which persisted until the end of the study (**Fig. 5.2E**). Plasma insulin levels were unchanged from values at the beginning of the Intervention Phase in both $RW_{EX}$ groups (**Fig. 5.2F**). $HbA1_c$ levels were not different in $\alpha1\alpha2^{lox/lox}$ and $\alpha1\alpha2^{lox/lox}$+Alb*cre* Sed (5.3±0.32 and 5.0±0.12) or $RW_{EX}$

(4.8±0.06 and 4.9±0.13, respectively) groups at the end of the Intervention Phase. Leptin uniformly increased over time in $\alpha1\alpha2^{lox/lox}$ and $\alpha1\alpha2^{lox/lox}$+Alb*cre* Sed mice (**Fig. 5.2G**). Though elevated by the end of the Intervention Phase, $RW_{EX}$ attenuated the increment in leptin at 17wks in $\alpha1\alpha2^{lox/lox}$ and $\alpha1\alpha2^{lox/lox}$+Alb*cre* mice. Thus, AMPK is not required for $RW_{EX}$ effects on blood glucose, insulin, and leptin during HF-feeding.

### *AMPK Mediates Effects on Hepatic Lipids but is Not Required for the Amelioration of Fatty Liver by Voluntary Exercise*

*Liver Triglycerides (TGs), Cholesterol Esters (CEs), and Diglycerides (DGs)*

Fatty liver is a condition defined by excessive TG accumulation. AMPK activation has been proposed to be involved in the reversal of fatty liver by exercise training (36). Liver TG composition and concentrations were not statistically different between $\alpha1\alpha2^{lox/lox}$ and $\alpha1\alpha2^{lox/lox}$+Alb*cre* Sed mice after 16wks of HF-feeding (**Fig. 5.3A**). 10wks of voluntary $RW_{EX}$ was sufficient to ameliorate fatty liver, independently of hepatic AMPK (**Fig. 5.3A**). $RW_{EX}$ elicited a 53±11 and 59±9% reduction in liver TGs in $\alpha1\alpha2^{lox/lox}$ and $\alpha1\alpha2^{lox/lox}$+Alb*cre* mice and induced a shift toward in TG polyunsaturation (**Fig. 5.3A**).

CE accumulation associates with fatty liver in rodents (36). Although modest $RW_{EX}$ effects were observed, CE content and composition were no different between $\alpha1\alpha2^{lox/lox}$ and $\alpha1\alpha2^{lox/lox}$+Alb*cre* Sed and $RW_{EX}$ mice (**Fig. 5.3B**). Likewise, liver AMPK deletion had no effect on hepatic DG levels in Sed and $RW_{EX}$ mice; however, DG polyunsaturation was elevated in $\alpha1\alpha2^{lox/lox}$+Alb*cre* $RW_{EX}$ mice (**Fig. 5.3D**).

*Liver Phospholipids (PLs)*

Aberrations in hepatic PLs have been reported in obesity (244) and fatty liver (36). Exercise exerted no effect on the total quantity or saturation of liver PLs in $\alpha1\alpha2^{lox/lox}$ mice (**Fig. 5.3C**). As observed in **Chapter III**, liver AMPK deletion resulted in a stark reduction in PLs in both Sed and $RW_{EX}$ groups (**Fig. 5.3C**), which corresponded to increased saturation and decreased polyunsaturation (**Fig. 5.3C**).

The gene effect on liver PLs corresponded to differences in metabolites utilized in PL synthesis. The *de novo* synthesis of the most abundant PL classes in eukaryotes, phosphatidylcholine (PC) and phosphatidylethanolamine (PE), is described by the Kennedy Pathway (245). $\alpha1\alpha2^{lox/lox}$+Alb*cre* Sed mice exhibited lower levels of choline, CDP-choline, and ethanolamine relative to controls (**Fig. 5.4A,B,E**). PC may also be synthesized through the tri-methylation of PE, with S-adenosylmethionine (SAM) serving as a methyl donor (245). Metabolites that cycle through SAM were disrupted by hepatic AMPK deletion (**Fig. 5.4F-I**). AMPK deletion reduced methionine and S-adenosylhomocysteine and increased SAM and 5-methylthioadenosine in Sed mice (**Fig. 5.4F-I**). $RW_{EX}$ largely mitigated the aberrations in PL-related metabolites in $\alpha1\alpha2^{lox/lox}$+Alb*cre* $RW_{EX}$ mice (**Fig. 5.4**). Despite these changes, liver PL levels in $\alpha1\alpha2^{lox/lox}$+Alb*cre* $RW_{EX}$ mice remained lower than in $\alpha1\alpha2^{lox/lox}$ $RW_{EX}$ mice (**Fig. 5.3C**).

***Deficits in Hepatic Energy State in the Absence of AMPK Associate with Alterations in TCA Cycle and Acylcarnitine Metabolites***

*Adenylate Energy Homeostasis and the TCA cycle*

Adenylate kinase catalyzes the interconversion of ATP, ADP, and AMP (38) which fluctuate in the liver during physiological or pharmacological perturbations in metabolism (16, 28, 30, 228). Dysregulated hepatic energy metabolism is characteristic of HF-feeding in rodents (16, 35) and obesity-related pathology in humans (31, 32, 146). These abnormalities may stem from the inefficient coupling of reduced cofactors with ATP production (35, 146, 147). The deletion of hepatic AMPK impairs mitochondrial function in chow-fed mice (**Chapter III**).

HF-feeding reduced ATP and ADP concentrations by 20±4 and 13±5%, respectively, in $\alpha1\alpha2^{lox/lox}$+Alb*cre* Sed mice (**Fig. 5.5A**), which corresponded to a 16±3% reduction in the total adenine nucleotide (TAN) pool (**Fig. 5.5B**). $RW_{EX}$ elicited an increment in hepatic ATP levels in $\alpha1\alpha2^{lox/lox}$ mice, which did not occur in the absence of AMPK (**Fig. 5.5A**). As a result, $RW_{EX}$ failed to increase energy charge (EC) or decrease the AMP/ATP ratio despite raising the TAN pool (3.7±0.14 to 4.3±0.11μmol·g$^{-1}$) in the absence of hepatic AMPK (**Fig. 5.5B-D**). Though AMPK-deficient livers exhibit a small recovery in ADP and TAN, AMPK is clearly essential for the maintenance and improvement of hepatic energy state during HF-feeding and $RW_{EX}$, respectively.

The TCA cycle couples substrate catabolism with oxidative phosphorylation. Liver AMPK deletion disrupted normal levels of TCA cycle intermediates and TCA-cycle related substrates. HF-feeding increased citrate, cis-aconitate and reduced fumarate and malate in $\alpha1\alpha2^{lox/lox}$+Alb*cre* mice compared to WT mice (**Fig. 5.6A,B,D,E**). No genotype-dependent changes in succinate were observed (**Fig. 5.6C**). Exercise training demonstrated remarkable

efficacy in normalizing TCA cycle intermediates. Indeed, citrate, cis-aconitate, succinate, fumarate, and malate levels were equivalent in $\alpha1\alpha2^{lox/lox}$ and $\alpha1\alpha2^{lox/lox}$+Alb*cre* $RW_{EX}$ mice and resulted from changes in both groups (**Fig. 5.6A-E**).

*Liver Acylcarnitine Metabolites*

The accumulation of acylcarnitine species in metabolic dysregulation may indicate incomplete or abnormal substrate oxidation (35, 82). Acylcarnitines of varying lengths emanate from tissue and organelle specific activities of carnitine acyltransferases (86, 246). In particular, short-chain acylcarnitines emanate from the catabolic pathway of branched chain amino (BCAA), keto (BCKA), and certain fatty acids. Degradation of the latter metabolites yields reducing cofactors, ketogenic (acetylCoA and acetoacetate) or anaplerotic (propionylCoA) moieties.

Interestingly, elevations in the aforementioned metabolites were observable only in the livers from $\alpha1\alpha2^{lox/lox}$+Alb*cre* mice (**Fig. 5.7A-F**). 3-methylglutaryl, glutaryl (trend), and succinylcarnitine were elevated in sedentary $\alpha1\alpha2^{lox/lox}$+Alb*cre* mice (**Fig. 5.7A-C**). The elevation in these metabolites was sustained with $RW_{EX}$. In fact, the carnitine conjugate of propionylCoA (propionylcarnitine) (**Fig. 5.7D**) increased with $RW_{EX}$ in $\alpha1\alpha2^{lox/lox}$+Alb*cre* mice. Moreover, acetylcarnitine—generated from the catalysis of carnitine and acetylCoA by carnitine acetyltransferase (247)—was elevated in $\alpha1\alpha2^{lox/lox}$+Alb*cre* $RW_{EX}$ mice (**Fig. 5.7E**).

Several small carbon chain substrates that enter the TCA cycle through anaplerosis or acetylCoA were also elevated with liver AMPK deletion. Glutamate, alanine, lactate, and 1,2-propanediol were elevated in either $\alpha1\alpha2^{lox/lox}$+Alb*cre* Sed or $RW_{EX}$ mice (**Fig. 5.7G-J**).

Exercise exerted no effect on these metabolites in $\alpha1\alpha2^{lox/lox}$ mice indicating that this phenotype is 1) dependent on liver AMPK deletion and 2) not correctable by chronic exercise in HF-feeding. Thus, hepatic AMPK deletion spurs a deficit in hepatic energy homeostasis that corresponds to an accumulation of anaplerotic and oxidizable carbon.

## Discussion

Dysregulated liver metabolism is associated with diabetes and obesity. Chronic HF-feeding impairs hepatic insulin signaling and associates with the development of fatty liver (36), altered mitochondrial function, and an induction of TCA cycle flux (35). These and other studies validate the capacity of exercise to reduce liver lipids (36, 152, 243). Regular voluntary exercise lowered circulating insulin, leptin, and whole-body adiposity. $RW_{EX}$ also improved hepatic energy state, which was associated with a shift in the relative amounts of TCA cycle intermediates. The following subsections discuss the degree to which the liver relies on AMPK for the hepatic effects of exercise training during overnutrition.

### *Hepatic AMPK is Unnecessary for the Reversal of Fatty Liver by Exercise*

Glucagon receptor signaling during regular exercise is a requisite for the reversal of fatty liver and an induction of genes that control oxidation in the liver (36). Glucagon action may increase AMPK-activation with chronic exercise training (36). In these studies, however, regular exercise ameliorated fatty liver through mechanisms independent of liver AMPK (**Fig. 5.3A**).

The effects of acute-moderate and high intensity exercise on hepatic AMPK activation are well documented (28, 62, 115, 248–251). Changes in hepatic energy state and AMPK activation after a single bout of exercise can be captured through rapid tissue excision and

storage. The effects of exercise training on AMPK activation are less uniform (36, 151, 252, 253). Discrepancies may stem from differences in exercise training protocols and duration from the last exercise bout.

Nevertheless, a body of literature substantiates AMPK's role in promoting fat oxidation and suppressing lipogenesis in the liver. AMPK phosphorylation regulates ACC (190, 191) and SREBP-1c (67). Administration of AMPK activators promote fat oxidation *in vitro* (136, 217) and reduce liver triglycerides *in vivo* (135, 213, 218). Moreover, genetic models that chronically activate (71) or remove (172) AMPK increase or impair fat utilization. In the present studies, we set out to determine the metabolic effects of hepatic AMPK deletion in HF-feeding and the requirement of AMPK for the exercise-mediated decrement in fatty liver. The results clearly demonstrate that exercise can employ mechanisms to reduce fatty liver independently of hepatic AMPK. In addition to reductions in liver TG content, $RW_{EX}$ elevated the percentage of TG polyunsaturation and decreased monounsaturation, regardless of genotype. A similar effect on hepatic lipid polyunsaturation has also been observed in humans following an acute exercise regimen (149).

Chronic exercise modalities may elicit changes in the body composition of mice. In these studies, the introduction of exercise offset the effects of HF-feeding on body weight and composition. Liver TGs are particularly sensitive to even modest changes in weight in humans (254). Dietary intervention in obese, HF-fed mice results in weight loss and large reductions in liver triglycerides (255). Furthermore, HF-feeding and exercise alter the phase and rhythm of voluntary exercise in mice (256). $RW_{EX}$ -mediated changes in feeding behvaior and whole-body adiposity may have contributed to the reversal of fatty liver and increase in TG polyunsaturation.

### *Hepatic AMPK is Necessary for the Effects of Regular Exercise on Energy Homeostasis during HF-Feeding*

Obesity and diabetes create a paradoxical energy state in the liver. Despite a chronic increase in nutrient availability, ATP consumption may exceed production and elicit a deficit in liver energy status (16). Impairments in hepatic ATP homeostasis have been observed in NASH (32) and type II diabetes (31). To this end, the ordinary coupling of TCA cycle flux (35), reducing cofactor (147) and hepatic glucose production become dysregulated (35). Recent *in vivo* research has made significant advances in measuring TCA cycle flux in the context of HF-feeding induced mitochondrial dysfunction (35). Indeed, HF-feeding alters mitochondrial content, function (35, 257), and TCA-cycle associated fluxes in the transition from 8 to 32wks of HF-feeding (35). A reduction in mitochondrial efficiency (State 3/State 4 respiration) combined with the increased energetic demands of gluconeogenesis during insulin resistance may necessitate a compensatory increase in TCA cycle flux (35). We demonstrate that regular exercise improves hepatic energy state through AMPK-dependent mechanisms.

Hepatic AMPK deletion impairs State 3 respiration, decreases mitochondrial respiration efficiency (State 3/State 2 respiration) and the expression of mitochondrial complexes II and III (**Chapter III**). Metabolic stress uncovers AMPK's role in maintaining energy homeostasis in the liver. AICAR delivery in chow-fed $\alpha1\alpha2^{lox/lox}$+Alb*cre* mice elicits a greater reduction in ATP, TAN, and energy charge than controls (**Chapter IV**). HF-feeding reduced ATP and TAN in sedentary, $\alpha1\alpha2^{lox/lox}$+Alb*cre* mice. Whereas $RW_{EX}$ increased ATP in WT mice, $RW_{EX}$ failed to improve deficits in ATP in the absence of liver AMPK. Thus, hepatic AMPK is required to dampen the energetic stress of HF-feeding with regular exercise.

Metabolomic analyses provided further evidence for an imbalance between substrate availability and oxidation in AMPK deficient livers. In $\alpha1\alpha2^{lox/lox}$+Alb*cre* Sed mice, the succinylCoA synthetase (SCS) step in the TCA cycle appears to serve as an important site of dysregulation in oxidative metabolism. Metabolites preceding SCS (citrate, cis-aconitate) accumulate and subsequent SCS (fumarate, malate) drop, with no apparent changes in succinate. Moreover, succinylcarnitine, which forms from succinylCoA, was elevated. When coupled with the reductions in ATP, TAN, and impaired mitochondrial function observed in chow-fed mice (**Chapter III**), the results strongly suggest that liver AMPK deletion causes inefficient or impaired substrate flux through the TCA cycle in high fat feeding.

Voluntary exercise normalized TCA-cycle intermediates in $\alpha1\alpha2^{lox/lox}$ and $\alpha1\alpha2^{lox/lox}$+Alb*cre* mice. Elevations in acylcarnitine metabolites, however, were augmented by exercise intervention in AMPK's absence. With the exception of 2-methylbutyrylcarnitine, acylcarnitine species with chain lengths between 2 and 6 carbons were increased. Some species derive primarily from amino acid catabolism (**Fig. 5.7A,B**) whereas others arise from odd-chain fatty acids, amino acids (**Fig. 5.7C,D**) or several substrates that yield acetylCoA (**Fig. 5.7E**). The acylcarnitine phenotype exhibited in liver AMPK-knockout mice shares a degree of overlap with other models of pathological or impaired oxidative metabolism (35, 88). In addition to the aforementioned acylcarnitine species, substrates that feed into pyruvate (i.e. lactate, alanine) were also elevated. The relative ATP deprivation in $\alpha1\alpha2^{lox/lox}$+Alb*cre* livers corresponds to an apparent accumulation of oxidizable/anaplerotic substrate.

AMPK has been strongly implicated in the control of hepatic fat oxidation, synthesis, and mitochondrial function (**Chapter III, IV**). In AMPK's absence, impairments in ATP production may be coupled to a metabolic switch that controls substrate selection. Though AMPK is not

required for the amelioration of fatty liver by $RW_{EX}$, energy deficits introduced by AMPK deletion may reflect an impairment or switch in the utilization of substrates targeted for the TCA cycle. Despite adequate amounts of oxidizable carbon, the liver may be kept in a perpetual state of pseudo-deprivation due to inefficient energy coupling.

***Novel Observations Concerning a Role for Liver AMPK in ER functions***

Hepatic AMPK has been a central molecular target in the investigation of *in vitro* and *in vivo* glucoregulation. The necessity of AMPK for normoglycemia and the action of AICAR/biguanides on hepatic glucose production has been evaluated in this dissertation and elsewhere (4, 34). No differences in plasma glucose or insulin emerged in HF-fed or exercised $\alpha1\alpha2^{lox/lox}$+Alb*cre* mice compared to $\alpha1\alpha2^{lox/lox}$ mice. Sedentary, $\alpha1\alpha2^{lox/lox}$+Alb*cre* mice exhibited a reduction in liver glycogen (**Fig. 5.8A**). Whole-body deletion of AMPKβ2 (214), but not β1 (172), also reduces liver glycogen levels. Glycogen is lengthened by the addition of the glucose moiety from UDP-glucose onto a nascent branch. Alternatively, UDP-glucose may be converted to UDP-glucuronate and conjugated to endo and xenobiotics or converted to ascorbate (258). We observed an elevation in metabolites of the glucuronidation and ascorbate synthesis pathways in liver AMPK knockout mice (**Fig. 5.8B-F**). Abnormalities in the "glycogenoreticular system" may be a cause or consequence of the abnormal reduction in liver glycogen observed in the absence of AMPK.

The endoplasmic reticulum (ER) serves as a key locus for glucuronidation, ascorbate (258) and PL synthesis in the liver (259). The absence of hepatic AMPK reduced liver PLs in sedentary and $RW_{EX}$ mice. Metabolic abnormalities in PC and PE biosynthetic pathways were

observed in $\alpha1\alpha2^{lox/lox}$+Alb*cre* Sed livers. These observations provide evidence for a role of AMPK in proper ER functioning.

***Summary***

The effectiveness of metformin and AICAR (**Chapter IV**) on glucoregulation has reemphasized energy state as an AMPK-independent regulator (4, 34). Thus, distinguishing between the AMPK-dependent and independent effects of physiological, pathophysiological, and pharmacological energy stress on liver metabolism is of central importance. These studies establish the liver AMPK-independent effectiveness of exercise training on liver metabolism in HF-feeding. Indeed, liver AMPK is not necessary to correct fatty liver, lower blood glucose, insulin, body weight and adiposity with regular exercise. Hepatic AMPK deletion resulted in several metabolic abnormalities with HF-feeding, some of which were normalized by regular exercise—namely intermediates of the TCA cycle and those of the phospholipid synthesis pathway. However, $RW_{EX}$ failed to improve hepatic energy state or mitigate aberrant acylcarnitine levels in the absence of AMPK. While pharmacological targeting of AMPK may reduce liver TGs and improve energy state, regular exercise can reduce fatty liver through mechanisms independent of this enzyme.

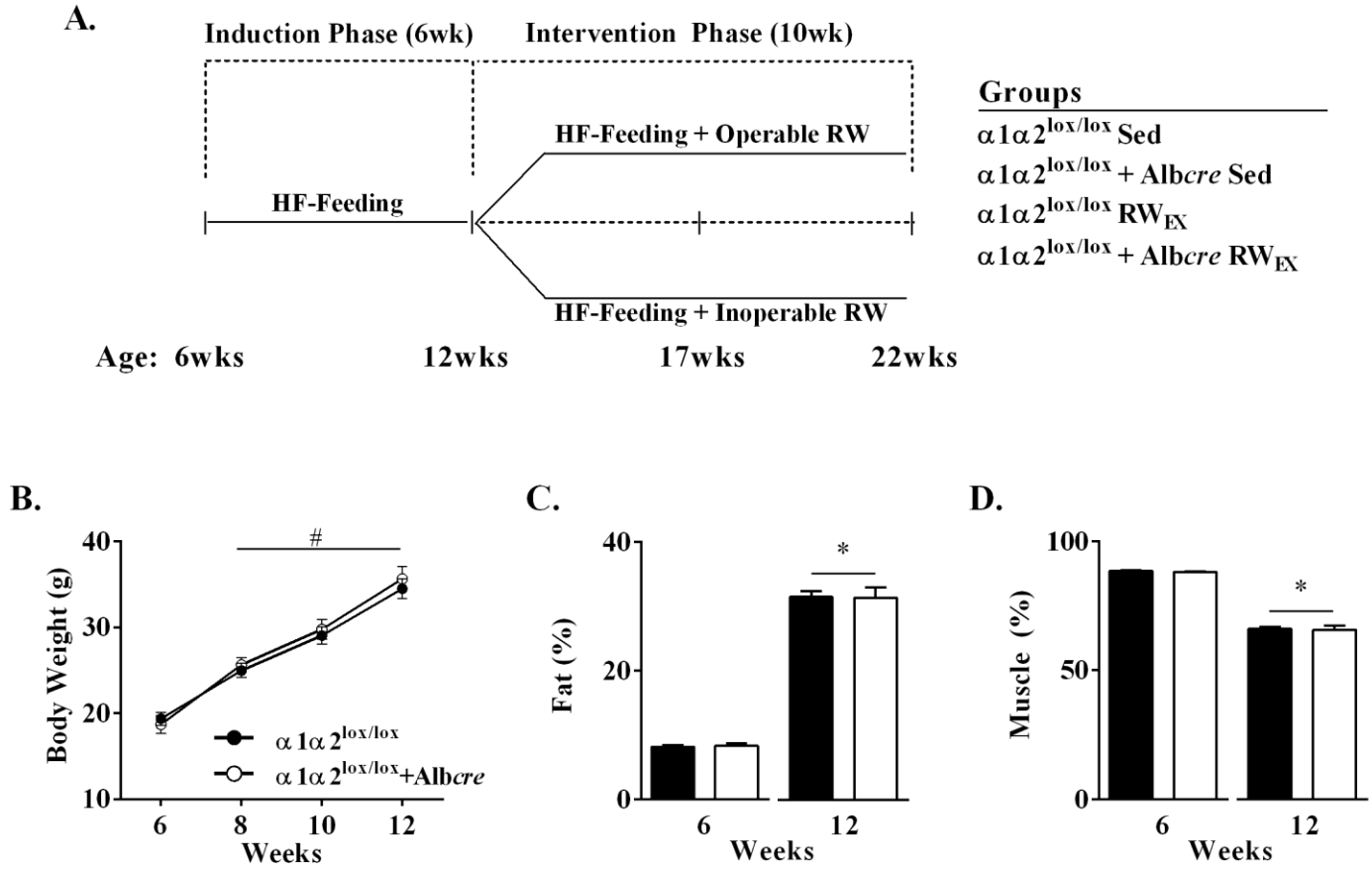


**Figure 5.1 – Induction Phase body weight and composition.** HF-feeding induced changes in body weight (**B**) and composition (**C, D**) in $\alpha1\alpha2^{lox/lox}$ and $\alpha1\alpha2^{lox/lox}$+Alb*cre* mice during the fatty liver Induction Phase. 6wk old mice were placed on a HFD for 6wks prior to $RW_{EX}$ intervention. A scheme has been included to describe the design for these studies (**A**). Data are expressed as means±SEM, *n=13-19* in each group. **p≤0.05* vs. 6wks. *#p≤0.05*, $\alpha1\alpha2^{lox/lox}$ and $\alpha1\alpha2^{lox/lox}$+Alb*cre* Sed vs. 6wks.

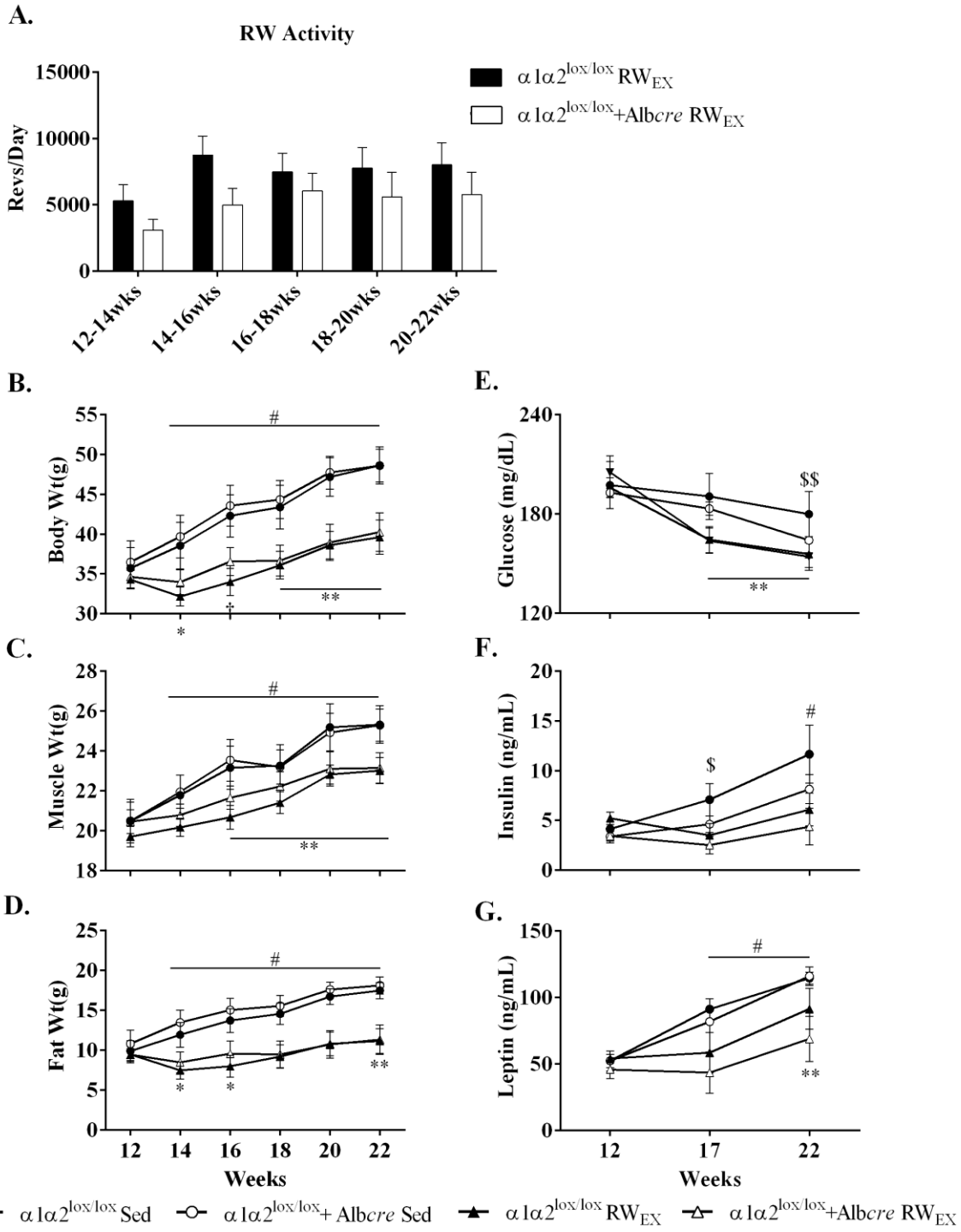


**Figure 5.2 – RW activity, body weight, composition, and plasma parameters during the Intervention Phase.** After 6wks of HF-feeding (12wks), α1α2$^{lox/lox}$ and α1α2$^{lox/lox}$+Alb*cre* mice were placed in cages with operable ($RW_{EX}$) or inoperable (Sed) running wheels for 10wks. Running wheel revolutions were continuously monitored using a digital counter and plotted as Revs/Day for every 2 weeks of the Intervention Phase (**A.)**. Body weight (**B.**) and composition (**C,D.**) were monitored biweekly and blood glucose (**E.**), insulin (**F.**), and leptin (**G.**) were measured every 5wks from the cut tail. Data were analyzed by Two-Way ANOVA RM and expressed as means±SEM, *n=5-7*. #$p \leq 0.05$, α1α2$^{lox/lox}$ and α1α2$^{lox/lox}$+Alb*cre* Sed vs. 12wks; \$$p \leq 0.05$, α1α2$^{lox/lox}$ Sed vs. 12wks; \$\$$p \leq 0.05$, α1α2$^{lox/lox}$+Alb*cre* Sed vs. 12wks; *$p \leq 0.05$, α1α2$^{lox/lox}$ $RW_{EX}$ vs. 12wks; †$p \leq 0.05$, α1α2$^{lox/lox}$+Alb*cre* $RW_{EX}$ vs. 12wks; **$p \leq 0.05$, α1α2$^{lox/lox}$ and α1α2$^{lox/lox}$+Alb*cre* $RW_{EX}$ vs. 12wks.

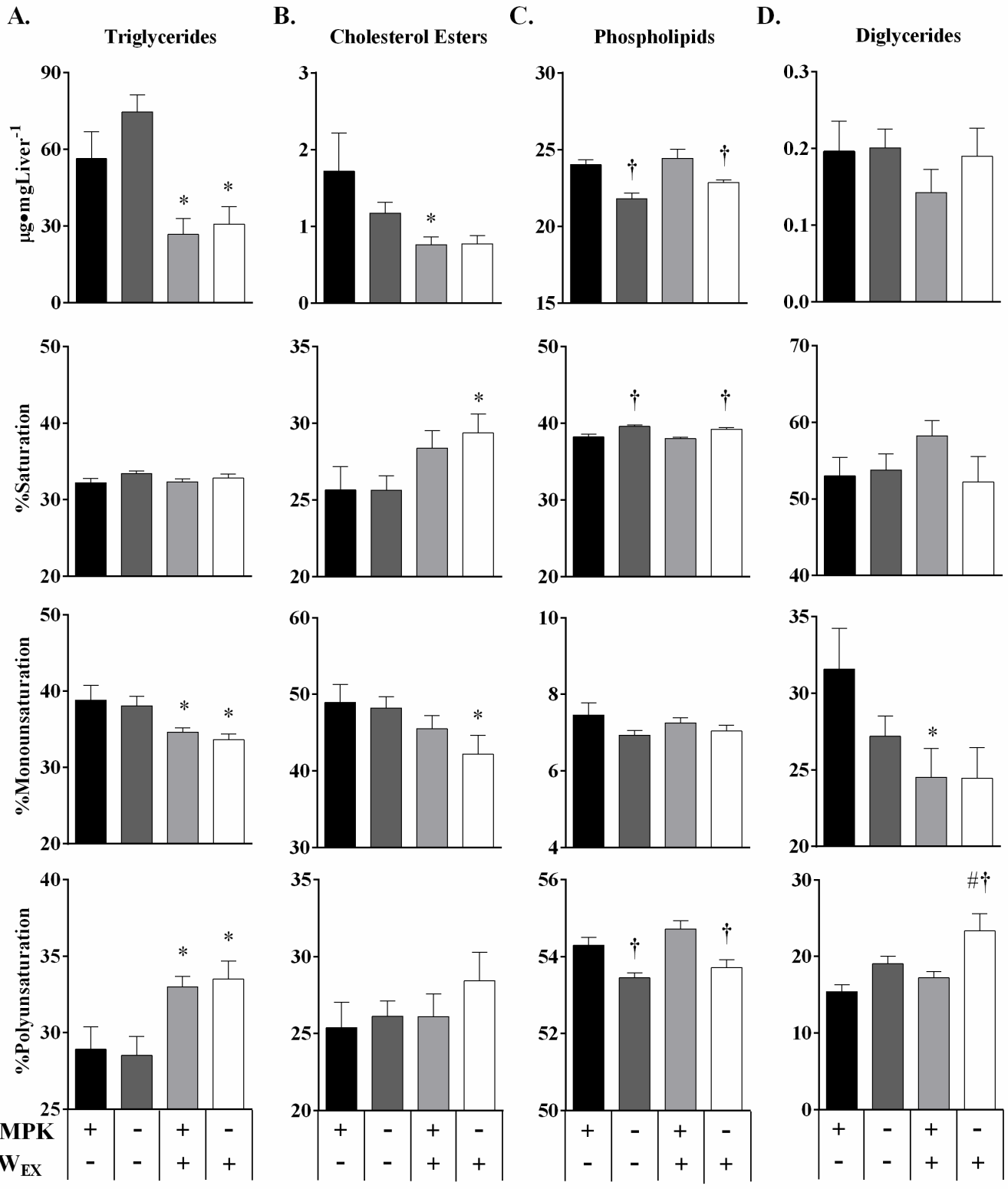


**Figure 5.3 – Hepatic lipids and saturation at the end of the Intervention Phase.** At the close of the study, mice were 22wks old and fed a HF-diet for 16wks (±10wks of $RW_{EX}$). 48hrs following the last bout of activity, mice were sacrificed and liver tissue was taken for analysis. Liver triglycerides (**A.**), cholesterol esters (**B.**), phospholipids (**C.**), and diglycerides (**D.**) were isolated through Folch extraction. Lipid saturation was calculated as a sum of the %contribution for individual saturated, monounsaturated, or polyunsaturated fatty acid species. Data are expressed as means±SEM, *n=5-7* in each group. **p≤0.05* vs. Sed*; †p≤0.05* vs. $\alpha1\alpha2^{lox/lox}$; *#p=0.056 vs.* Sed.

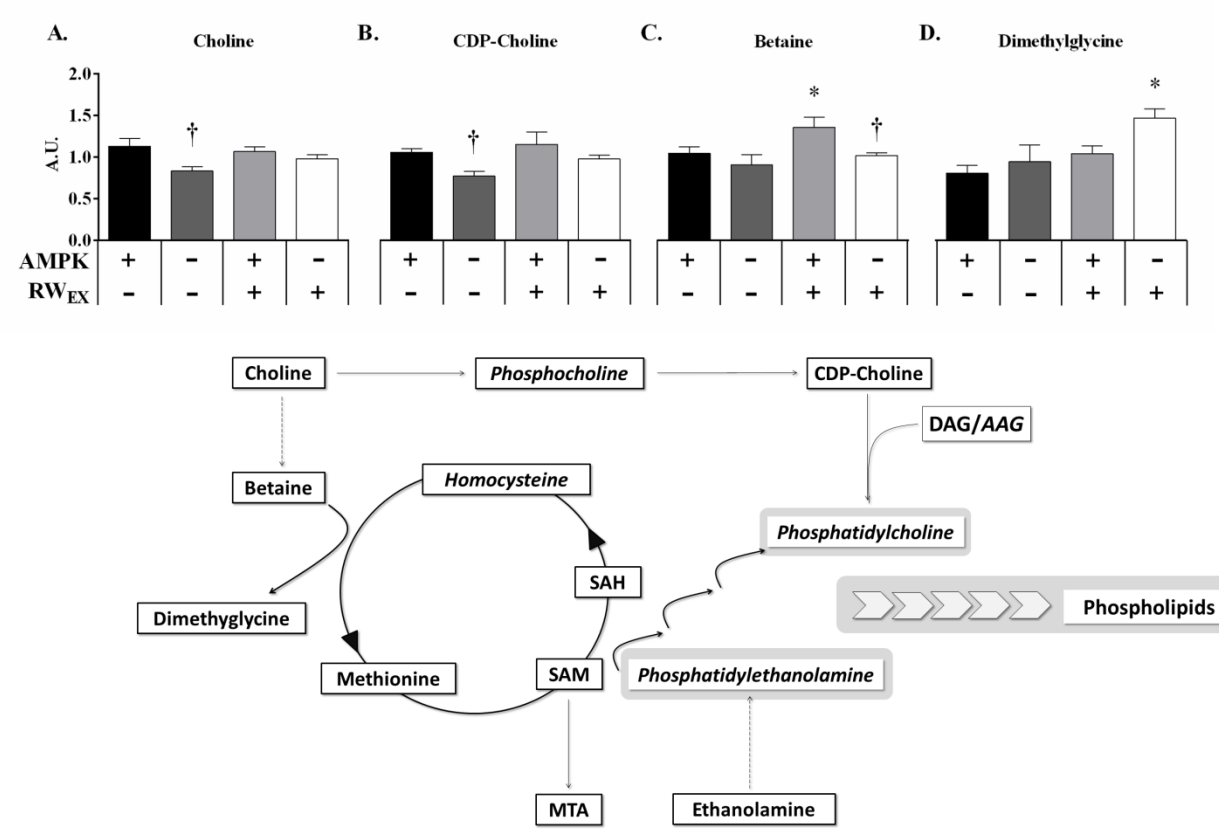


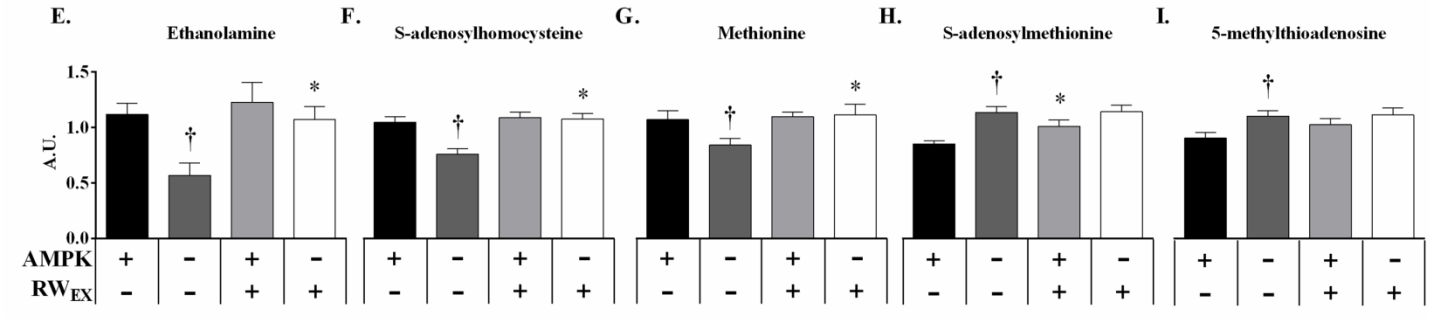


**Figure 5.4 – Metabolites related to the *de novo* synthesis of phosphatidylcholine (PC) and phosphatidylethanolamine (PE).** The listed metabolites contribute to the Kennedy or alternative PC synthesis pathways (**A-I.**). Metabolites were determined from liver tissue excised 48Hrs following the last bout of $RW_{EX}$ (16wks of HF-feeding±10wks $RW_{EX}$). A minimal metabolite pathway scheme is provided for reference (adapted from (259, 263)) and is not intended to reflect all reactions and directionality in the network; metabolites not provided (italicized) are included for clarity. Dotted lines indicate multiple enzymatic steps between reactants and products. Data are expressed as means±SEM, *n=6-7* in each group. *$p \leq 0.05$ vs. Sed; †$p \leq 0.05$ vs. $\alpha 1\alpha 2^{lox/lox}$.

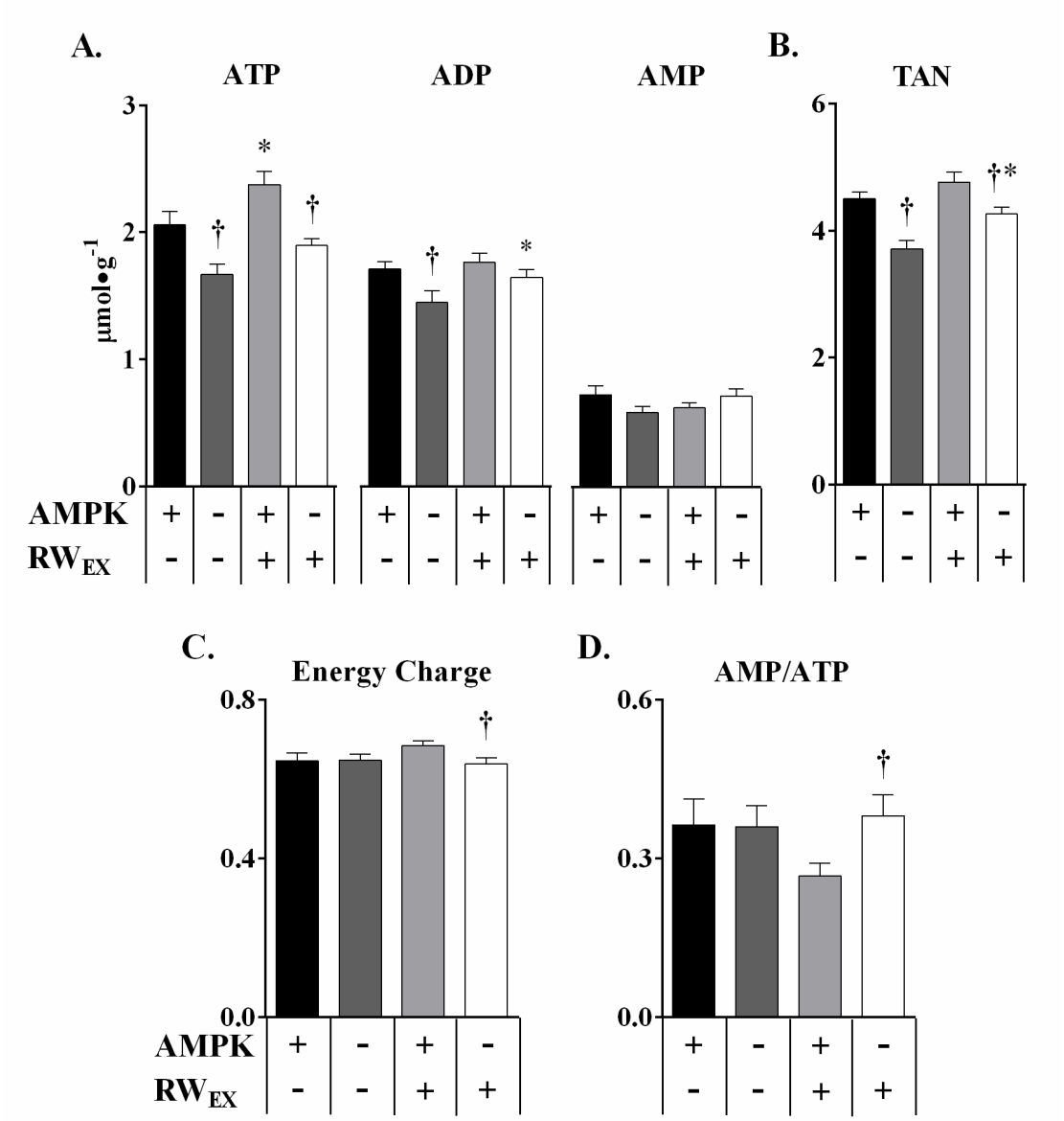


**Figure 5.5 – Hepatic adenine nucleotides and energy state.** Hepatic adenine nucleotides (**A.**) and the total adenine nucleotide pool (TAN) (**B.**) were measured by HPLC from liver extracts taken from $\alpha1\alpha2^{lox/lox}$ and $\alpha1\alpha2^{lox/lox}$+Alb*cre* mice at the close of the Intervention Phase. Energy charge (**C.**) was calculated by the equation EC=([ATP]+0.5[ADP])/([ATP]+[ADP]+[AMP]). The AMP/ATP ratio (**D.**) was provided for each group. Data are expressed as means±SE, *n=5-6* in each group. *$p \leq 0.05$ vs. Sed; †$p \leq 0.05$ vs. $\alpha1\alpha2^{lox/lox}$.

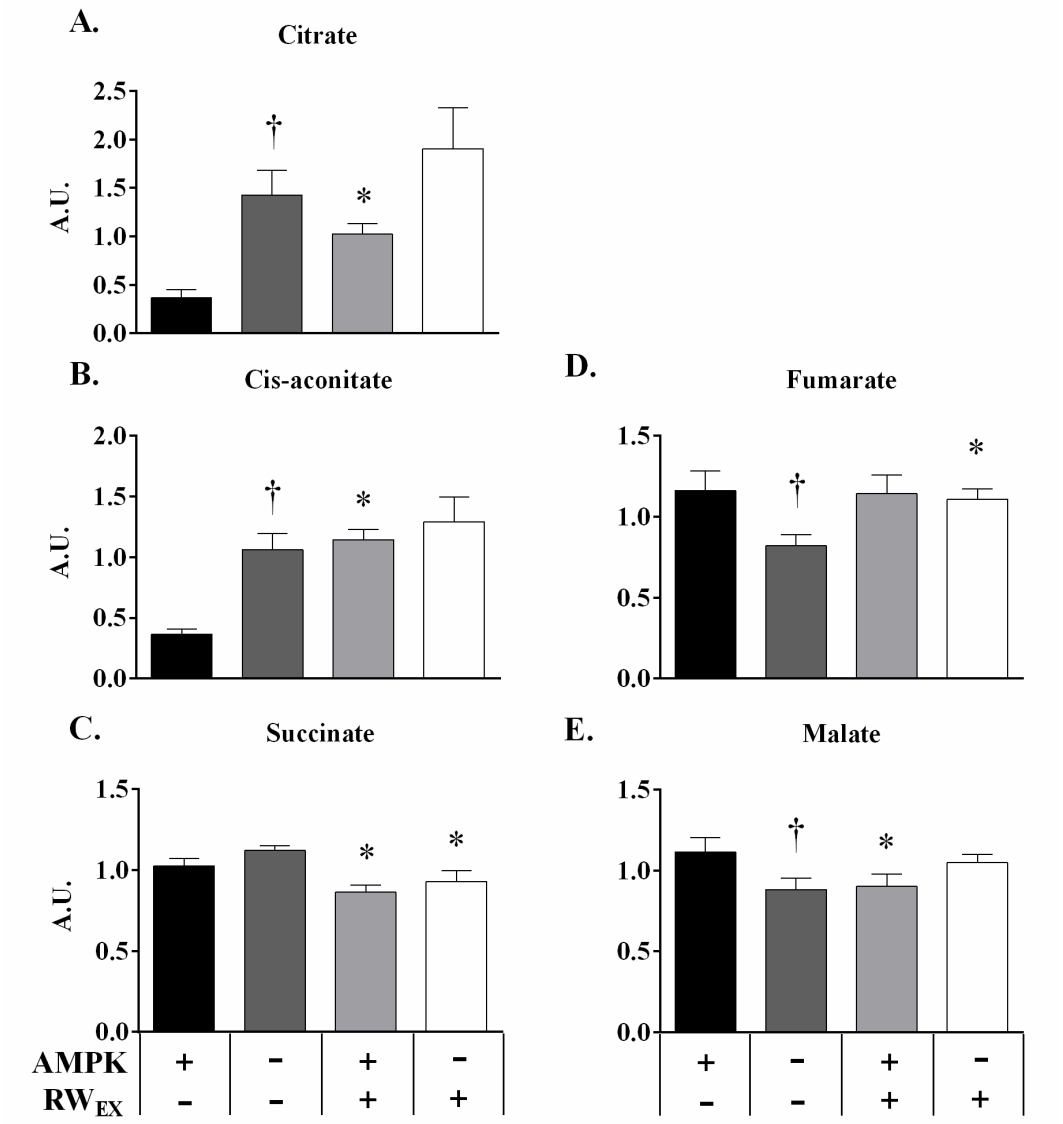


**Figure 5.6 – Hepatic TCA cycle intermediates**. TCA cycle metabolites (**A-E.**) were determined for liver samples taken at the end of the Intervention Phase from $\alpha1\alpha2^{lox/lox}$ and $\alpha1\alpha2^{lox/lox}$+Alb*cre* Sed and $RW_{EX}$ mice. Data are expressed as means±SEM, *n=6-7* in each group. *$p \leq 0.05$ vs. Sed; †$p \leq 0.05$ vs. $\alpha1\alpha2^{lox/lox}$.

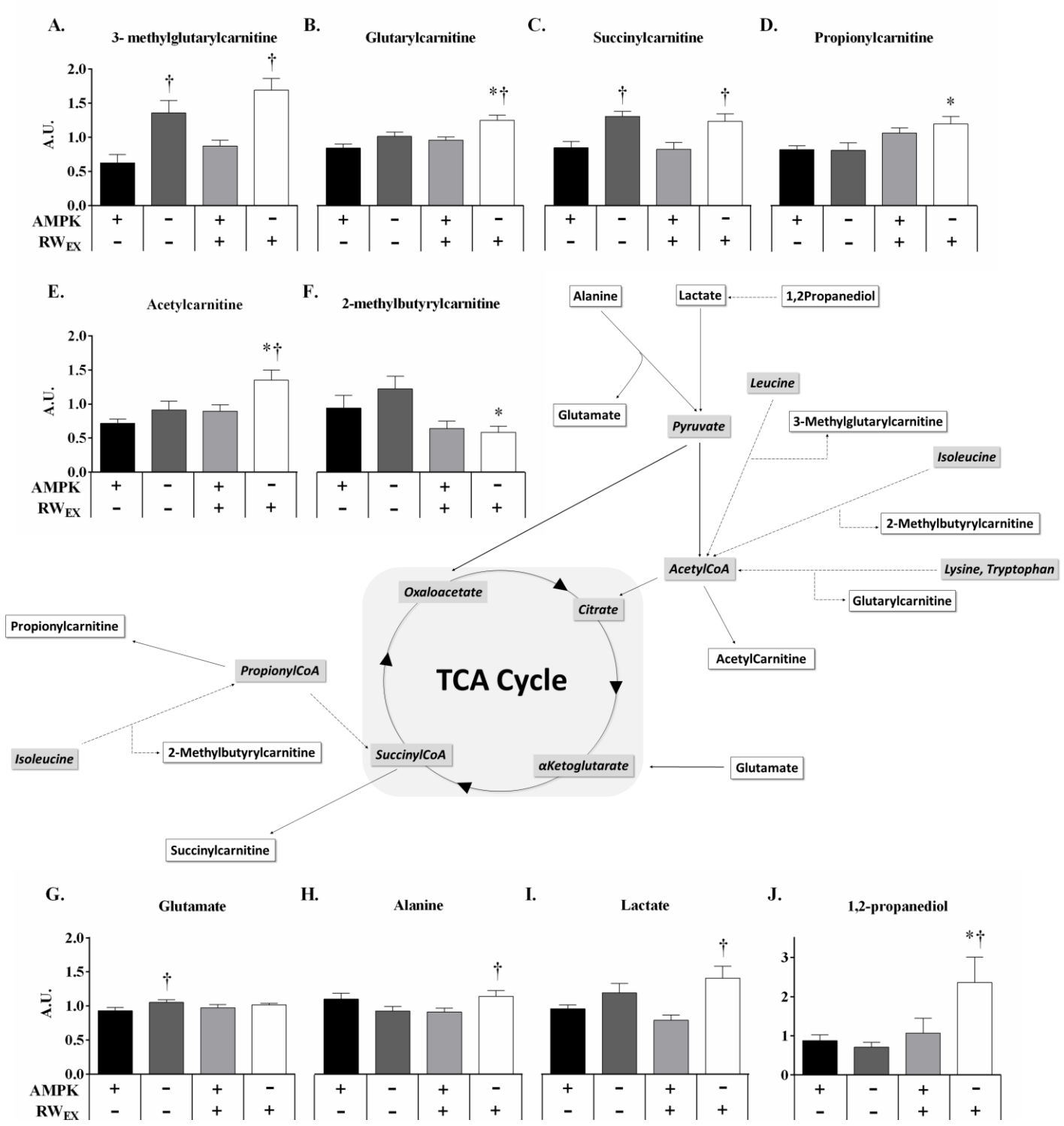


**Figure 5.7 –Acylcarnitine and TCA cycle related liver metabolites.** Acylcarnitine species (**A-F.**) and anaplerotic metabolites (**G-J.**) from liver tissue excised after the Intervention Phase in $\alpha1\alpha2^{lox/lox}$ and $\alpha1\alpha2^{lox/lox}$+Alb*cre* Sed and $RW_{EX}$ mice. A minimal molecular pathway scheme is provided for reference and is not intended to reflect all possible reactions and directionality in the network; metabolites not provided (italicized) are included for clarity. Dotted lines indicate multiple enzymatic steps between reactants and products. The carnitine-linked reactions emphasized in this diagram do not necessarily reflect reactions exclusive to liver mitochondria, as subcellular organelle carnitine acyltransferase activity may vary between tissues (246). Data are expressed as means±SEM, *n=6-7* in each group. *$p \leq 0.05$ vs. Sed; †$p \leq 0.05$ vs. $\alpha1\alpha2^{lox/lox}$.

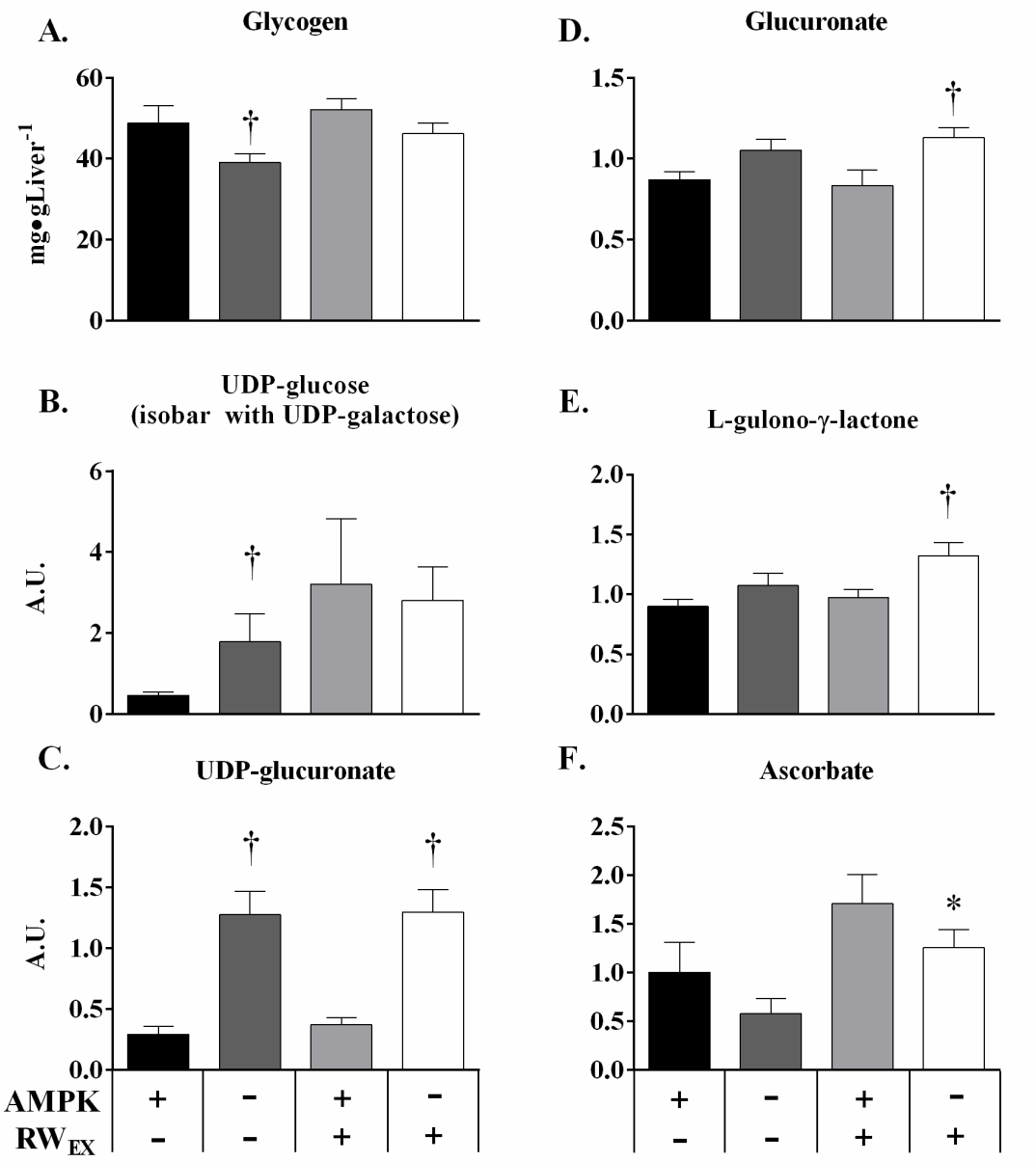


**Figure 5.8 – Glucuronidation and ascorbate-related metabolites.** Liver glycogen (**A.**) and metabolites involved in glucuronidation and ascorbate synthesis (**B-F.**) in the livers of $\alpha1\alpha2^{lox/lox}$ and $\alpha1\alpha2^{lox/lox}$+Alb*cre* Sed and $RW_{EX}$ mice. Data are expressed as means±SEM, *n=6-7* in each group. *$p \leq 0.05$ vs. Sed; †$p \leq 0.05$ vs. $\alpha1\alpha2^{lox/lox}$.

# Chapter VI

# CONCLUSIONS

## Summary

Collectively, this dissertation demonstrates that hepatic AMPK preserves energy state during physiological and pharmacological stress by coordinating substrate availability and oxidative capacity with ATP production in the liver. These studies advance an understanding hepatic AMPK function in three *in vivo* settings of central value to metabolic science: (1) varying degrees of nutrient deprivation, (2) pharmacological inhibition of hepatic glucose production, and (3) regular, voluntary exercise in HF-feeding. An ancillary benefit of this work was gauging the liver's metabolic capacity independent of AMPK activation. Fluctuations in adenine nucleotides are an ordinary feature of hepatic metabolism caused by a number of stressors. AMPK coordinates a signaling circuit that limits the ATP nadir observed in physiological and pharmacological energy stress.

Glucagon action stimulates mechanisms for substrate uptake and utilization in the liver which sustain gluconeogenesis during fasting and exercise (8, 10, 12, 240). The net effect of conditions characterized by sustained glucagon action is an apparent discharge of the liver's energy state (16, 28–30). Accordingly, AMPK is activated by glucagon receptor signaling during fasting (115), exercise (28, 115), and hyperglucagonemia (16), which serves as the impetus for the experiments described in Chapter III and V.

A salient finding from these studies is that AMPK action buffers reductions in liver ATP that result from pharmacological or physiological states. However, one cannot help but notice

that even in the presence of AMPK activation, fasting-mediated deficits in energy state are maintained. Therefore, AMPK works to keep changes in adenine nucleotides within a range integral for physiological processes in a long term fasted state. These observations support the postulate that products of AMPK-supported oxidation—e.g. acetylCoA and NADH—are crucial for sustaining gluconeogenesis and ketogenesis. Fasting and exercise mediated reductions in hepatic energy state, perhaps, facilitate the production of the aforementioned metabolites through AMPK activation. This rationale would explain, in part, the importance of a plastic energy state in the liver.

Indeed, energy coupling in the liver is unique in that substrates oxidized in the TCA cycle are linked with sustained gluconeogenesis. Results here and elsewhere (210) clearly demonstrate that glucose production in the long term fasted mouse is almost entirely dependent on gluconeogenesis, predominantly from PEP flux. Albeit modest, long term fasting induces a decrement in the rate of flux through the TCA cycle ($\boldsymbol{V_7}$) while maintaining normal rates of gluconeogenesis. Persistent carbon flow to glucose (OAA→PEP) may diminish TCA cycle intermediates, lessen $\boldsymbol{V_7}$, and drain liver energy state in response to a long term fast. In these conditions, the abundance of acetylCoA and NADH derived from fat oxidation may sustain flux through gluconeogenic reactions (98). Livers from starved rats may also exhibit a decrease in TCA cycle flux and an increase ketogenesis (69).

From these measurements we conclude that AMPK synchronizes ATP balance with fasting-mediated changes in substrate utilization in the liver. In the absence of AMPK, glucose and oxidative fluxes become discordant. Reductions in glycogenolytic flux to glucose associate with increases in fatty acids, aberrant medium and short chain metabolites, and a reduction in the total adenine nucleotide pool in a short term fast. Extending the fast duration in absence of liver

AMPK leads to greater deficits in hepatic ATP. Unlike what is observed in long term fasted controls, $\boldsymbol{V_7}$ remains elevated in conjunction with the larger fall in ATP, which coincides with a relative elevation in BCAA/BCKA-related metabolites.

Physiological changes in adenine nucleotides—which require glucagon-receptor signaling—may emanate from several sources. As shown in **Fig. 1.1**, multiple processes that support anaplerotic or oxidative substrate provision to the TCA cycle require ATP. Nitrogen disposal through ureagenesis requires ATP. The priming of fatty acids with CoA requires ATP hydrolysis; moreover, fatty acids may exert an uncoupling effect on mitochondria that dissociates electron transport from ATP synthesis. These events may contribute to liver energy state when gluconeogenic glucose production predominates. Research presented here (**Chapter IV**) and elsewhere (4, 34) imply that energy state exerts AMPK-independent control over energy consuming processes. Albeit important, AMPK is one component of a regulatory unit in the liver that harmonizes metabolic flux with energy production.

The results here also demonstrate the AMPK reliant, preservative nature of liver energy status during stress. Chapters III-V provide substantial evidence that AMPK supports structures (mitochondria) and pathways that keep energy status within a limited range. This claim is most clearly illustrated in Chapter III. The livers of short-fasted $\alpha1\alpha2^{lox/lox}$+Alb*cre* mice exhibit several complications that would either induce or exacerbate energy deprivation. First and foremost, liver AMPK deletion impairs maximal mitochondrial responsiveness (State 3) and efficiency (State3/State2); thus, the capacity and efficiency of the cell's powerhouse diminishes in the absence of AMPK. Accordingly, AMPK deletion causes greater deficits in liver energy state following the acute delivery of a compound that consumes ATP and interferes with

complex I (AICAR). Chronic HF-feeding elicits reductions in hepatic ATP that cannot be corrected by regular exercise in the absence of AMPK.

Acute AMPK activation promotes fatty acid transport and regulates lipogenesis by inhibiting malonylCoA synthesis (**Fig. 1.3**). Chapters III -V provide evidence that AMPK promotes the appropriate coupling of fatty and amino acids with TCA cycle metabolism. For simplicity, the process that mediates complete LCFA oxidation can be partitioned into 3 intracellular steps: 1) mitochondrial transport, 2) β-oxidation and 3) acetylCoA oxidation. LCFAs must be conjugated to carnitine by CPT1 (**Fig. 1.3**) to cross the mitochondrial membrane; once in the matrix, CPT2 reintroduces CoA allowing for β-oxidation. Unlike long chains, medium chain fatty acids bypass the transport regulatory step. AMPK deletion induces a selective elevation in long, but not short chain fatty acids in the liver. These data coincide with a decrease in CoA levels. Moreover, liver TGs, DGs, and CEs are equivalent to controls. Without AMPK-supported transport, the buildup of LCFAs may contribute to a deficit in liver energy state. These results are corroborated by the AICAR-mediated reduction in hepatic TGs in $\alpha1\alpha2^{lox/lox}$ but not $\alpha1\alpha2^{lox/lox}$ +Alb*cre* mice.

It is acknowledged that the evidence for impaired LCFA flux into the mitochondria is correlative. Moreover, these studies do not discern whether the early elevation in LCFAs results from impairments in oxidation or re-esterification, provision from PL biosynthetic/degradative pathways, or enhanced delivery to the liver. Liver LCFA levels are not elevated above controls in long term fasted liver AMPK knockout mice—despite greater deficits in ATP and TAN. However, a larger increment in liver CEs was observed in the absence of AMPK, which might be a compensatory mechanism to combat FA lipotoxicity in a system with impaired LCFA intramitochondrial transport. Interpreting the results from the acute AICAR studies are

complicated by similar limitations. Though liver TGs are elevated in hepatic AMPK knockout mice following the AICAR infusion, it remains unclear whether this results from sustained hepatic TG assembly and/or impairments in fat oxidation.

This dissertation also presents substantial evidence that liver AMPK deletion increases metabolites in non-canonical, energetically less economical pathways that feed carbon to the TCA cycle. Metabolites that emanate from amino acid catabolism—primarily BCAA or branched-chain α-keto acid (BCKA)—are atypically elevated in the livers of short and long term fasted liver AMPK knockout mice. Branched-chain aminotransferase (BCAT) catalyzes the transamination of BCAAs to BCKAs, which utilizes α-ketoglutarate to generate BCKA and glutamate. BCKA dehydrogenase (BCKDH) catalyzes BCKA decarboxylation, committing BCAA/BCKAs to degradation (260). Distinct from other metabolically active organs, BCAT and BCKDH activities in the liver are uniquely low and high, respectively (261). In addition to the α-keto acid derived from leucine deamination (4-methyl-2-oxopentanoate), metabolites that stem primarily from the BCAA/BCKA catabolic pathway were elevated (**Chapter III, V**). The former metabolite is proposed to indirectly activate BCKDH activity (260). Breakdown of BCAA/BCKAs yield gluconeogenic and ketogenic products (gluconeogenic = succinylCoA and propionylCoA, ketogenic = acetoacetate and acetylCoA). An atypical elevation in BCAA/BCKA metabolism, perhaps, sustains $\boldsymbol{V_7}$ in long-term fasted, liver AMPK knockout mice. This hypothesis should be considered with caution, as the subcellular distribution of carnitine acyltransferase activity is not uniform in all tissues (246). Furthermore, propionylCoA is generated through the metabolism of certain amino and fatty acid species.

Though amino acid metabolism may yield reduced cofactors, gluconeogenic and ketogenic products in the liver, the energy costs associated with amino acid deamination and

nitrogen disposal might contribute to the larger energy deficits observed in liver AMPK knockout mice. While augmenting BCAA/BCKA-related metabolites, AMPK deletion increases N-acetylglutamate, an activating cofactor of the ureagenic enzyme carbomoyl-phosphate synthetase I. These results do not unequivocally prove that AMPK deletion accelerates BCAA/BCKA catabolism in short and long term fasting. It is plausible that substrate load may simply exceed the rate of carbon extraction by the TCA cycle. Such a condition could manifest during impairments in oxidation and/or during periods of substrate excess. For example, others observe an increase in short, medium, and long chain acylcarnitines in chronic high fat feeding—which corresponds to a sustained increase in oxidative flux through the TCA cycle (35). Indeed, long term fasting increases liver acetylcarnitine in $\alpha1\alpha2^{lox/lox}$ and $\alpha1\alpha2^{lox/lox}$+Alb*cre* mice, which serves as the carnitine conjugate of acetylCoA. It is acknowledged that the provision of BCAA/BCKA-related metabolites from extrahepatic tissues may be an alternative mechanism to explain the phenotype observed in these studies (82, 87). A complete analysis of short, medium, and long chain fatty acylcarnitine species would be helpful to better elucidate carbon flux. Several long and medium chain acylcarnitines may also be elevated in the livers of hepatic AMPK knockout mice.

An understanding of the acute mechanistic control of glucose production and gluconeogenic enzyme expression is crucial for developing therapeutics to treat obesity-related hyperglycemia. For the reasons outlined in the introduction, AMPK is often invoked as a central enzyme in the molecular regulation of hepatic glucose production. The studies performed here and elsewhere (4, 34) demonstrate that metformin and AICAR acutely inhibit glucose production independent of AMPK (**Chapter IV**), potentially through a mechanism that lowers energy state. Unlike the aforementioned studies, blood glucose levels were clamped *in vivo* and, thus, the

metabolic consequences of swings in glycemia were abrogated. The deleterious effect of AICAR on energy state is profound, even during the provision of exogenous glucose. AMPK protects against the depletion of the adenine nucleotide pool and energy state in this pharmacological setting. Though this dissertation focused on the ability of AICAR to inhibit glucose production in the absence of hepatic AMPK, AMPK may actually impede the effectiveness of antiglycemic compounds whose actions depend on a reduction in energy state. An interesting corollary study would be the administration of AICAR/biguanides in the presence of constitutively active AMPK. One might hypothesize that adaptations to chronic AMPK activation would prime the liver to combat the effects of these compounds on energy depletion, thereby decreasing their glucose-lowering effectiveness. Various exercise modalities also deplete hepatic energy state. It stands to reason that, in the absence of AMPK, reductions in liver energy state are exacerbated by exhaustive exercise. The ability of the liver to sustain glucose production during exhaustive exercise may require hepatic AMPK. Moreover, liver compensation to chronic bouts of high intensity exercise may also require AMPK signaling.

When taking into account the novel flux methods developed in this dissertation, a plethora of future directions concerning hepatic metabolism may be extrapolated from this work. Studies in this dissertation did not move beyond simple stressors in examining hepatic metabolic fluxes; this decision was made deliberately to 1) avoid an additional layer of complexity in a novel *in vivo* technique and 2) provide a reasonable basis of comparison to the results of others investigating similar fluxes. The results in Chapter III and in unpublished validation studies provide sufficient reason to move this technique into other *in vivo* stressors.

## Future Directions for Flux Analysis *In Vivo*

The effects of acute exercise on hepatic energy state and AMPK activation have been demonstrated (16, 28, 115). Moreover, our laboratory has made sizeable contributions to understanding the role of glucagon in substrate uptake and utilization in the liver during an exercise-mediated increment in glucose production. The techniques developed here provide for the investigation of TCA cycle and glucose-related fluxes during an acute bout of exercise in wild-type and transgenic mice. The hypothesis that acute, moderate and exhaustive exercise accelerate flux through the TCA cycle and gluconeogenesis could be investigated in the mouse *in vivo*. Repeated bouts of exercise have been demonstrated to improve the liver's responsiveness to glucagon (262); thus, the effects of regular exercise on energetic adaptations in the liver associated with glucose and oxidative fluxes could be tested. Moreover, these methods may be applied to investigate the acute and chronic effects of endogenous (e.g. FGF21, adiponectin, saturated/unsaturated fatty acid emulsions) and pharmaceutical agents on liver metabolic flux. The "insulin-resistant" and gluconeogenic effect of acute hyperlipidemia (Intralipid infusion) may emanate from the effects of excess fatty acids on oxidative metabolism. These future directions in wild-type mice are, by far, not an exhaustive list.

## Hepatic AMPK and Nutrient Sensor Specific Future Directions

Chronic $RW_{EX}$ ameliorated fatty liver independent of hepatic AMPK. The reduction in liver TGs associated with an increase in polyunsaturation and decrease in monounsaturation. Likewise, insulin, blood glucose, and leptin were no different in control and liver AMPK knockout mice. These results demonstrate that long-term voluntary exercise is capable of mitigating many of the pathological effects of high-fat feeding. However, abnormalities in

BCAA/BCKA-related acylcarnitines and energy state persisted despite exercise intervention. Interpreting the AMPK-independence of $RW_{EX}$-mediated reductions in fatty liver is complicated by differences in whole-body adiposity and large variations in RW activity. A more conclusive investigation would standardize chronic exercise workload and prevent changes in body weight and adiposity. A predefined, daily treadmill exercise regimen could conceivably mitigate the aforementioned complications; indeed, AMPK may be important for the amelioration of fatty liver when differences in body weight and composition are prevented. Moreover, chronic administration of AMPK activators (AICAR, biguanides, A-769662) may require liver AMPK for lowering hepatic triglycerides and blood glucose during high-fat feeding. The flux methods described in Chapter III could be applied in HF-fed, $\alpha1\alpha2^{lox/lox}$ ± Alb*cre* and ± acute/chronic AICAR administration, for example.

The AICAR dose selected in Chapter IV was intended to bring hepatic ZMP levels within the medium to high range and, thus, test the absolute requirements of AMPK for AICAR effects *in vivo*. While AICAR and metformin appear to stimulate hepatocyte fat oxidation, it is unclear whether they stimulate mitochondrial β-oxidation or the subsequent complete oxidation of acetylCoA. Evidence suggests both pharmacological agents inhibit respiration (125, 127) and elevate AMP. It is reasonable to suspect that these compounds also inhibit TCA cycle flux through feedback inhibition (227). In this setting, AMPK would support β-oxidation through the influx of LCFAs into the mitochondria yet the complete oxidation of acetylCoA may be impaired. A combination of *in vivo* and *in vitro* tracer flux modeling strategies could be employed to test the hypotheses that (1) AICAR promotes β-oxidation while inhibiting TCA cycle flux (2) AMPK activation is essential for the coordination of both processes.

A series of "pulse-chase" like experiments could also be used to test the hypothesis that AMPK is essential for recharging hepatic energy state following a pharmacological or physiological stress (i.e. high intensity exercise). These studies could be performed in the presence and absence of liver AMPK. Since AMPK is also important for mitochondrial function, medium-chain FAs could be supplemented during the recharge phase to bypass complications associated with LCFA import into the mitochondria. A variation of the stable-isotopic tracer technique could be applied during the "pulse" and "chase" phases to measure liver intermediary metabolism.

These and several other energy-centric experiments can be performed in an array of mouse models with transgenic or knockout of nutrient/energy sensing enzymes. Severe hyperglycemia ensues following liver LKB1 deletion, which implies a dramatic increase in hepatic anaplerotic and gluconeogenic fluxes (137). LKB1-deletion may drain hepatic energy state and disrupt redox balance; a compensatory increase in anaplerotic and oxidative substrate may fuel elevated glucose production in the context of upregulated gluconeogenic enzyme expression. The effects of AMPK inactivity would be compounded by a decrease in the activity of several LKB1-dependent kinases (174) .

## Concluding Remarks

The results presented in this dissertation provide the most complete *in vivo* investigation of AMPK action in the control of fundamental liver physiology. AMPK is crucial for protecting energy status during a mild and extreme stressor (overnight fasting and AICAR administration, respectively) by supporting the coupling of oxidative flux with ATP homeostasis in the liver. However, the liver is capable of preventing gross impairments in glucose and oxidative

metabolism even in the absence of AMPK. Thus, AMPK is postured as an important control element of a broader signaling network that regulates metabolic state in the liver.

## REFERENCES


1. Malik, V. S., Willett, W. C., and Hu, F. B. (2013) Global obesity: trends, risk factors and policy implications. *Nat. Rev. Endocrinol.* **9**, 13–27

2. Wasserman, D. H. (2009) Four grams of glucose. *Am. J. Physiol. Endocrinol. Metab.* **296**, E11–21

3. Moller, D. E. (2012) Metabolic Disease Drug Discovery- "Hitting the Target" Is Easier Said Than Done. *Cell Metab.* **15**, 19–24

4. Miller, R. A., Chu, Q., Xie, J., Foretz, M., Viollet, B., and Birnbaum, M. J. (2013) Biguanides suppress hepatic glucagon signalling by decreasing production of cyclic AMP. *Nature* **494**, 256–60

5. Unger, R. H., and Cherrington, A. D. (2012) Glucagonocentric restructuring of diabetes : a pathophysiologic and therapeutic makeover. *J. Clin. Invest.* **122**, 4–12

6. Moore, M. C., Cherrington, A. D., and Wasserman, D. H. (2003) Regulation of hepatic and peripheral glucose disposal. *Best Pract. Res. Clin. Endocrinol. Metab.* **17**, 343–364

7. Brosnan, J. T. (2003) Interorgan Amino Acid Transport and its Regulation. *J. Nutr.* **133**, 2068–2072

8. Wasserman, D. H., Williams, P. E., Lacy, D. B., Green, D. R., and Cherrington, A. D. (1988) Importance of intrahepatic mechanisms to gluconeogenesis from alanine during exercise and recovery. *Am. J. Physiol.* **254**, E518–25

9. Wasserman, D. H., Spalding, J. A., Lacy, D. B., Colburn, C. A., Goldstein, R. E., and Cherrington, A. D. (1989) Glucagon is a primary controller of hepatic glycogenolysis and gluconeogenesis during muscular work. *Am. J. Physiol.* **257**, E108–17

10. Wasserman, D. H., Spalding, J. A., Bracy, D., Lacy, D. B., and Cherrington, A. D. (1989) Exercise-Induced Rise in Glucagon and Ketogenesis During Prolonged Muscular Work. *Diabetes* **38**, 799–807

11. Wasserman, D. H., and Cherrington, A. D. (1991) Hepatic fuel metabolism during muscular work: role and regulation. *Am. J. Physiol. Endocrinol. Metab.* **260**, E811–24

12. Hendrick, G. K., Wasserman, D. H., Frizzell, R. T., Williams, P. E., Lacy, D. B., Jaspan, J. B., and Cherrington, A. D. (1992) Importance of basal glucagon in maintaining hepatic glucose production during a prolonged fast in conscious dogs. *Am. J. Physiol. Endocrinol. Metab.* **263**, E541–E549

13. Woodside, K. H., Ward, W. F., and Mortimore, G. E. (1974) Effects of Glucagon on General Protein Degradation and Synthesis in Perfused Rat Liver. *J. Biol. Chem.* **249**, 5458–5463

14. Ayuso-Parrilla, M. S., Martin-Requero, A., Perez-Diaz, J., and Parrilla, R. (1976) Role of Glucagon on the Control of Hepatic Protein Synthesis and Degradation in the Rat in Vivo. *J. Biol. Chem.* **251**, 7785–7790

15. Ezaki, J., Matsumoto, N., Takeda-Ezaki, M., Komatsu, M., Takahashi, K., Hiraoka, Y., Taka, H., Fujimura, T., Takehana, K., Yoshida, M., Iwata, J., Tanida, I., Furuya, N., Zheng, D.-M., Tada, N., Tanaka, K., Kominami, E., and Ueno, T. (2011) Liver autophagy contributes to the maintenance of blood glucose and amino acid levels. *Autophagy* **7**, 727–736

16. Berglund, E. D., Lee-young, R. S., Lustig, D. G., Lynes, S. E., Donahue, E. P., Camacho, R. C., Meredith, M. E., Magnuson, M. A., Charron, M. J., and Wasserman, D. H. (2009) Hepatic energy state is regulated by glucagon receptor signaling in mice. *J. Clin. Invest.* **119**, 2412–2422

17. Lafontan, M., and Langin, D. (2009) Lipolysis and lipid mobilization in human adipose tissue. *Prog. Lipid Res.* **48**, 275–97

18. Wasserman, D. H., Lacy, D. B., Goldstein, R. E., Williams, P. E., and Cherrington, A. D. (1989) Exercise-Induced Fall in Insulin and Increase in Fat Metabolism During Prolonged Muscular Work. *Diabetes* **38**, 484–90

19. Mcgarry, J. D., Meier, J. M., and Foster, D. W. (1973) The Effects of Starvation and Refeeding on Carbohydrate and Lipid Metabolism in Vivo and in the Perfused Rat Liver: THE RELATIONSHIP BETWEEN FATTY ACID OXIDATION AND ESTERIFICATION IN THE REGULATION OF KETOGENESIS. *J. Biol. Chem.* **248**, 270–278

20. McGarry, J. D., Wright, P. H., and Foster, D. W. (1975) Hormonal Control of Ketogenesis. RAPID ACTIVATION OF KETOGENIC CAPACITY IN FED RATS BY ANTI-INSULIN SERUM AND GLUCAGON. *J. Clin. Invest.* **55**, 1202–9

21. Longuet, C., Sinclair, E. M., Maida, A., Baggio, L. L., Maziarz, M., Charron, M. J., and Drucker, D. J. (2008) The Glucagon Receptor Is Required for the Adaptive Metabolic Response to Fasting. *Cell Metab.* **8**, 359–71

22. Brown, M. S., and Goldstein, J. L. (2008) Selective versus Total Insulin Resistance: A Pathogenic Paradox. *Cell Metab.* **7**, 95–6

23. Kawamori, D., and Kulkarni, R. N. (2009) Insulin modulation of glucagon secretion. The role of insulin and other factors in the regulation of glucagon secretion. *Islets* **1**, 276–279

24. Kawamori, D., Kurpad, A. J., Hu, J., Liew, C. W., Shih, J. L., Ford, E. L., Herrera, P. L., Polonsky, K. S., McGuinness, O. P., and Kulkarni, R. N. (2009) Insulin Signaling in α Cells Modulates Glucagon Secretion In Vivo. *Cell Metab.* **9**, 350–61

25. Unger, R. H. (1978) Role of Glucagon in the Pathogenesis of Diabetes: The Status of the Controversy. *Metabolism* **27**, 1691–1709

26. Lee, Y., Berglund, E. D., Wang, M. Y., Fu, X., Yu, X., Charron, M. J., Burgess, S. C., and Unger, R. H. (2012) Metabolic manifestations of insulin deficiency do not occur without glucagon action. *Proc. Natl. Acad. Sci. U. S. A.* **109**, 14972–14976

27. Lee, Y., Wang, M. Y., Du, X. Q., Charron, M. J., and Unger, R. H. (2011) Glucagon Receptor Knockout Prevents Insulin-Deficient Type 1 Diabetes in Mice. *Diabetes* **60**, 391–7

28. Camacho, R. C., Donahue, E. P., James, F. D., Berglund, E. D., and Wasserman, D. H. (2006) Energy state of the liver during short-term and exhaustive exercise in C57BL/6J mice. *Am. J. Physiol. Endocrinol. Metab.* **290**, E405–8

29. Start, C., and Newsholme, E. A. (1968) The Effects of Starvation and Alloxan-Diabetes on the Contents of Citrate and other Metabolic Intermediates in Rat Liver. *Biochem. J.* **107**, 411–5

30. Dohm, G. L., and Newsholme, E. A. (1983) Metabolic control of hepatic gluconeogenesis during exercise. *Biochem. J.* **212**, 633–9

31. Szendroedi, J., Chmelik, M., Schmid, A. I., Nowotny, P., Brehm, A., Krssak, M., Moser, E., and Roden, M. (2009) Abnormal Hepatic Energy Homeostasis in Type 2 Diabetes. *Hepatology* **50**, 1079–86

32. Cortez-Pinto, H., Chatham, J., Chacko, V. P., Arnold, C., Rashid, A., and Diehl, A. M. (1999) Alterations in Liver ATP Homeostasis in Human Nonalcoholic Steatohepatitis: A Pilot Study. *JAMA* **282**, 1659–64

33. Vincent, M. F., Erion, M. D., Gruber, H. E., and Van den Berghe, G. (1996) Hypoglycaemic effect of AICAriboside in mice. *Diabetologia* **39**, 1148–55

34. Foretz, M., Hébrard, S., Leclerc, J., Zarrinpashneh, E., Soty, M., Mithieux, G., Sakamoto, K., Andreelli, F., and Viollet, B. (2010) Metformin inhibits hepatic gluconeogenesis in mice independently of the LKB1/AMPK pathway via a decrease in hepatic energy state. *J. Clin. Invest.* **120**, 2355–2369

35. Satapati, S., Sunny, N. E., Kucejova, B., Fu, X., He, T. T., Méndez-Lucas, A., Shelton, J. M., Perales, J. C., Browning, J. D., and Burgess, S. C. (2012) Elevated TCA cycle function in the pathology of diet-induced hepatic insulin resistance and fatty liver. *J. Lipid Res.* **53**, 1080–92

36. Berglund, E. D., Lustig, D. G., Baheza, R. A., Hasenour, C. M., Lee-Young, R. S., Donahue, E. P., Lynes, S. E., Swift, L. L., Charron, M. J., Damon, B. M., and Wasserman, D. H. (2011) Hepatic Glucagon Action Is Essential for Exercise-Induced Reversal of Mouse Fatty Liver. *Diabetes* **60**, 2720–2729

37. Steinberg, G. R., and Kemp, B. E. (2009) AMPK in Health and Disease. *Physiol. Rev.* **89**, 1025–1078

38. Hardie, D. G., and Hawley, S. A. (2001) AMP-activated protein kinase: the energy charge hypothesis revisited. *Bioessays* **23**, 1112–9

39. Taketa, K., and Pogell, B. M. (1965) Allosteric Inhibition of Rat Liver Fructose 1,6-Diphosphatase by Adenosine 5'-Monophosphate. *J. Biol. Chem.* **240**, 651–662

40. Atkinson, D. E. (1968) The Energy Charge of the Adenylate Pool as a Regulatory Parameter. Interaction with Feedback Modifiers. *Biochemistry* **7**, 4030–4

41. Lee-Young, R. S., Palmer, M. J., Linden, K. C., LePlastrier, K., Canny, B. J., Hargreaves, M., Wadley, G. D., Kemp, B. E., and McConell, G. K. (2006) Carbohydrate ingestion does not alter skeletal muscle AMPK signaling during exercise in humans. *Am. J. Physiol. Endocrinol. Metab.* **291**, E566–573

42. Jansson, E., Dudley, G. A., Norman, B., and Tesch, P. A. (1987) ATP and IMP in single human muscle fibres after high intensity exercise. *Clin. Physiol.* **7**, 337–45

43. Norman, B., Sollevi, A., Kaijser, L., and Jansson, E. (1987) ATP breakdown products in human skeletal muscle during prolonged exercise to exhaustion. *Clin. Physiol.* **7**, 503–10

44. Dudley, G. A., and Terjung, R. L. (1985) Influence of aerobic metabolism on IMP accumulation in fast-twitch muscle. *Am. J. Physiol.* **248**, C37–42

45. Meyer, R. A., and Terjung, R. L. (1979) Differences in ammonia and adenylate metabolism in contracting fast and slow muscle. *Am. J. Physiol.* **237**, C111–8

46. Atkinson, D. E. (1977) CELLULAR ENERGY METABOLISM AND ITS REGULATION. *Acad. Press*

47. Woods, H. F., Eggleston, L. V, and Krebs, H. A. (1970) The Cause of Hepatic Accumulation of Fructose 1-Phosphate on Fructose Loading. *Biochem. J.* **119**, 501–10

48. Woods, H. F., and Krebs, H. A. (1973) The Effect of Glycerol and Dihydroxyacetone on Hepatic Adenine Nucleotides. *Biochem J* **132**, 55–60

49. Chapman, A. G., and Atkinson, D. E. (1973) Stabilization of Adenylate Energy Charge by the Adenylate Deaminase Reaction. *J. Biol. Chem.* **248**, 8309–8312

50. Gowans, G. J., Hawley, S. A., Ross, F. A., and Hardie, D. G. (2013) AMP Is a True Physiological Regulator of AMP-Activated Protein Kinase by Both Allosteric Activation and Enhancing Net Phosphorylation. *Cell Metab.* **18**, 556–66

51. Oakhill, J. S., Scott, J. W., and Kemp, B. E. (2012) AMPK functions as an adenylate charge-regulated protein kinase. *Trends Endocrinol. Metab.* **23**, 125–32

52. McGarry, J. D., and Foster, D. W. (1980) REGULATION OF HEPATIC FATTY ACID OXIDATION AND KETONE BODY PRODUCTION. *Annu. Rev. Biochem.* **49**, 395–420

53. McGarry, J. D., Leatherman, G. F., and Foster, D. W. (1978) Carnitine palmitoyltransferase I. The site of inhibition of hepatic fatty acid oxidation by malonyl-CoA. *J. Biol. Chem.* **253**, 4128–36

54. Mcgarry, J. D., and Foster, D. W. (1981) Importance of experimental conditions in evaluating the malonyl-CoA sensitivity of liver carnitine acyltransferase. *Biochem. J.* **200**, 217–223

55. Brownsey, R. W., Boone, A. N., Elliott, J. E., Kulpa, J. E., and Lee, W. M. (2006) Regulation of acetyl-CoA carboxylase. *Biochem. Soc. Trans.* **34**, 223–7

56. Munday, M. R., Milic, M. R., Takhar, S., Holness, M. J., and Sugden, M. C. (1991) The short-term regulation of hepatic acetyl-CoA carboxylase during starvation and re-feeding in the rat. *Biochem. J.* **280**, 733–7

57. Holland, R., Witters, L. A., and Hardie, D. G. (1984) Glucagon inhibits fatty acid synthesis in isolated hepatocytes via phosphorylation of acetyl-CoA carboxylase by cyclic-AMP-dependent protein kinase. *Eur. J. Biochem.* **140**, 325–33

58. Sim, A. T. R., and Hardie, D. G. (1988) The low activity of acetyl-CoA carboxylase in basal and glucagon-stimulated hepatocytes is due to phosphorylation by the AMP-activated protein kinase and not cyclic AMP-dependent protein kinase. *FEBS Lett.* **233**, 294–8

59. Jungermann, K., and Kietzmann, T. (1996) ZONATION OF PARENCHYMAL AND NONPARENCHYMAL METABOLISM IN LIVER. *Annu. Rev. Nutr.* **16**, 179–203

60. Witters, L. A., Gao, G., Kemp, B. E., and Quistorff, B. (1994) Hepatic 5′-AMP-Activated Protein Kinase: Zonal Distribution and Relationship to Acetyl-CoA Carboxylase Activity in Varying Nutritional States. *Arch. Biochem. Biophys.* **308**, 413–419

61. Heimberg, M., Weinstein, I., and Kohout, M. (1969) The Effects of Glucagon, Dibutyryl Cyclic Adenosine 3’-5'-Monophosphate, and Cencentration of Free Fatty Acid on Hepatic Lipid Metabolism. *J. Biol. Chem.* **244**, 5131–5139

62. Carlson, C. L., and Winder, W. W. (1999) Liver AMP-activated protein kinase and acetyl-CoA carboxylase during and after exercise. *J. Appl. Physiol.* **86**, 669–74

63. Williamson, J. R., Scholz, R., and Browning, E. T. (1969) Control Mechanisms of Gluconeogenesis and Ketogenesis: II. INTERACTIONS BETWEEN FATTY ACID OXIDATION AND THE CITRIC ACID CYCLE IN PERFUSED RAT LIVER. *J. Biol. Chem.* **244**, 4617–4627

64. McGarry, J. D., and Foster, D. W. (1980) Effects of Exogenous Fatty Acid Concentration on Glucagon-induced Changes in Hepatic Fatty Acid Metabolism. *Diabetes* **29**, 236–40

65. Watt, M. J., Steinberg, G. R., Chen, Z.-P., Kemp, B. E., and Febbraio, M. A. (2006) Fatty acids stimulate AMP-activated protein kinase and enhance fatty acid oxidation in L6 myotubes. *J. Physiol.* **574**, 139–47

66. Foretz, M., Pacot, C., Dugail, I., Lemarchand, P., Guichard, C., Le Lièpvre, X., Berthelier-Lubrano, C., Spiegelman, B., Kim, J. B., Ferré, P., and Foufelle, F. (1999) ADD1/SREBP-1c Is Required in the Activation of Hepatic Lipogenic Gene Expression by Glucose. *Mol. Cell. Biol.* **19**, 3760–8

67. Li, Y., Xu, S., Mihaylova, M. M., Zheng, B., Hou, X., Jiang, B., Park, O., Luo, Z., Lefai, E., Shyy, J. Y.-J., Gao, B., Wierzbicki, M., Verbeuren, T. J., Shaw, R. J., Cohen, R. A., and Zang, M. (2011) AMPK Phosphorylates and Inhibits SREBP Activity to Attenuate Hepatic Steatosis and Atherosclerosis in Diet-Induced Insulin-Resistant Mice. *Cell Metab.* **13**, 376–88

68. Hasenour, C. M., Berglund, E. D., and Wasserman, D. H. (2013) Emerging role of AMP-activated protein kinase in endocrine control of metabolism in the liver. *Mol. Cell. Endocrinol.* **366**, 152–62

69. McGarry, J. D., and Foster, D. W. (1971) The Regulation of Ketogenesis from Octanoic Acid: THE ROLE OF THE TRICARBOXYLIC ACID CYCLE AND FATTY ACID SYNTHESIS. *J. Biol. Chem.* **246**, 1149–59

70. Mcgarry, J. D., and Foster, D. W. (1971) The Regulation of Ketogenesis from Oleic Acid and the Influence of Antiketogenic Agents. *J. Biol. Chem.* **246**, 6247–53

71. Foretz, M., Ancellin, N., Andreelli, F., Saintillan, Y., Grondin, P., Kahn, A., Thorens, B., Vaulont, S., and Viollet, B. (2005) Short-Term Overexpression of a Constitutively Active Form of AMP-Activated Protein Kinase in the Liver Leads to Mild Hypoglycemia and Fatty Liver. *Diabetes* **54**, 1331–9

72. Mallette, L. E., Exton, J. H., and Park, C. R. (1969) Effects of Glucagon on Amino Acid Transport and Utilization in the Perfused Rat Liver. *J. Biol. Chem.* **244**, 5724–5728

73. Kimball, S. R., Siegfried, B. A., and Jefferson, L. S. (2004) Glucagon Represses Signaling through the Mammalian Target of Rapamycin in Rat Liver by Activating AMP-activated protein kinase. *J. Biol. Chem.* **279**, 54103–9

74. Izzo, J. L., and Glasser, S. R. (1961) COMPARATIVE EFFECTS OF GLUCAGON, HYDROCORTISONE AND EPINEPHRINE ON THE PROTEIN METABOLISM OF THE FASTING RAT. *Endocrinology* **68**, 189–198

75. Yin, X. M., Ding, W. X., and Gao, W. (2008) Autophagy in the Liver. *Hepatology* **47**, 1773–85

76. Baum, J. I., Kimball, S. R., and Jefferson, L. S. (2009) Glucagon acts in a dominant manner to repress insulin-induced mammalian target of rapamycin complex 1 signaling in perfused rat liver. *Am. J. Physiol. Endocrinol. Metab.* **297**, 410–415

77. Dubbelhuis, P. F., and Meijer, A. J. (2002) Hepatic amino acid-dependent signaling is under the control of AMP-dependent protein kinase. *FEBS Lett.* **521**, 39–42

78. Inoki, K., Zhu, T., and Guan, K.-L. (2003) TSC2 Mediates Cellular Energy Response to Control Cell Growth and Survival. *Cell* **115**, 577–90

79. Gwinn, D. M., Shackelford, D. B., Egan, D. F., Mihaylova, M. M., Mery, A., Vasquez, D. S., Turk, B. E., and Shaw, R. J. (2008) AMPK Phosphorylation of Raptor Mediates a Metabolic Checkpoint. *Mol. Cell* **30**, 214–26

80. Kim, J., Kundu, M., Viollet, B., and Guan, K. L. (2011) AMPK and mTOR regulate autophagy through direct phosphorylation of Ulk1. *Nat. Cell Biol.* **13**, 132–41

81. Dunlop, E. A., and Tee, A. R. (2013) The kinase triad, AMPK, mTORC1 and ULK1, maintains energy and nutrient homoeostasis. *Biochem. Soc. Trans.* **41**, 939–43

82. Newgard, C. B. (2012) Interplay between Lipids and Branched-Chain Amino Acids in Development of Insulin Resistance. *Cell Metab.* **15**, 606–14

83. Koves, T. R., Ussher, J. R., Noland, R. C., Slentz, D., Mosedale, M., Ilkayeva, O., Bain, J., Stevens, R., Dyck, J. R. B., Newgard, C. B., Lopaschuk, G. D., and Muoio, D. M. (2008) Mitochondrial overload and incomplete fatty acid oxidation contribute to skeletal muscle insulin resistance. *Cell Metab.* **7**, 45–56

84. Muoio, D. M., and Newgard, C. B. (2008) Mechanisms of disease: molecular and metabolic mechanisms of insulin resistance and β-cell failure in type 2 diabetes. *Nat. Rev. Mol. Cell Biol.* **9**, 193–205

85. Makowski, L., Noland, R. C., Koves, T. R., Xing, W., Ilkayeva, O. R., Muehlbauer, M. J., Stevens, R. D., and Muoio, D. M. (2009) Metabolic profiling of PPARα-/- mice reveals

defects in carnitine and amino acid homeostasis that are partially reversed by oral carnitine supplementation. *FASEB J.* **23**, 586–604

86. Zammit, V. A. (1999) Carnitine acyltransferases: functional significance of subcellular distribution and membrane topology. *Prog. Lipid Res.* **38**, 199–224

87. Schooneman, M. G., Vaz, F. M., Houten, S. M., and Soeters, M. R. (2013) Acylcarnitines: Reflecting or Inflicting Insulin Resistance? *Diabetes* **62**, 1–8

88. Kucejova, B., Sunny, N. E., Nguyen, A. D., Hallac, R., Fu, X., Peña-Llopis, S., Mason, R. P., Deberardinis, R. J., Xie, X. J., DeBose-Boyd, R., Kodibagkar, V. D., Burgess, S. C., and Brugarolas, J. (2011) Uncoupling hypoxia signaling from oxygen sensing in the liver results in hypoketotic hypoglycemic death. *Oncogene* **30**, 2147–60

89. Struck, E., Ashmore, J., and Wieland, O. (1966) EFFECTS OF GLUCAGON AND LONG CHAIN FATTY ACIDS ON GLUCOSE PRODUCTION BY ISOLATED PERFUSED RAT LIVER. *Adv. Enzyme Regul.* **4**, 219–224

90. Williamson, J. R., Kreisberg, R. A., and Felts, P. (1966) MECHANISM FOR THE STIMULATION OF GLUCONEOGENESIS BY FATTY ACIDS IN PERFUSED RAT LIVER. *Proc. Natl. Acad. Sci. U. S. A.* **56**, 247–254

91. Teufel, H., Menahan, L. A., Shipp, J. C., Boning, S., and Wieland, O. (1967) Effect of Oleic Acid on the Oxidation and Gluconeogenesis from [1-14C]Pyruvate in the Perfused Rat Liver. *Eur. J. Biochem.* **2**, 182–186

92. Friedmann, B., Goodman, E. H., and Weinhouse, S. (1967) Effects of Insulin and Fatty Acids on Gluconeogenesis in the Rat. *J. Biol. Chem.* **242**, 3620–3627

93. Williamson, J. R., Browning, E. T., and Scholz, R. (1969) Control Mechanisms of Gluconeogenesis and Ketogenesis: I. EFFECTS OF OLEATE ON GLUCONEOGENESIS IN PERFUSED RAT LIVER. *J. Biol. Chem.* **244**, 4607–4616

94. Chu, C. A., Sherck, S. M., Igawa, K., Sindelar, D. K., Neal, D. W., Emshwiller, M., and Cherrington, A. D. (2002) Effects of free fatty acids on hepatic glycogenolysis and gluconeogenesis in conscious dogs. *Am. J. Physiol. Endocrinol. Metab.* **282**, E402–11

95. Roden, M., Stingl, H., Chandramouli, V., Schumann, W. C., Hofer, A., Landau, B. R., Nowotny, P., Waldhäusl, W., and Shulman, G. I. (2000) Effects of Free Fatty Acid Elevation on Postabsorptive Endogenous Glucose Production and Gluconeogenesis in Humans. *Diabetes* **49**, 701–707

96. Wolf, H. P. O., and Engel, D. W. (1985) Decrease of fatty acid oxidation, ketogenesis and gluconeogenesis in isolated perfused rat liver by phenylalkyl oxirane carboxylate (B 807-27) due to inhibition of CPT I (EC 2.3.1.21). *Eur. J. Biochem.* **146**, 359–63

97. Conti, R., Mannucci, E., Pessotto, P., Tassoni, E., Carminati, P., Giannessi, F., and Arduini, A. (2011) Selective Reversible Inhibition of Liver Carnitine Palmitoyl-Transferase 1 by Teglicar Reduces Gluconeogenesis and Improves Glucose Homeostasis. *Diabetes* **60**, 644–51

98. Ruderman, N. B., Toews, C. J., and Shafrir, E. (1969) Role of Free Fatty Acids in Glucose Homeostasis. *Arch. Intern. Med.* **123**, 299–313

99. González-Manchón, C., Ayuso, M. S., and Parrilla, R. (1989) Control of Hepatic Gluconeogenesis: Role of Fatty Acid Oxidation. *Arch. Biochem. Biophys.* **271**, 1–9

100. Blumenthal, S. A. (1983) Stimulation of Gluconeogenesis by Palmitic Acid in Rat Hepatocytes: Evidence That This Effect Can Be Dissociated From the Provision of Reducing Equivalents. *Metabolism* **32**, 971–976

101. Egnatchik, R. A., Leamy, A. K., Noguchi, Y., Shiota, M., and Young, J. D. (2014) Palmitate-induced Activation of Mitochondrial Metabolism Promotes Oxidative Stress and Apoptosis in H4IIEC3 Rat Hepatocytes. *Metabolism.* **63**, 283–95

102. Williamson, J. R., and Cooper, R. H. (1980) REGULATION OF THE CITRIC ACID CYCLE IN MAMMALIAN SYSTEMS. *FEBS Lett.* **117**, K73–85

103. Jones, J. G., Naidoo, R., Sherry, A. D., Jeffrey, F. M. H., Cottam, G. L., and Malloy, C. R. (1997) Measurement of gluconeogenesis and pyruvate recycling in the rat liver: a simple analysis of glucose and glutamate isotopomers during metabolism of [1,2,3-13C3]propionate. *FEBS Lett.* **412**, 131–137

104. She, P., Shiota, M., Shelton, K. D., Chalkley, R., Postic, C., and Magnuson, M. A. (2000) Phosphoenolpyruvate Carboxykinase Is Necessary for the Integration of Hepatic Energy Metabolism. *Mol. Cell. Biol.* **20**, 6508–6517

105. Burgess, S. C., Hausler, N., Merritt, M., Jeffrey, F. M. H., Storey, C., Milde, A., Koshy, S., Lindner, J., Magnuson, M. A., Malloy, C. R., and Sherry, A. D. (2004) Impaired Tricarboxylic Acid Cycle Activity in Mouse Livers Lacking Cytosolic Phosphoenolpyruvate Carboxykinase. *J. Biol. Chem.* **279**, 48941–9

106. Blackshear, P. J., Holloway, P. A., and Aberti, K. G. M. M. (1975) The Effects of Inhibition of Gluconeogenesis on Ketogenesis in Starved and Diabetic Rats. *Biochem. J.* **148**, 353–62

107. Burgess, S. C., Leone, T. C., Wende, A. R., Croce, M. A., Chen, Z., Sherry, A. D., Malloy, C. R., and Finck, B. N. (2006) Diminished Hepatic Gluconeogenesis via Defects in Tricarboxylic Acid Cycle Flux in Peroxisome Proliferator-activated Receptor γ Coactivator-1α (PGC-1α)-deficient mice. *J. Biol. Chem.* **281**, 19000–8

108. Leone, T. C., Lehman, J. J., Finck, B. N., Schaeffer, P. J., Wende, A. R., Boudina, S., Courtois, M., Wozniak, D. F., Sambandam, N., Bernal-Mizrachi, C., Chen, Z., Holloszy, J. O., Medeiros, D. M., Schmidt, R. E., Saffitz, J. E., Abel, E. D., Semenkovich, C. F., and Kelly, D. P. (2005) PGC-1α Deficiency Causes Multi-System Energy Metabolic Derangements: Muscle Dysfunction, Abnormal Weight Control and Hepatic Steatosis. *PLoS Biol.* **3**, e101

109. Rakhshandehroo, M., Sanderson, L. M., Matilainen, M., Stienstra, R., Carlberg, C., de Groot, P. J., Müller, M., and Kersten, S. (2007) Comprehensive Analysis of PPARα-Dependent Regulation of Hepatic Lipid Metabolism by Expression Profiling. *PPAR Res.* **2007**, 26839

110. Leone, T. C., Weinheimer, C. J., and Kelly, D. P. (1999) A critical role for the peroxisome proliferator-activated receptor α (PPARα) in the cellular fasting response: The PPARα-null mouse as a model of fatty acid oxidation disorders. *Proc. Natl. Acad. Sci. U. S. A.* **96**, 7473–7478

111. Kersten, S., Seydoux, J., Peters, J. M., Gonzalez, F. J., Desvergne, B., and Wahli, W. (1999) Peroxisome proliferator-activated receptor α mediates the adaptive response to fasting. *J. Clin. Invest.* **103**, 1489–98

112. Rankin, E. B., Rha, J., Selak, M. A., Unger, T. L., Keith, B., Liu, Q., and Haase, V. H. (2009) Hypoxia-Inducible Factor 2 Regulates Hepatic Lipid Metabolism. *Mol. Cell. Biol.* **29**, 4527–38

113. Kucejova, B., Sunny, N. E., Nguyen, A. D., Hallac, R., Fu, X., Peña-Llopis, S., Mason, R. P., Deberardinis, R. J., Xie, X. J., DeBose-Boyd, R., Kodibagkar, V. D., Burgess, S. C., and Brugarolas, J. (2011) Uncoupling hypoxia signaling from oxygen sensing in the liver results in hypoketotic hypoglycemic death. *Oncogene* **30**, 2147–2160

114. Burgess, S. C., He, T. T., Yan, Z., Lindner, J., Sherry, A. D., Malloy, C. R., Browning, J. D., and Magnuson, M. A. (2007) Cytosolic Phosphoenolpyruvate Carboxykinase Does Not Solely Control the Rate of Hepatic Gluconeogenesis in the Intact Mouse Liver. *Cell Metab.* **5**, 313–20

115. Berglund, E. D., Kang, L., Lee-Young, R. S., Hasenour, C. M., Lustig, D. G., Lynes, S. E., Donahue, E. P., Swift, L. L., Charron, M. J., and Wasserman, D. H. (2010) Glucagon and lipid interactions in the regulation of hepatic AMPK signaling and expression of PPARα and FGF21 transcripts in vivo. *Am. J. Physiol. Endocrinol. Metab.* **299**, E607–614

116. Rodgers, J. T., Lerin, C., Haas, W., Gygi, S. P., Spiegelman, B. M., and Puigserver, P. (2005) Nutrient control of glucose homeostasis through a complex of PGC-1α and SIRT1. *Nature* **434**, 113–118

117. Houtkooper, R. H., Pirinen, E., and Auwerx, J. (2012) Sirtuins as regulators of metabolism and healthspan. *Nat. Rev. Mol. Cell Biol.* **13**, 225–38

118. Buler, M., Aatsinki, S.-M., Izzi, V., and Hakkola, J. (2012) Metformin Reduces Hepatic Expression of SIRT3, the Mitochondrial Deacetylase Controlling Energy Metabolism. *PLoS One* **7**, e49863

119. Hirschey, M. D., Shimazu, T., Goetzman, E., Jing, E., Schwer, B., Lombard, D. B., Grueter, C. A., Harris, C., Biddinger, S., Ilkayeva, O. R., Stevens, R. D., Li, Y., Saha, A. K., Ruderman, N. B., Bain, J. R., Newgard, C. B., Farese Jr, R. V, Alt, F. W., Kahn, C. R., and Verdin, E. (2010) SIRT3 regulates mitochondrial fatty-acid oxidation by reversible enzyme deacetylation. *Nature* **464**, 121–5

120. Fulco, M., Cen, Y., Zhao, P., Hoffman, E. P., McBurney, M. W., Sauve, A. A., and Sartorelli, V. (2008) Glucose Restriction Inhibits Skeletal Myoblast Differentiation by Activating SIRT1 through AMPK-Mediated Regulation of Nampt. *Dev. Cell* **14**, 661–73

121. Cantó, C., Gerhart-Hines, Z., Feige, J. N., Lagouge, M., Noriega, L., Milne, J. C., Elliott, P. J., Puigserver, P., and Auwerx, J. (2009) AMPK regulates energy expenditure by modulating NAD+ metabolism and SIRT1 activity. *Nature* **458**, 1056–1060

122. Um, J. H., Park, S. J., Kang, H., Yang, S., Foretz, M., McBurney, M. W., Kim, M. K., Viollet, B., and Chung, J. H. (2010) AMP-Activated Protein Kinase-Deficient Mice Are Resistant to the Metabolic Effects of Resveratrol. *Diabetes* **59**, 554–563

123. O'Neill, H. M., Maarbjerg, S. J., Crane, J. D., Jeppesen, J., Jørgensen, S. B., Schertzer, J. D., Shyroka, O., Kiens, B., van Denderen, B. J., Tarnopolsky, M. A., Kemp, B. E., Richter, E. A., and Steinberg, G. R. (2011) AMP-activated protein kinase (AMPK) β1β2 muscle null mice reveal an essential role for AMPK in maintaining mitochondrial content and glucose uptake during exercise. *Proc. Natl. Acad. Sci. U. S. A.* **108**, 16092–16097

124. Ruderman, N. B., Xu, X. J., Nelson, L., Cacicedo, J. M., Saha, A. K., Lan, F., and Ido, Y. (2010) AMPK and SIRT1: a long-standing partnership? *Am. J. Physiol. Endocrinol. Metab.* **298**, E751–60

125. El-Mir, M.-Y., Nogueira, V., Fontaine, E., Averet, N., Rigoulet, M., and Leverve, X. (2000) Dimethylbiguanide Inhibits Cell Respiration via an Indirect Effect Targeted on the Respiratory Chain Complex I. *J. Biol. Chem.* **275**, 223–228

126. Cantó, C., Gerhart-Hines, Z., Feige, J. N., Lagouge, M., Noriega, L., Milne, J. C., Elliott, P. J., Puigserver, P., and Auwerx, J. (2009) AMPK regulates energy expenditure by modulating NAD+ metabolism and SIRT1 activity. *Nature* **458**, 1056–60

127. Guigas, B., Taleux, N., Foretz, M., Detaille, D., Andreelli, F., Viollet, B., and Hue, L. (2007) AMP-activated protein kinase-independent inhibition of hepatic mitochondrial oxidative phosphorylation by AICA riboside. *Biochem. J.* **404**, 499–507

128. Brunmair, B., Staniek, K., Gras, F., Scharf, N., Althaym, A., Clara, R., Roden, M., Gnaiger, E., Nohl, H., Waldhausl, W., and Furnsinn, C. (2004) Thiazolidinediones, Like

Metformin, Inhibit Respiratory Complex I: A Common Mechanism Contributing to Their Antidiabetic Actions? *Diabetes* **53**, 1052–1059

129. Corton, J. M., Gillespie, J. G., Hawley, S. A., and Hardie, D. G. (1995) 5-Aminoimidazole-4-carboxamide ribonucleoside. A specific method for activating AMP-activated protein kinase in intact cells? *Eur. J. Biochem.* **229**, 558–565

130. Moore, F., Weekes, J., and Hardie, D. G. (1991) Evidence that AMP triggers phosphorylation as well as direct allosteric activation of rat liver AMP-activated protein kinase. A sensitive mechanism to protect the cell against ATP depletion. *Eur. J. Biochem.* **199**, 691–7

131. Ramaiah, A., Hathaway, J. A., and Atkinson, D. E. (1964) Adenylate as a Metabolic Regulator: EFFECT ON YEAST PHOSPHOFRUCTOKINASE KINETICS. *J. Biol. Chem.* **239**, 3619–3622

132. Johnson, L. N. (1992) Glycogen phosphorylase: effectors control by phosphorylation and allosteric effectors. *FASEB J.* **6**, 2274–2282

133. Bergeron, R., Previs, S. F., Cline, G. W., Perret, P., Russell III, R. R., Young, L. H., and Shulman, G. I. (2001) Effect of 5-Aminoimidazole-4-Carboxamide-1-β-D-Ribofuranoside Infusion on In Vivo Glucose and Lipid Metabolism in Lean and Obese Zucker Rats. *Diabetes* **50**, 1076–1082

134. Bergeron, R., Russell III, R. R., Young, L. H., Ren, J. M., Marcucci, M., Lee, A., and Shulman, G. I. (1999) Effect of AMPK activation on muscle glucose metabolism in conscious rats. *Am. J. Physiol. Endocrinol. Metab.* **276**, E938–44

135. Iglesias, M. A., Ye, J. M., Frangioudakis, G., Saha, A. K., Tomas, E., Ruderman, N. B., Cooney, G. J., and Kraegen, E. W. (2002) AICAR Administration Causes an Apparent Enhancement of Muscle and Liver Insulin Action in Insulin-Resistant High-Fat-Fed Rats. *Diabetes* **51**, 2886–2894

136. Zhou, G., Myers, R., Li, Y., Chen, Y., Shen, X., Fenyk-Melody, J., Wu, M., Ventre, J., Doebber, T., Fujii, N., Musi, N., Hirshman, M. F., Goodyear, L. J., and Moller, D. E. (2001) Role of AMP-activated protein kinase in mechanism of metformin action. *J. Clin. Invest.* **108**, 1167–1174

137. Shaw, R. J., Lamia, K. A., Vasquez, D., Koo, S.-H., Bardeesy, N., DePinho, R. A., Montminy, M., and Cantley, L. C. (2005) The Kinase LKB1 Mediates Glucose Homeostasis in Liver and Therapeutic Effects of Metformin. *Science (80-. ).* **310**, 1642–1646

138. He, L., Sabet, A., Djedjos, S., Miller, R., Sun, X., Hussain, M. A., Radovick, S., and Wondisford, F. E. (2009) Metformin and Insulin Suppress Hepatic Gluconeogenesis through Phosphorylation of CREB Binding Protein. *Cell* **137**, 635–46

139. Obika, M., and Noguchi, H. (2012) Diagnosis and Evaluation of Nonalcoholic Fatty Liver Disease. *Exp. Diabetes Res.* **2012**, 145754

140. Targher, G., and Byrne, C. D. (2013) Nonalcoholic Fatty Liver Disease: A Novel Cardiometabolic Risk Factor for Type 2 Diabetes and Its Complications. *J. Clin. Endocrinol. Metab.* **98**, 483–95

141. Quiroga, A. D., and Lehner, R. (2011) Role of endoplasmic reticulum neutral lipid hydrolases. *Trends Endocrinol. Metab.* **22**, 218–25

142. Malhi, H., and Gores, G. J. (2008) Molecular Mechanisms of Lipotoxicity in Nonalcoholic Fatty Liver Disease. *Semin. Liver Dis.* **28**, 360–369

143. Listenberger, L. L., Han, X., Lewis, S. E., Cases, S., Farese, R. V, Ory, D. S., and Schaffer, J. E. (2003) Triglyceride accumulation protects against fatty acid-induced lipotoxicity. *Proc. Natl. Acad. Sci. U. S. A.* **100**, 3077–82

144. Leamy, A. K., Egnatchik, R. A., and Young, J. D. (2013) Molecular mechanisms and the role of saturated fatty acids in the progression of non-alcoholic fatty liver disease. *Prog. Lipid Res.* **52**, 165–74

145. Diraison, F., Moulin, P. H., and Beylot, M. (2003) Contribution of hepatic de novo lipogenesis and reesterification of plasma non esterified fatty acids to plasma triglyceride synthesis during non-alcoholic fatty liver disease. *Diabetes Metab.* **29**, 478–485

146. Sunny, N. E., Parks, E. J., Browning, J. D., and Burgess, S. C. (2011) Excessive Hepatic Mitochondrial TCA Cycle and Gluconeogenesis in Humans with Nonalcoholic Fatty Liver Disease. *Cell Metab.* **14**, 804–10

147. Kim, H. J., Kim, J. H., Noh, S., Hur, H. J., Sung, M. J., Hwang, J. T., Park, J. H., Yang, H. J., Kim, M. S., Kwon, D. Y., and Yoon, S. H. (2011) Metabolomic Analysis of Livers and Serum from High-Fat Diet Induced Obese Mice. *J. Proteome Res.* **10**, 722–31

148. Fealy, C. E., Haus, J. M., Solomon, T. P., Pagadala, M., Flask, C. A., McCullough, A. J., and Kirwan, J. P. (2012) Short-term exercise reduces markers of hepatocyte apoptosis in nonalcoholic fatty liver disease. *J. Appl. Physiol.* **113**, 1–6

149. Haus, J. M., Solomon, T. P., Kelly, K. R., Fealy, C. E., Kullman, E. L., Scelsi, A. R., Lu, L., Pagadala, M. R., McCullough, A. J., Flask, C. A., and Kirwan, J. P. (2013) Improved Hepatic Lipid Composition Following Short-Term Exercise in Nonalcoholic Fatty Liver Disease. *J. Clin. Endocrinol. Metab.* **98**, E1181–1188

150. Johnson, N. A., Sachinwalla, T., Walton, D. W., Smith, K., Armstrong, A., Thompson, M. W., and George, J. (2009) Aerobic Exercise Training Reduces Hepatic and Visceral Lipids in Obese Individuals Without Weight Loss. *Hepatology* **50**, 1105–12

151. Rector, R. S., Thyfault, J. P., Morris, R. T., Laye, M. J., Borengasser, S. J., Booth, F. W., and Ibdah, J. A. (2008) Daily exercise increases hepatic fatty acid oxidation and prevents steatosis in Otsuka Long-Evans Tokushima Fatty rats. *Am. J. Physiol. Gastrointest. Liver Physiol.* **294**, G619–G626

152. Borengasser, S. J., Rector, R. S., Uptergrove, G. M., Morris, E. M., Perfield II, J. W., Booth, F. W., Fritsche, K. L., Ibdah, J. A., and Thyfault, J. P. (2012) Exercise and Omega-3 Polyunsaturated Fatty Acid Supplementation for the Treatment of Hepatic Steatosis in Hyperphagic OLETF Rats. *J. Nutr. Metab.* **2012**, 268680

153. Vieira, V. J., Valentine, R. J., Wilund, K. R., Antao, N., Baynard, T., and Woods, J. A. (2009) Effects of exercise and low-fat diet on adipose tissue inflammation and metabolic complications in obese mice. *Am. J. Physiol. Endocrinol. Metab.* **296**, E1164–E1171

154. Rector, R. S., Uptergrove, G. M., Morris, E. M., Borengasser, S. J., Laughlin, M. H., Booth, F. W., Thyfault, J. P., and Ibdah, J. A. (2011) Daily exercise vs. caloric restriction for prevention of nonalcoholic fatty liver disease in the OLETF rat model. *Am. J. Physiol. Gastrointest. Liver Physiol.* **300**, G874–883

155. Andreelli, F., Foretz, M., Knauf, C., Cani, P. D., Perrin, C., Iglesias, M. A., Pillot, B., Bado, A., Tronche, F., Mithieux, G., Vaulont, S., Burcelin, R., and Viollet, B. (2006) Liver Adenosine Monophosphate-Activated Kinase-α2 Catalytic Subunit is a Key Target for the Control of Hepatic Glucose Production by Adiponectin and Leptin but Not Insulin. *Endocrinology* **147**, 2432–41

156. Altarejos, J. Y., and Montminy, M. (2011) CREB and the CRTC co-activators: sensors for hormonal and metabolic signals. *Nat. Rev. Mol. Cell Biol.* **12**, 141–51

157. Gonzalez, G. A., and Montminy, M. R. (1989) Cyclic AMP Stimulates Somatostatin Gene Transcription by Phosphorylation of CREB at Serine 133. *Cell* **59**, 675–80

158. Herzig, S., Long, F., Jhala, U. S., Hedrick, S., Quinn, R., Bauer, A., Rudolph, D., Schutz, G., Yoon, C., Puigserver, P., Spiegelman, B., and Montminy, M. (2001) CREB regulates hepatic gluconeogenesis through the coactivator PGC-1. *Nature* **413**, 179–83

159. Yoon, J. C., Puigserver, P., Chen, G., Donovan, J., Wu, Z., Rhee, J., Adelmant, G., Stafford, J., Kahn, C. R., Granner, D. K., Newgard, C. B., and Spiegelman, B. M. (2001) Control of hepatic gluconeogenesis through the transcriptional coactivator PGC-1. *Nature* **413**, 131–8

160. Rhee, J., Inoue, Y., Yoon, J. C., Puigserver, P., Fan, M., Gonzalez, F. J., and Spiegelman, B. M. (2003) Regulation of hepatic fasting response by PPARγ coactivator-1α (PGC-1): Requirement for hepatocyte nuclear factor 4α in gluconeogenesis. *Proc. Natl. Acad. Sci. U. S. A.* **100**, 4012–7

161. Puigserver, P., Rhee, J., Donovan, J., Walkey, C. J., Yoon, J. C., Oriente, F., Kitamura, Y., Altomonte, J., Dong, H., Accili, D., and Spiegelman, B. M. (2003) Insulin-regulated hepatic gluconeogenesis through FOXO1–PGC-1α interaction. *Nature* **423**, 550–555

162. Hong, Y. H., Varanasi, U. S., Yang, W., and Leff, T. (2003) AMP-activated Protein Kinase Regulates HNF4α Transcriptional Activity by Inhibiting Dimer Formation and Decreasing Protein Stability. *J. Biol. Chem.* **278**, 27495–501

163. Leclerc, I., Lenzner, C., Gourdon, L., Vaulont, S., Kahn, A., and Viollet, B. (2001) Hepatocyte Nuclear Factor-4α Involved in Type I Mature-Onset Diabetes of the Young Is a Novel Target of AMP-Activated Protein Kinase. *Diabetes* **50**, 1515–1521

164. Handschin, C., Lin, J., Rhee, J., Peyer, A.-K., Chin, S., Wu, P.-H., Meyer, U. A., and Spiegelman, B. M. (2005) Nutritional Regulation of Hepatic Heme Biosynthesis and Porphyria through PGC-1α. *Cell* **122**, 505–15

165. Dentin, R., Liu, Y., Koo, S. H., Hedrick, S., Vargas, T., Heredia, J., Yates III, J., and Montminy, M. (2007) Insulin modulates gluconeogenesis by inhibition of the coactivator TORC2. *Nature* **449**, 366–9

166. Koo, S. H., Flechner, L., Qi, L., Zhang, X., Screaton, R. A., Jeffries, S., Hedrick, S., Xu, W., Boussouar, F., Brindle, P., Takemori, H., and Montminy, M. (2005) The CREB coactivator TORC2 is a key regulator of fasting glucose metabolism. *Nature* **437**, 1109–14

167. Le Lay, J., Tuteja, G., White, P., Dhir, R., Ahima, R., and Kaestner, K. H. (2009) CRTC2 (TORC2) Contributes to the Transcriptional Response to Fasting in the Liver but is Not Required for the Maintenance of Glucose Homeostasis. *Cell Metab.* **10**, 55–62

168. Mihaylova, M. M., Vasquez, D. S., Ravnskjaer, K., Denechaud, P.-D., Yu, R. T., Alvarez, J. G., Downes, M., Evans, R. M., Montminy, M., and Shaw, R. J. (2011) Class IIa Histone Deacetylases Are Hormone-Activated Regulators of FOXO and Mammalian Glucose Homeostasis. *Cell* **145**, 607–21

169. Wang, B., Moya, N., Niessen, S., Hoover, H., Mihaylova, M. M., Shaw, R. J., Yates III, J. R., Fischer, W. H., Thomas, J. B., and Montminy, M. (2011) A Hormone-Dependent Module Regulating Energy Balance. *Cell* **145**, 596–606

170. Holland, W. L., Miller, R. A., Wang, Z. V, Sun, K., Barth, B. M., Bui, H. H., Davis, K. E., Bikman, B. T., Halberg, N., Rutkowski, J. M., Wade, M. R., Tenorio, V. M., Kuo, M. S., Brozinick, J. T., Zhang, B. B., Birnbaum, M. J., Summers, S. A., and Scherer, P. E. (2011) Receptor-mediated activation of ceramidase activity initiates the pleiotropic actions of adiponectin. *Nat. Med.* **17**, 55–63

171. Miller, R. A., Chu, Q., Le Lay, J., Scherer, P. E., Ahima, R. S., Kaestner, K. H., Foretz, M., Viollet, B., and Birnbaum, M. J. (2011) Adiponectin suppresses gluconeogenic gene

expression in mouse hepatocytes independent of LKB1-AMPK signaling. *J. Clin. Invest.* **121**, 2518–2528

172. Dzamko, N., van Denderen, Bryce J W Hevener, A. L., Jørgensen, S. B., Honeyman, J., Galic, S., Chen, Z. P., Watt, M. J., Campbell, D. J., Steinberg, G. R., and Kemp, B. E. (2010) AMPKβ1 Deletion Reduces Appetite, Preventing Obesity and Hepatic Insulin Resistance. *J. Biol. Chem.* **285**, 115–22

173. Scott, J. W., van Denderen, B. J. W., Jorgensen, S. B., Honeyman, J. E., Steinberg, G. R., Oakhill, J. S., Iseli, T. J., Koay, A., Gooley, P. R., Stapleton, D., and Kemp, B. E. (2008) Thienopyridone Drugs Are Selective Activators of AMP-Activated Protein Kinase β1-Containing Complexes. *Chem. Biol.* **15**, 1220–30

174. Shackelford, D. B., and Shaw, R. J. (2009) The LKB1-AMPK pathway: metabolism and growth control in tumour suppression. *Nat. Rev. Cancer* **9**, 563–75

175. Screaton, R. A., Conkright, M. D., Katoh, Y., Best, J. L., Canettieri, G., Jeffries, S., Guzman, E., Niessen, S., Yates III, J. R., Takemori, H., Okamoto, M., and Montminy, M. (2004) The CREB Coactivator TORC2 Functions as a Calcium- and cAMP-Sensitive Coincidence Detector. *Cell* **119**, 61–74

176. Witters, L. A., and Kemp, B. E. (1992) Insulin Activation of Acetyl-CoA Carboxylase Accompanied by Inhibition of 5'-AMP-activated Protein Kinase. *J. Biol. Chem.* **267**, 2864–2867

177. Horman, S., Vertommen, D., Heath, R., Neumann, D., Mouton, V., Woods, A., Schlattner, U., Wallimann, T., Carling, D., Hue, L., and Rider, M. H. (2006) Insulin Antagonizes Ischemia-induced Thr172 Phosphorylation of AMP-activated Protein Kinase α-Subunits in Heart via Hierarchical Phosphorylation of Ser485/491. *J. Biol. Chem.* **281**, 5335–40

178. Rivera, N., Ramnanan, C. J., An, Z., Farmer, T., Smith, M., Farmer, B., Irimia, J. M., Snead, W., Lautz, M., Roach, P. J., and Cherrington, A. D. (2010) Insulin-induced hypoglycemia increases hepatic sensitivity to glucagon in dogs. *J. Clin. Invest.* **120**, 4425–4435

179. Inoki, K., Li, Y., Zhu, T., Wu, J., and Guan, K. L. (2002) TSC2 is phosphorylated and inhibited by Akt and suppresses mTOR signalling. *Nat. Cell Biol.* **4**, 648–57

180. Kim, Y. D., Park, K. G., Lee, Y. S., Park, Y. Y., Kim, D. K., Nedumaran, B., Jang, W. G., Cho, W. J., Ha, J., Lee, I. K., Lee, C. H., and Choi, H. S. (2008) Metformin Inhibits Hepatic Gluconeogenesis Through AMP-Activated Protein Kinase-Dependent Regulation of the Orphan Nuclear Receptor SHP. *Diabetes* **57**, 306–314

181. Granner, D., Andreone, T., Sasaki, K., and Beale, E. (1983) Inhibition of transcription of the phosphoenolpyruvate carboxykinase gene by insulin. *Nature* **305**, 549–551

182. Biggs III, W. H., Meisenhelder, J., Hunter, T., Cavenee, W. K., and Arden, K. C. (1999) Protein kinase B/Akt-mediated phosphorylation promotes nuclear exclusion of the winged helix transcription factor FKHR1. *Proc. Natl. Acad. Sci. U. S. A.* **96**, 7421–6

183. Nakae, J., Park, B.-C., and Accili, D. (1999) Insulin Stimulates Phosphorylation of the Forkhead Transcription Factor FKHR on Serine 253 through a Wortmannin-sensitive Pathway. *J. Biol. Chem.* **274**, 15982–15985

184. Li, X., Monks, B., Ge, Q., and Birnbaum, M. J. (2007) Akt/PKB regulates hepatic metabolism by directly inhibiting PGC-1α transcription coactivator. *Nature* **447**, 1012–6

185. Mabrouk, G. M., Helmy, I. M., Thampy, K. G., and Wakil, S. J. (1990) Acute hormonal control of acetyl-CoA carboxylase. The roles of insulin, glucagon, and epinephrine. *J. Biol. Chem.* **265**, 6330–6338

186. Li, S., Brown, M. S., and Goldstein, J. L. (2010) Bifurcation of insulin signaling pathway in rat liver: mTORC1 required for stimulation of lipogenesis, but not inhibition of gluconeogenesis. *Proc. Natl. Acad. Sci. U. S. A.* **107**, 3441–6

187. Wan, M., Leavens, K. F., Saleh, D., Easton, R. M., Guertin, D. A., Peterson, T. R., Kaestner, K. H., Sabatini, D. M., and Birnbaum, M. J. (2011) Postprandial Hepatic Lipid Metabolism Requires Signaling through Akt2 Independent of the Transcription Factors FoxA2, FoxO1, and SREBP1c. *Cell Metab.* **14**, 516–27

188. Yecies, J. L., Zhang, H. H., Menon, S., Liu, S., Yecies, D., Lipovsky, A. I., Gorgun, C., Kwiatkowski, D. J., Hotamisligil, G. S., Lee, C. H., and Manning, B. D. (2011) Akt Stimulates Hepatic SREBP1c and Lipogenesis through Parallel mTORC1-Dependent and Independent Pathways. *Cell Metab.* **14**, 21–32

189. Horton, J. D., Goldstein, J. L., and Brown, M. S. (2002) SREBPs : activators of the complete program of cholesterol and fatty acid synthesis in the liver. *J. Clin. Invest.* **109**, 1125–1131

190. Munday, M. R., Campbell, D. G., Carling, D., and Hardie, D. G. (1988) Identification by amino acid sequencing of three major regulatory phosphorylation sites on rat acetyl-CoA carboxylase. *Eur. J. Biochem.* **175**, 331–8

191. Fullerton, M. D., Galic, S., Marcinko, K., Sikkema, S., Pulinilkunnil, T., Chen, Z. P., O'Neill, H. M., Ford, R. J., Palanivel, R., O'Brien, M., Hardie, D. G., Macaulay, S. L., Schertzer, J. D., Dyck, J. R. B., van Denderen, B. J., Kemp, B. E., and Steinberg, G. R. (2013) Single phosphorylation sites in Acc1 and Acc2 regulate lipid homeostasis and the insulin-sensitizing effects of metformin. *Nat. Med.* **19**, 1649–1654

192. Ingebritsen, T. S., Geelen, M. J., Parker, R. A., Evenson, K. J., and Gibson, D. M. (1979) Modulation of hydroxymethylglutaryl-CoA reductase activity, reductase kinase activity,

and cholesterol synthesis in rat hepatocytes in response to insulin and glucagon. *J. Biol. Chem.* **254**, 9986–9989

193. Clarke, P. R., and Hardie, D. G. (1990) Regulation of HMG-CoA reductase: identification of the site phosphorylated by the AMP-activated protein kinase in vitro and in intact rat liver. *EMBO J.* **9**, 2439–46

194. Carling, D., Zammit, V. A., and Hardie, D. G. (1987) A common bicyclic protein kinase cascade inactivates the regulatory enzymes of fatty acid and cholesterol biosynthesis. *FEBS Lett.* **223**, 217–22

195. Awazawa, M., Ueki, K., Inabe, K., Yamauchi, T., Kaneko, K., Okazaki, Y., Bardeesy, N., Ohnishi, S., Nagai, R., and Kadowaki, T. (2009) Adiponectin suppresses hepatic SREBP1c expression in an AdipoR1/LKB1/AMPK dependent pathway. *Biochem. Biophys. Res. Commun.* **382**, 51–6

196. Austin, S., and St-Pierre, J. (2012) PGC1α and mitochondrial metabolism - emerging concepts and relevance in ageing and neurodegenerative disorders. *J. Cell Sci.* **125**, 4963–71

197. Ayala, J. E., Bracy, D. P., Malabanan, C., James, F. D., Ansari, T., Fueger, P. T., McGuinness, O. P., and Wasserman, D. H. (2011) Hyperinsulinemic-euglycemic Clamps in Conscious, Unrestrained Mice. *J. Vis. Exp.* **57**, e3188

198. Kang, L., Ayala, J. E., Lee-Young, R. S., Zhang, Z., James, F. D., Neufer, P. D., Pozzi, A., Zutter, M. M., and Wasserman, D. H. (2011) Diet-Induced Muscle Insulin Resistance Is Associated With Extracellular Matrix Remodeling and Interaction With Integrin α2β1in Mice. *Diabetes* **60**, 416–26

199. Shearer, J., Fueger, P. T., Rottman, J. N., Bracy, D. P., Martin, P. H., and Wasserman, D. H. (2004) AMPK stimulation increases LCFA but not glucose clearance in cardiac muscle in vivo. *Am. J. Physiol. Endocrinol. Metab.* **287**, E871–E877

200. Befroy, D. E., Perry, R. J., Jain, N., Dufour, S., Cline, G. W., Trimmer, J. K., Brosnan, J., Rothman, D. L., Petersen, K. F., and Shulman, G. I. (2014) Direct assessment of hepatic mitochondrial oxidative and anaplerotic fluxes in humans using dynamic (13)C magnetic resonance spectroscopy. *Nat. Med.* **20**, 98–102

201. Antoniewicz, M. R., Kelleher, J. K., and Stephanopoulos, G. (2011) Measuring Deuterium Enrichment of Glucose Hydrogen Atoms by Gas Chromatography/Mass Spectrometry. *Anal. Chem.* **83**, 3211–6

202. Young, J. D. (2014) INCA: a computational platform for isotopically non-stationary metabolic flux analysis. *Bioinformatics*, 1–3

203. Romestaing, C., Piquet, M.-A., Letexier, D., Rey, B., Mourier, A., Servais, S., Belouze, M., Rouleau, V., Dautresme, M., Ollivier, I., Favier, R., Rigoulet, M., Duchamp, C., and Sibille, B. (2008) Mitochondrial adaptations to steatohepatitis induced by a methionine- and choline-deficient diet. *Am. J. Physiol. Endocrinol. Metab.* **294**, E110–119

204. Hughey, C. C., Hittel, D. S., Johnsen, V. L., and Shearer, J. (2011) Respirometric Oxidative Phosphorylation Assessment in Saponin-permeabilized Cardiac Fibers. *J. Vis. Exp.* **48**, e2431

205. Davies, S. P., Carling, D., Munday, M. R., and Hardie, D. G. (1992) Diurnal rhythm of phosphorylation of rat liver acetyl-CoA carboxylase by the AMP-activated protein kinase, demonstrated using freeze-clamping. Effects of high fat diets. *Eur. J. Biochem.* **203**, 615–23

206. Chan, T. M., and Exton, J. H. (1976) A Rapid Method for the Determination of Glycogen Content and Radioactivity in Small Quantities of Tissue or Isolated Hepatocytes. *Anal. Biochem.* **71**, 96–105

207. Folch, J., Lees, M., and Sloane Stanley, G. H. (1957) A SIMPLE METHOD FOR THE ISOLATION AND PURIFICATION OF TOTAL LIPIDES FROM ANIMAL TISSUES. *J. Biol. Chem.* **226**, 497–509

208. Morrison, W. R., and Smith, L. M. (1964) Preparation of fatty acid methyl esters and dimethylacetals from lipids with boron fluoride-methanol. *J. Lipid Res.* **5**, 600–8

209. Steele, R., Wall, J. S., de Bodo, R. C., and Altszuler, N. (1956) Measurement of Size and Turnover Rate of Body Glucose Pool by the Isotope Dilution Method. *Am. J. Physiol.* **187**, 15–24

210. Burgess, S. C., Jeffrey, F. M. H., Storey, C., Milde, A., Hausler, N., Merritt, M. E., Mulder, H., Holm, C., Sherry, A. D., and Malloy, C. R. (2005) Effect of murine strain on metabolic pathways of glucose production after brief or prolonged fasting. *Am. J. Physiol. Endocrinol. Metab.* **289**, E53–61

211. Jensen, T. L., Kiersgaard, M. K., Sørensen, D. B., and Mikkelsen, L. F. (2013) Fasting of mice: a review. *Lab. Anim.* **47**, 225–40

212. Michalik, L., Desvergne, B., and Wahli, W. (2004) PEROXISOME-PROLIFERATOR-ACTIVATED RECEPTORS AND CANCERS: COMPLEX STORIES. *Nat. Rev. Cancer* **4**, 61–70

213. Cool, B., Zinker, B., Chiou, W., Kifle, L., Cao, N., Perham, M., Dickinson, R., Adler, A., Gagne, G., Iyengar, R., Zhao, G., Marsh, K., Kym, P., Jung, P., Camp, H. S., and Frevert, E. (2006) Identification and characterization of a small molecule AMPK activator that treats key components of type 2 diabetes and the metabolic syndrome. *Cell Metab.* **3**, 403–16

214. Steinberg, G. R., O'Neill, H. M., Dzamko, N. L., Galic, S., Naim, T., Koopman, R., Jørgensen, S. B., Honeyman, J., Hewitt, K., Chen, Z. P., Schertzer, J. D., Scott, J. W., Koentgen, F., Lynch, G. S., Watt, M. J., van Denderen, B. J. W., Campbell, D. J., and Kemp, B. E. (2010) Whole Body Deletion of AMP-Activated Protein Kinase β2 Reduces Muscle AMPK Activity and Exercise Capacity. *J. Biol. Chem.* **285**, 37198–209

215. Park, S. K., Haase, V. H., and Johnson, R. S. (2007) von Hippel Lindau tumor suppressor regulates hepatic glucose metabolism by controlling expression of glucose transporter 2 and glucose 6-phosphatase. *Int. J. Oncol.* **30**, 341–8

216. Krebs, H. (1964) The Croonian Lecture, 1963: Gluconeogenesis. *Proc. R. Soc. Biol. Sci.* **159**, 545–564

217. Velasco, G., Geelen, M. J. H., and Guzmán, M. (1997) Control of Hepatic Fatty Acid Oxidation by 5'-AMP-Activated Protein Kinase Involves a Malonyl-CoA-Dependent and a Malonyl-CoA-Independent Mechanism. *Arch. Biochem. Biophys.* **337**, 169–75

218. Song, X. M., Fiedler, M., Galuska, D., Ryder, J. W., Fernström, M., Chibalin, A. V, Wallberg-Henriksson, H., and Zierath, J. R. (2002) 5-Aminoimidazole-4-carboxamide ribonucleoside treatment improves glucose homeostasis in insulin-resistant diabetic (ob/ob) mice. *Diabetologia* **45**, 56–65

219. Iglesias, M. A., Furler, S. M., Cooney, G. J., Kraegen, E. W., and Ye, J. M. (2004) AMP-Activated Protein Kinase Activation by AICAR Increases both Muscle Fatty Acid and Glucose Uptake in White Muscle of Insulin-Resistant Rats In Vivo. *Diabetes* **53**, 1649–54

220. Buhl, E. S., Jessen, N., Pold, R., Ledet, T., Flyvbjerg, A., Pedersen, S. B., Pedersen, O., Schmitz, O., and Lund, S. (2002) Long-Term AICAR Administration Reduces Metabolic Disturbances and Lowers Blood Pressure in Rats Displaying Features of the Insulin Resistance Syndrome. *Diabetes* **51**, 2199–206

221. Fryer, L. G. D., Parbu-Patel, A., and Carling, D. (2002) The Anti-diabetic Drugs Rosiglitazone and Metformin Stimulate AMP-activated Protein Kinase through Distinct Signaling Pathways. *J. Biol. Chem.* **277**, 25226–32

222. Vincent, M. F., Marangos, P. J., Gruber, H. E., and Van den Berghe, G. (1991) Inhibition by AICA Riboside of Gluconeogenesis in Isolated Rat Hepatocytes. *Diabetes* **40**, 1259–66

223. Shirai, T., Inoue, E., Ishimi, Y., and Yamauchi, J. (2011) AICAR response element binding protein (AREBP), a key modulator of hepatic glucose production regulated by AMPK in vivo. *Biochem. Biophys. Res. Commun.* **414**, 287–91

224. Chanda, D., Kim, S. J., Lee, I. K., Shong, M., and Choi, H. S. (2008) Sodium arsenite induces orphan nuclear receptor SHP gene expression via AMP-activated protein kinase to inhibit gluconeogenic enzyme gene expression. *Am. J. Physiol. Endocrinol. Metab.* **295**, E368–79

225. Yamauchi, T., Kamon, J., Minokoshi, Y., Ito, Y., Waki, H., Uchida, S., Yamashita, S., Noda, M., Kita, S., Ueki, K., Eto, K., Akanuma, Y., Froguel, P., Foufelle, F., Ferre, P., Carling, D., Kimura, S., Nagai, R., Kahn, B. B., and Kadowaki, T. (2002) Adiponectin stimulates glucose utilization and fatty-acid oxidation by activating AMP-activated protein kinase. *Nat. Med.* **8**, 1288–95

226. Lochhead, P. A., Salt, I. P., Walker, K. S., Hardie, D. G., and Sutherland, C. (2000) 5-Aminoimidazole-4-Carboxamide Riboside Mimics the Effects of Insulin on the Expression of the 2 Key Gluconeogenic Genes PEPCK and Glucose-6-Phosphatase. *Diabetes* **49**, 896–903

227. Miller, R. A., and Birnbaum, M. J. (2010) An energetic tale of AMPK-independent effects of metformin. *J. Clin. Invest.* **120**, 2267–2270

228. Pencek, R. R., Shearer, J., Camacho, R. C., James, F. D., Brooks, D. B., Fueger, P. T., Donahue, E. P., Snead, W., and Wasserman, D. H. (2005) 5-Aminoimidazole-4-Carboxamide-1-β-D-Ribofuranoside Causes Acute Hepatic Insulin Resistance In Vivo. *Diabetes* **54**, 355–360

229. Vincent, M. F., Bontemps, F., and Van den Berghe, G. (1992) Inhibition of glycolysis by 5-amino-4-imidazolecarboxamide riboside in isolated rat hepatocytes. *Biochem. J.* **281**, 267–72

230. Mukhtar, M. H., Payne, V. A., Arden, C., Harbottle, A., Khan, S., Lange, A. J., and Agius, L. (2008) Inhibition of glucokinase translocation by AMP-activated protein kinase is associated with phosphorylation of both GKRP and 6-phosphofructo-2-kinase/fructose-2,6-bisphosphatase. *Am. J. Physiol. Regul. Integr. Comp. Physiol.* **294**, R766–774

231. Guigas, B., Bertrand, L., Taleux, N., Foretz, M., Wiernsperger, N., Vertommen, D., Andreelli, F., Viollet, B., and Hue, L. (2006) 5-Aminoimidazole-4-Carboxamide-1-β-D-Ribofuranoside and Metformin Inhibit Hepatic Glucose Phosphorylation by an AMP-Activated Protein Kinase-Independent Effect on Glucokinase Translocation. *Diabetes* **55**, 865–874

232. Hunter, R. W., Treebak, J. T., Wojtaszewski, J. F. P., and Sakamoto, K. (2011) Molecular Mechanism by Which AMP-Activated Protein Kinase Activation Promotes Glycogen Accumulation in Muscle. *Diabetes* **60**, 766–74

233. García-Villafranca, J., Guillén, A., and Castro, J. (2008) Ethanol consumption impairs regulation of fatty acid metabolism by decreasing the activity of AMP-activated protein kinase in rat liver. *Biochimie* **90**, 460–6

234. Foretz, M., Carling, D., Guichard, C., Ferré, P., and Foufelle, F. (1998) AMP-activated Protein Kinase Inhibits the Glucose-activated Expression of Fatty Acid Synthase Gene in Rat Hepatocytes. *J. Biol. Chem.* **273**, 14767–14771

235. Muoio, D. M., Seefeld, K., Witters, L. A., and Coleman, R. A. (1999) AMP-activated kinase reciprocally regulates triacylglycerol synthesis and fatty acid oxidation in liver and muscle : evidence that sn-glycerol-3-phosphate acyltransferase is a novel target. *Biochem J* **338**, 783–791

236. Wasserman, D. H., Lickley, H. L. A., and Vranic, M. (1985) Important role of glucagon during exercise in diabetic dogs. *J. Appl. Physiol.* **59**, 1272–81

237. Wasserman, D. H., Lickley, H. L. A., and Vranic, M. (1984) Interactions between Glucagon and Other Counterregulatory Hormones during Normoglycemic and Hypoglycemic Exercise in Dogs. *J. Clin. Invest.* **74**, 1404–13

238. Hippen, A. R., She, P., Young, J. W., Beitz, D. C., Lindberg, G. L., Richardson, L. F., and Tucker, R. W. (1999) Alleviation of Fatty Liver in Dairy Cows with 14-Day Intravenous Infusions of Glucagon. *J. Dairy Sci.* **82**, 1139–52

239. Nafikov, R. A., Ametaj, B. N., Bobe, G., Koehler, K. J., Young, J. W., and Beitz, D. C. (2006) Prevention of Fatty Liver in Transition Dairy Cows by Subcutaneous Injections of Glucagon. *J. Dairy Sci.* **89**, 1533–45

240. Krishna, M. G., Coker, R. H., Lacy, D. B., Zinker, B. A., Halseth, A. E., and Wasserman, D. H. (2000) Glucagon response to exercise is critical for accelerated hepatic glutamine metabolism and nitrogen disposal. *Am. J. Physiol. Endocrinol. Metab.* **279**, E638–E645

241. Kim, K. H., Kim, S. H., Min, Y. K., Yang, H. M., Lee, J. B., and Lee, M. S. (2013) Acute Exercise Induces FGF21 Expression in Mice and in Healthy Humans. *PLoS One* **8**, e63517

242. Inagaki, T., Dutchak, P., Zhao, G., Ding, X., Gautron, L., Parameswara, V., Li, Y., Goetz, R., Mohammadi, M., Esser, V., Elmquist, J. K., Gerard, R. D., Burgess, S. C., Hammer, R. E., Mangelsdorf, D. J., and Kliewer, S. A. (2007) Endocrine Regulation of the Fasting Response by PPARα-Mediated Induction of Fibroblast Growth Factor 21. *Cell Metab.* **5**, 415–25

243. Cintra, D. E., Ropelle, E. R., Vitto, M. F., Luciano, T. F., Souza, D. R., Engelmann, J., Marques, S. O., Lira, F. S., de Pinho, R. A., Pauli, J. R., and De Souza, C. T. (2012) Reversion of hepatic steatosis by exercise training in obese mice: The role of sterol regulatory element-binding protein-1c. *Life Sci.* **91**, 395–401

244. Fu, S., Yang, L., Li, P., Hofmann, O., Dicker, L., Hide, W., Lin, X., Watkins, S. M., Ivanov, A. R., and Hotamisligil, G. S. (2011) Aberrant lipid metabolism disrupts calcium homeostasis causing liver endoplasmic reticulum stress in obesity. *Nature* **473**, 528–31

245. Gibellini, F., and Smith, T. K. (2010) The Kennedy Pathway- De Novo Synthesis of Phosphatidylethanolamine and Phosphatidylcholine. *IUBMB Life* **62**, 414–28

246. Muoio, D. M., Noland, R. C., Kovalik, J. P., Seiler, S. E., Davies, M. N., DeBalsi, K. L., Ilkayeva, O. R., Stevens, R. D., Kheterpal, I., Zhang, J., Covington, J. D., Bajpeyi, S., Ravussin, E., Kraus, W., Koves, T. R., and Mynatt, R. L. (2012) Muscle-Specific Deletion of Carnitine Acetyltransferase Compromises Glucose Tolerance and Metabolic Flexibility. *Cell Metab.* **15**, 764–77

247. Seiler, S. E., Martin, O. J., Noland, R. C., Slentz, D. H., DeBalsi, K. L., Ilkayeva, O. R., An, J., Newgard, C. B., Koves, T. R., and Muoio, D. M. (2014) Obesity and Lipid Stress Inhibit Carnitine Acetyltransferase Activity. *J. Lipid Res.* **55**, 635–44

248. Park, H., Kaushik, V. K., Constant, S., Prentki, M., Przybytkowski, E., Ruderman, N. B., and Saha, A. K. (2002) Coordinate Regulation of Malonyl-CoA Decarboxylase, sn-Glycerol-3-phosphate Acyltransferase, and Acetyl-CoA Carboxylase by AMP-activated Protein Kinase in Rat Tissues in Response to Exercise. *J. Biol. Chem.* **277**, 32571–7

249. Kelly, M., Keller, C., Avilucea, P. R., Keller, P., Luo, Z., Xiang, X., Giralt, M., Hidalgo, J., Saha, A. K., Pedersen, B. K., and Ruderman, N. B. (2004) AMPK activity is diminished in tissues of IL-6 knockout mice: the effect of exercise. *Biochem. Biophys. Res. Commun.* **320**, 449–54

250. Reiter, A. K., Bolster, D. R., Crozier, S. J., Kimball, S. R., and Jefferson, L. S. (2008) AMPK represses TOP mRNA translation but not global protein synthesis in liver. *Biochem. Biophys. Res. Commun.* **374**, 345–50

251. Hoene, M., Lehmann, R., Hennige, A. M., Pohl, A. K., Häring, H. U., Schleicher, E. D., and Weigert, C. (2009) Acute regulation of metabolic genes and insulin receptor substrates in the liver of mice by one single bout of treadmill exercise. *J. Physiol.* **587**, 241–52

252. Cui, M., Yu, H., Wang, J., Gao, J., and Li, J. (2013) Chronic Caloric Restriction and Exercise Improve Metabolic Conditions of Dietary-Induced Obese Mice in Autophagy Correlated Manner without Involving AMPK. *J. Diabetes Res.* **2013**, 852754

253. Dobrzyn, P., Pyrkowska, A., Jazurek, M., Szymanski, K., Langfort, J., and Dobrzyn, A. (2010) Endurance training-induced accumulation of muscle triglycerides is coupled to upregulation of stearoyl-CoA desaturase 1. *J. Appl. Physiol.* **109**, 1653–1661

254. Magkos, F. (2010) Exercise and fat accumulation in the human liver. *Curr. Opin. Lipidol.* **21**, 507–17

255. Wang, Q., Perrard, X. D., Perrard, J. L., Mansoori, A., Raya, J. L., Hoogeveen, R., Smith, C. W., Ballantyne, C. M., and Wu, H. (2011) Differential effect of weight loss with low-fat diet or high-fat diet restriction on inflammation in the liver and adipose tissue of mice with diet-induced obesity. *Atherosclerosis* **219**, 100–108

256. Pendergast, J. S., Branecky, K. L., Huang, R., Niswender, K. D., and Yamazaki, S. (2014) Wheel-running activity modulates circadian organization and the daily rhythm of eating behavior. *Front. Psychol.* **5**, 1–9

257. Mantena, S. K., Vaughn, D. P., Andringa, K. K., Eccleston, H. B., King, A. L., Abrams, G. A., Doeller, J. E., Kraus, D. W., Darley-Usmar, V. M., and Bailey, S. M. (2009) High fat diet induces dysregulation of hepatic oxygen gradients and mitochondrial function in vivo. *Biochem. J.* **417**, 183–93

258. Bánhegyi, G., and Mandl, J. (2001) The Hepatic Glycogenoreticular System. *Pathol. Oncol. Reasearch* **7**, 107–110

259. Cole, L. K., Vance, J. E., and Vance, D. E. (2012) Phosphatidylcholine biosynthesis and lipoprotein metabolism. *Biochim. Biophys. Acta* **1821**, 754–61

260. Shimomura, Y., Honda, T., Shiraki, M., Murakami, T., Sato, J., Kobayashi, H., Mawatari, K., Obayashi, M., and Harris, R. A. (2006) Branched-Chain Amino Acid Catabolism in Exercise and Liver Disease. *J. Nutr.* **136**, 250S–253S

261. Harper, A. E., Miller, R. H., and Block, K. P. (1984) BRANCHED-CHAIN AMINO ACID METABOLISM. *Annu. Rev. Nutr.* **4**, 409–54

262. Drouin, R., Robert, G., Milot, M., Massicotte, D., Péronnet, F., and Lavoie, C. (2004) Swim Training Increases Glucose Output From Liver Perfused In Situ with Glucagon in Fed and Fasted Rats. *Metabolism* **53**, 1027–1031

263. Friesen, R. W., Novak, E. M., Hasman, D., and Innis, S. M. (2007) Relationship of Dimethylglycine, Choline, and Betaine with Oxoproline in Plasma of Pregnant Women and Their Newborn Infants. *J. Nutr.* **137**, 2641–2646